



NTNU – Trondheim
Norwegian University of
Science and Technology

Energy efficiency improvement of industrial refrigeration systems within the pelagic fish industry

Ephraim Gukelberger

Master's Thesis

Submission date: April 2014

Supervisor: Trygve Magne Eikevik, EPT

Norwegian University of Science and Technology
Department of Energy and Process Engineering

EPT-M-2013-150

MASTER THESIS

for

Ephraim Gukelberger

Autumn 2013

Energy efficiency improvement of industrial refrigeration systems within the pelagic fish industry

Forbedring av energieffektivitet i industrielle kuldetekniske systemer for pelagisk industri

Background and objective

Pelagic fish is by far the largest Norwegian industry based on wild-caught fish. Norway's share of herring and mackerel will represent over 750 000 tonnes in 2013. In addition imported fish from other countries is processed and refined in the Norwegian pelagic industry. The total value added in the sector in 2011 was ~1 billion € and gross margin over the past year was an average of 0.2 billion €. Although the processing industry has struggled with earnings in recent years, the industry has had profitability in total.

Rational and efficient cooling and freezing systems are the main basis for an economic processing of fish. A change in fishing patterns and the amount of fish from the vessels requires rationalization of systems with new technology, even with many freezing systems and an excess of freezing capacity. Today, pelagic fishing boats have become larger. This means landing of larger amount of fish as well as the land-based processing facilities have not increased their freezing capacities. To maintain the quality of the fish it is necessary to improve the efficiency of the freezing equipment to ensure that the time does not increase from the fish arrives to shore until it is deep-frozen.

Cooling systems using ammonia (NH₃) are applied in a wide range in this kind of installations. Air supply temperatures are in the range of -40 to 42 °C and lower at the end of the freezing period, to be able to reverse the freezing tunnels within a day cycle. These low freezing temperatures are challenging for ordinary NH₃ systems and result in greatly reduced performance and low energy efficiency. Rational freezing solutions with efficient refrigeration systems for low temperatures have to be developed.

Main focus of the master thesis will be to evaluate various alternative system solutions.

The following tasks are to be considered:

1. Literature review of freezing equipment applied in the pelagic fishing industry.
2. Analysis of measurement data from state of the art equipment.
3. Theoretical evaluation of alternative system enhancements and solutions.
4. Calculation of potential energy savings compared with current baseline equipment.
5. Prepare a draft scientific paper from the results of the thesis.
6. Make proposals for further work.

Within 14 days of receiving the written text on the master thesis, the candidate shall submit a research plan for his project to the department.

When the thesis is evaluated, emphasis is put on processing of the results, and that they are presented in tabular and/or graphic form in a clear manner, and that they are analyzed carefully.

The thesis should be formulated as a research report with summary both in English and German, conclusion, literature references, table of contents etc. During the preparation of the text, the candidate should make an effort to produce a well-structured and easily readable report. In order to ease the evaluation of the thesis, it is important that the cross-references are correct. In the making of the report, strong emphasis should be placed on both a thorough discussion of the results and an orderly presentation.

The candidate is requested to initiate and keep close contact with his/her academic supervisor(s) throughout the working period. The candidate must follow the rules and regulations of NTNU as well as passive directions given by the Department of Energy and Process Engineering.

Risk assessment of the candidate's work shall be carried out according to the department's procedures. The risk assessment must be documented and included as part of the final report. Events related to the candidate's work adversely affecting the health, safety or security, must be documented and included as part of the final report.

Pursuant to "Regulations concerning the supplementary provisions to the technology study program/Master of Science" at NTNU §20, the Department reserves the permission to utilize all the results and data for teaching and research purposes as well as in future publications.

The final report is to be submitted digitally in DAIM (<http://daim.idi.ntnu.no/>). An executive summary of the thesis including title, student's name, supervisor's name, year, department name, and NTNU's logo and name, shall be submitted to the department as a separate pdf file. The final report (in editable format), with summary and all other material and documents have to be given to the academic supervisor in digital format on a CD. Deadline 25th of March 2014.

Department of Energy and Process Engineering, September 18th 2013



Prof. Olav Bolland
Department Head



Prof. Trygve M. Eikevik
Academic Supervisor
e-mail: trygve.m.eikevik@ntnu.no

Research Advisors:

Tom Ståle Nordtvedt, SINTEF Energy Research, e-mail: tom.s.nordtvedt@sintef.no
Armin Hafner, SINTEF Energy Research, e-mail: armin.hafner@sintef.no

Declaration of Authorship

I hereby declare that this thesis entitled “Energy efficiency improvement of industrial refrigeration systems within the pelagic industry” and the work presented in is the result of my own investigation and was not written with the help by others. Moreover I confirm that I haven’t used any other sources and documents than listed below in my thesis.

This thesis is being submitted for the degree of Master of Science in Environmental Engineering obtained at the University Stuttgart, Germany.

.....
Stuttgart, April 12th 2014



.....
Ephraim Gukelberger

Acknowledgement

First of all I want to thank my supervisors Prof. Trygve M. Eikevik and Apl. Prof. Dr.-Ing. Klaus Spindler. This research would not have been possible without their support and expertise. Mr. Eikevik contributed with his profound knowledge and Mr. Spindler also with his support from Germany. I felt very comfortable with the warm welcome I received from the team of SINTEF Energy Research. Final thanks go to Dr. Armin Hafner, my second examiner, who naturally took over this position.

I truly enjoyed working at SINTEF and many thanks to the project leader Tom Ståle Nordtvedt, who always supported me in my intentions and deliberations. Moreover I am also obliged to Krzysztof Banasiak and Daniel Rohde who supported me with their fundamental knowledge about Dymola Control that helped me to perform my simulations in a targeted manner. In addition, I appreciated the help of all the persons who were further involved in this project. I enjoyed working with Ole Stavset as a friendly and professional team member but I am also grateful for the valuable experience given by Per A. Moen from PAM-Refrigeration and Yves Ladam. I appreciate the efforts they took to help me completing my work successfully. This acknowledgement is also devoted to Ola Magnus Magnussen who was truly a master in the field of refrigeration and motivated me the most with his kind and fortunate nature. Unfortunately I could not thank him personally for his help and knowledge and his views he supported me with.

Besides my working hours I felt always safe and home in Trondheim and was astonished of the beautiful nature in Norway. The friendly, obliging society and the employees of SINTEF always made my stay even more pleasant.

The work and study within this thesis was financial supported by SINTEF Energi AS and the German Academic Exchange Service.

Abstract

Nowadays a high quality standard of fish products, either fresh or frozen, is desired. Therefore a fast processing is of the highest priority. Since the world-wide consumption is rising steadily, larger refrigeration plants and warehouses are being built. Consequently, the energy usage of such facilities is increasing. To offset the additional electricity costs, the energy efficiency must be improved either by inventing and investigating new and highly efficient industrial processes. Furthermore, increasingly stringent environmental standards impose even higher efforts on developing refrigeration systems with natural refrigerants. Ammonia is known as the thermodynamic most efficient refrigerant and is used for many applications, including the state of the art industrial refrigeration of the pelagic fish. However there are limitations of using ammonia as a coolant. As an example, the application is limited below -40°C and the efficiency reduces significantly due to the required high pressure ratio and the high specific volume. Opposed to ammonia, carbon dioxide with its high volumetric efficiency has unique benefits in the temperature range between -40°C and -50°C . Due to the smaller system components, capacity enhancements have been realized for offshore applications in cascade systems with ammonia as high temperature media. Although many NH_3/CO_2 cascade systems have proven to be highly efficient in various applications all over the world, this technology has not yet been established for onshore plants within the pelagic fish industry in Norway. Therefore the motivation for this thesis was the investigation of a cascade refrigeration system for a given freezing tunnel provided by Norway Pelagic AS. The main tool was the objective-orientated, declarative modelling language *Modelica* with the simulation environment *Dymola Control*. Besides the investigation of various system parameters that mainly affected the freezing process time and the energy consumption, an energy recovery system was designed and a laboratory facility was constructed. Additionally, the effect of the substantial vulnerability for pressure losses and the resulting temperature reduction on the evaporator side was discussed. Since the cutting-edge cascade technology is not yet existent in onshore plants within the pelagic fish industry, positive feedback and an understanding of the technical and economical background and a literature review was an important indication which allowed different approaches for the project in the future.

Kurzfassung

Der stetig wachsende weltweite Fischverbrauch, vor allem an Hering und Makrele, erfordert immer größere industrielle Verarbeitungs- und Lagerzentren. Auf Norwegen, eines der weltweit größten Exportländer für ozeanischen Fisch, kommt hier eine besondere Rolle zu. Neben exportiertem, frischem Fisch nimmt auch der Wunsch nach gefrorenen Fischprodukten zu. Das dabei die Qualität nicht darunter leiden darf ist genauso selbstverständlich wie die Forderung nach günstigen Produkten. Um hier auch in Zukunft wirtschaftlich produzieren zu können bedarf es neben der Instandhaltung aktueller Produktionsmethoden neue, schnellere und kapazitätsintensivere industrielle Prozessschritte. Durch den heutigen Klimawandel, der auch die Fischbestände stark schwanken lässt, nimmt auch die Anforderung an die Flexibilität solcher Systeme zu. Natürliche Kältemittel wie Ammoniak und Kohlenstoffdioxid haben sich bereits mehrfach bewährt und werden auch in Zukunft eine immer wichtigere Rolle einnehmen. Ein Grund dafür sind die immer strengeren, politischen Auflagen im Angesicht des Klimawandels. Neben der klimaneutralen Bilanz hat Ammoniak auch die höchste thermodynamische Effizienz aller natürlichen Kältemittel und gilt als heutiger „Stand der Technik“ in großtechnischen Kälteanlagen. Die Toxizität und die eingeschränkte Anwendung unterhalb Temperaturen von -42°C sind allerdings Nachteile von Ammoniak und machen alternative Kältemittel notwendig. Kohlenstoffdioxid bringt mit seiner hohen volumetrischen Kälteleistung Vorteile in der Dimensionierung und besonders bei tiefen Temperaturen zwischen -40°C und -50°C eine Kapazitätserhöhung im Vergleich zu konventionellen Ammoniakanlagen. Insbesondere als Kaskadenkälteanlage in Verbindung mit Ammoniak wird CO_2 bereits weltweit in Supermärkten und auch auf Fischerbooten eingesetzt. Jedoch hat sich diese Technologie noch nicht auf dem Norwegischen Festland durchgesetzt. Ziel dieser Arbeit war es, effiziente Methoden für einen durch *Norway Pelagic AS* vorgegebenen Produktionsstandort zu untersuchen und Vorschläge für eine flexible, energieeffiziente Anlage zur Luftstromgefrierung zu machen. In diesem Rahmen wurde eine NH_3/CO_2 Kaskadenkälteanlage auf ihre Vor- und Nachteile hin untersucht und die Ergebnisse zu einer herkömmlichen, zweistufigen Ammoniakanlage verglichen. Hauptinstrument war dabei die objektorientierte Programmiersprache *Modelica*, welche mit der Simulationsumgebung *Dymola Control* umgesetzt wurde. Neben der Einflussuntersuchung verschiedener Prozessparameter auf die Energieeffizienz sowie die Prozesszeit für

das entworfene Modell wurde auch der Einsatz eines Energierückgewinnungssystems diskutiert und ein Vorschlag zu einem Laboraufbau ausführlich beschrieben und unterbreitet. Die hierbei gewonnenen Erkenntnisse dienen zur weiteren Aufklärung über die Kaskadentechnik und den Einsatz von CO₂ in großtechnischem Maßstab.

Content

1.	Introduction	1
2.	Previous work	2
2.1	Data measurement of current baseline	2
2.2	Air flow field simulation.....	3
2.3	Simulation element and comparison to measurements.....	4
2.4	Compressor.....	6
2.5	Maintenance of cooling fan	7
3.	Fundamentals of refrigeration systems	8
3.1	Thermodynamic fundamentals	8
3.1.1	Physical Process	8
3.1.2	Basic considerations and energy saving potentials.....	10
3.1.3	Energetic analysis	12
3.1.4	Exergetic analysis.....	14
3.2	Refrigerants.....	16
3.2.1	Ammonia	17
3.2.2	Carbon dioxide	18
4.	Refrigeration systems within the pelagic industry	20
4.1	Considerations of freezing fish	20
4.2	Application and usage in contemporary industry	21
4.2.1	Contact freezer	22
4.2.2	Blast freezing.....	23
4.2.3	Immersion freezing	24
4.3	Development and future trends.....	25
5.	Material and methods	27
5.1	NH ₃ /CO ₂ cascade system	28
5.1.1	Simulation model	28

5.1.2	Problem definition of the air and water intake	31
5.1.3	Pressure loss and hydraulic adjustment of the evaporator	32
5.2	Cold thermal energy storage	35
5.2.1	Physical basics of the storing process	36
5.2.2	CO ₂ used as phase change material.....	39
5.2.3	Laboratory setup.....	40
5.2.4	Pipe geometry simulation.....	41
5.2.5	Ice Slurry system	43
6.	Experimental results	46
6.1	Modelica simulation of NH ₃ /CO ₂ cascade system	46
6.1.1	Cooling capacity adjustment	46
6.1.2	Cascade heat exchanger optimization	48
6.1.3	Condensing pressure investigation	50
6.1.4	Refrigeration pump	51
6.2	System comparison.....	52
6.2.1	Total energy consumption.....	52
6.2.2	Coefficient of Performance	53
6.2.3	Tunnel capacity	54
6.2.4	Economical view	55
7.	Conclusion	56
8.	Further work.....	58
9.	References	59
10.	Appenix	62
11.	Paper.....	68

List of Figures

Figure 1: Freezing tunnel outline	3
Figure 2: Air velocity distribution and values at different fan speed operations (1).....	4
Figure 3: Measurements and simulation results (1).....	5
Figure 4: Speed regulation of a screw compressor (6), (1).....	6
Figure 5: Simple refrigeration cycle with main components.....	8
Figure 6: Two-stage refrigeration system	9
Figure 7: R717/R744 cascade system.....	10
Figure 8: Pressure curve of different refrigerants (14).....	17
Figure 9: Product cooling curve	21
Figure 10: Horizontal (left) and vertical (right) contact freezing (21).....	22
Figure 11: Product box, freezing tunnel and air flow simulation with Airpak (1), (17)	23
Figure 12: Immersion spray – and liquid N ₂ immersion freezer (21).....	25
Figure 13: Dymola, NH ₃ /CO ₂ cascade model	29
Figure 14: Fin and tube evaporator (FINCOIL/Alfa Laval) and evaporator pipeline ..	32
Figure 15: Temperature drop calculations and resulting pressure drop.....	33
Figure 16: Temperature and resulting freezing time (right) with R717	34
Figure 17: Temperature and resulting freezing time (right) with R744	34
Figure 18: Enhancement of the efficiency by an energy storage system.....	35
Figure 19: Outline of the storage system.....	36
Figure 20: Heat transfer coefficient of the charging process	38
Figure 21: Heat transfer coefficient of the discharge process.....	38
Figure 22: Phase diagram of CO ₂	39
Figure 23: Laboratory setup of a Cold thermal energy storage system	41
Figure 24: Heat flow simulation, QuickField.....	42

Figure 25: Outline of an Ice Slurry storage system added to the cascade system ...	43
Figure 26: Enthalpy-phase diagram of different ethyl alcohol-water compounds.....	44
Figure 27: Heat transfer coefficient, solutions with different ice contents (35).....	45
Figure 28: Evaporation temperature curve	47
Figure 29: Cooling capacity adjustment.....	48
Figure 30: Parameter regulation of the cascade heat exchanger	49
Figure 31: Condensing pressure investigation.....	50
Figure 32: New system with adjusted parameters	51
Figure 33: Energy consumption, system comparison	52
Figure 34: Percentage composition of the total energy consumption	53
Figure 35: COP, system comparison.....	54

List of Tables

Table 1: Reference values of the two-stage ammonia system	5
Table 2: Specified boundary conditions by <i>Northern Pelagic AS</i>	27
Table 3: Reference values, two-stage ammonia system	27
Table 4: Variable simulation parameters	30
Table 5: Cooling capacity enhancement due to a cascade system	54
Table 6: Values of basis cascade system, re-calculated with 500 kW	63
Table 7: Values for cascade heat exchange study	63
Table 8: Condensing pressure investigation, parameters.....	63
Table 9: Simulation parameters and selected values	66

Symbols

T	°C	temperature
ΔT	K	temperature difference
\dot{Q}	kW	heat flow
P	kW	power consumption
E	kWh/MWh	energy consumption
Ne	-	Newton-number
ρ	kg/m ³	density
n	min ⁻¹	rotational speed
d	m	diameter
Q	kWh ; kJ	heat quantity
\dot{m}	kg/s	mass flow
Δh	kJ/kg	enthalpy difference
V	m ³	volume
λ	W/m ² *K	thermal conductivity
k	W/m ² *K	heat transfer coefficient
α	W/m*K	heat transfer coefficient
s	m	thickness
t	sec	time
A	m ²	surface
c_p	kJ/kg*K	specific heat capacity
h_i	kJ/kg	enthalpy
\dot{W}	kW	specific work
w	m/s	velocity
h	m	height
h_s	kJ/kg	isentropic entropy
p_0	Pa	ambient pressure
ΔE_{xv}	kW	exergetic loss
e_{xj}	kJ/kg	specific exergy
s	kJ/kg*K	entropy

Abbreviations

COP	Coefficient of Performance
RT	room temperature
CTES	Cold thermal energy storage
CO ₂	Carbon dioxide
R744	Carbon dioxide
NH ₃	Ammonia
R717	Ammonia
R12	Dichlorodifluoromethane
N ₂	Nitrogen
HT	high temperatur
LT	low temperature
MWh	Megawatt hours
kWh	Kilowatt hour

1. Introduction

Fish, after oil, gas and metals, is the third largest export good of Norway. Mainly sold to Russia, Japan and Denmark, the demand on fresh, dried and especially frozen fish is constantly increasing. This growth requires higher cooling capacities to ensure a good and steady quality of the frozen fish during the long transport routes. Since Norway covered almost 98% of its electricity consumption with water power plants and was therefore extensively available, the development of refrigeration technologies has stagnated over the last years (1). Ecological changes and the highly fluctuating precipitation rates have a particularly strong impact on the electricity market prices. In addition, the fast increasing production rate makes an economic freezing and the production process paramount to stay competitive in long-term. Although the energy costs for one kilogram of frozen pelagic fish was only 0.12 NOK in 2008, the total costs for a 100 day season of a refrigeration plant with a 200 t capacity accumulated to 10% of the investment for an industrial plant (2). To reduce that amount, considerable efforts must be taken in exploring new and more efficient cooling processes. Only if the energy consumption can be minimized, a sustainable economy can be obtained.

In total, the amount of pelagic fish caught by *Norway Pelagic* was 828.000 t in 2013 where Herring makes up the majority with 42% (28% White Herring, 14% North Sea Herring), followed by the Blue Whiting with 24%. Fish species such as Mackerel or Capelin were also exported in large amounts (3). Due to the different sizes and cell structure of fish, it is of utmost interest to find a freezing process that can ensure a constant quality for all products. As a result, the air blast freezing process is commonly used in industrial plants for pelagic fish. Lower energy consumption also reduces the negative impact on the environment. Additionally, the greenhouse gas emissions are declined, leading to an improvement of the greenhouse effect. Political discussions about the climate change, the results and possible control approaches are nowadays held and will also lead to a change of the energy policies. The Kyoto and the Montreal Protocol already limited the emissions and the application for certain refrigerants and the use of natural refrigerants will further increase. Ammonia and CO₂ are already established in the US, Japan, and Europe and the objective must be the introduction in the Norwegian onshore industry.

2. Previous work

For achieving the target objectives of this thesis it is of utmost importance to get a broad base and a good understanding of the entire industrial process first above all. This chapter answers issues of the basic rules and physical proceedings of common air blast freezer installed in the pelagic fish industry. The discussed subjects will serve as a reference process for further interventions and are the part for the calculations, reflections and strategies performed in this thesis.

2.1 *Data measurement of current baseline*

One essential aspect of the efficiency enhancement of a refrigeration system for the pelagic fish industry is the design of the freezing tunnels where the product is frozen as fast as possible to prevent bacterial growth. Not only the evaporating pressure and temperature but also the air velocity and distribution have a big influence on the freezing process. Since air is the cooling media within the tunnel, it transports the heat of the fish to the evaporator where it is exchanged with the primary refrigerant. The better the contact of the air to the product and the better the air transport through the tunnel the higher the cooling rate and thus the quality of the product. Considering the rackets where the cartons are placed, high turbulences occur between the shelves and the product boxes. It is important to have a steady air distribution field throughout the whole tunnel, independent of the height or the place of the product, to reach a batch with constant quality.

One of the baseline freezing tunnels has been investigated in 2006 by Kristina Norne Widell. The focus of measurements was given on the temperature, the pressure and air velocity in different places of the rackets and in the products itself. The result should give a better knowledge of the flow pattern and the process for current tunnel designs in the Norwegian pelagic fish industry. The simulation models used in (4) were conducted and evaluated to get a fundamental strategy for a more efficient freezing process. It is now essential to compare the models that have been build and the measurements of freezing tunnel in the field. The results will show the accuracy of the simulation and thereby enables a much better prediction for the real fish freez-

ing process. This chapter deals with the important approach of linking theory and practice.

Divided into three sectors, a sketch of one of these tunnel sections is shown in Figure 1. Confined space between the product boxes and the shelves obstructed a proper installation of pressure sensor and consequential the data logging of the air velocity. As a consequence only the temperature profile was recorded and the flow field was simulated complementary with Airpack (see Figure 2). The pressure drop and the turbulences that occur due to the rackets and the product boxes and the corresponding uneven air distribution in the whole tunnel lead to an unfavourable freezing in areas with a low air velocity. To maintain that all boxes are frozen properly, the freezing process is conducted longer and than necessary for a consistent freezing of all products.

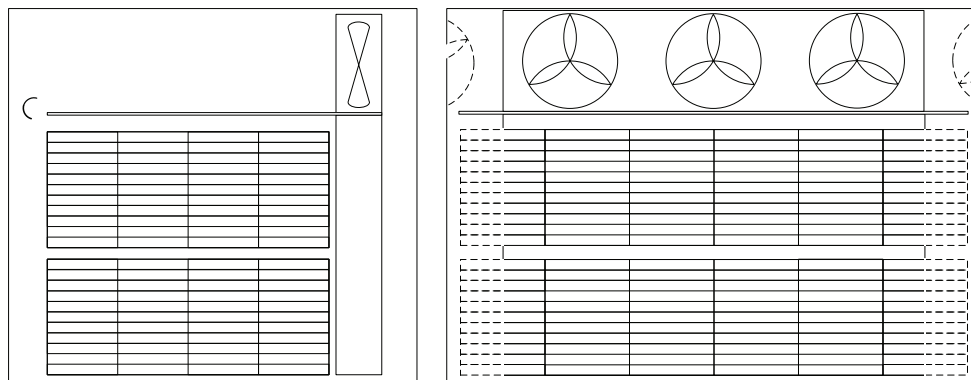


Figure 1: Freezing tunnel outline

2.2 Air flow field simulation

As a simplified 1-D model the results do not reflect reality but still essential findings for the freezing process can be made. As one result, Widell K. Found out that a guiding plate at the end of the inner ceiling helps to get a more even air distribution and especially the freezing time of the product boxes on the top shelves can be reduced what is beneficial for the freezing process. The pressure loss and the turbulences between the shelves (black patches) also reduce the air velocity and that lowers the heat transfer and the freezing rate. It should be also noticed that almost one third of the cooled air is pushed through the gap between the top shelves and the false sealing and lead back to the evaporator almost unused.

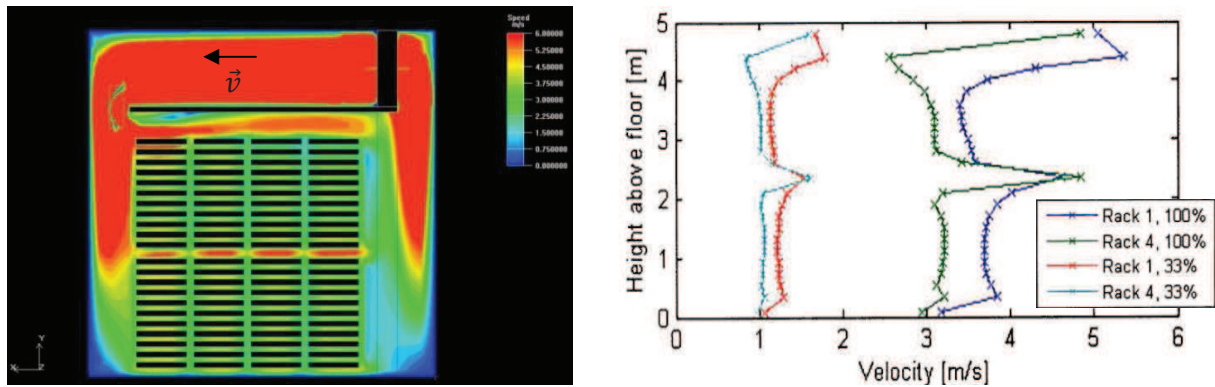


Figure 2: Air velocity distribution and values at different fan speed operations (1)

This information shows that also more investigations about the placing of such guiding plates and also the fans should be performed. More fans could increase the air velocity or lead to a more even air distribution. The heat emission of the fans is comparatively low, however at the end the significance on the total heat load increases substantially. The power consumption, calculated with $P = \frac{1}{2} * \rho_L * \pi * r^2 * v_L^3$, shows that an air speed reduction of $\frac{1}{2} v_L$ reduces the power consumption to $\frac{1}{8} P$. Since only the velocity quantity changes by a fan speed reduction (Figure 2) it can be assumed that the flow behaviour and the cooling characteristic remains the same. As a consequence a fan speed control should be proceeded in the end of the freezing period where only small heat transfer coefficients are required and a low rotational fan speed is sufficient. Commonly the evaporator fan speed is reduced to 50% of its nominal rotational speed after 9 hours of operation what brings great benefit in energy savings. Further influences of the fan speed reduction and its effects on the entire system were also discussed in (1).

2.3 Simulation element and comparison to measurements

The model that was used for the Dymola simulations is described in detail in (5) which was also used in (1). The main focus was given on the product temperature, density and the air velocity in the freezing tunnel.

Figure 3 shows the comparison of the simulation results and the measurements taken in the plant. While the simulation results are inserted as a solid line, the dashed line represents the measured values. Differences in the cooling rate between the curves may be due the simplification of the product box design or the different plac-

ing of the temperature sensors while the simulated temperature profiles were calculated in the middle of all boxes. The resulting different distance to the box wall of the sensors influenced the convective heat transfer.

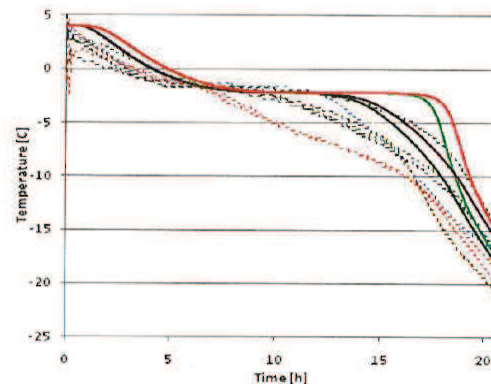


Figure 3: Measurements and simulation results (1)

Also contributing is the fact of idealized fish and the air gap between the product and the lid. The package used in the simulations also leads to a slower cooling rate. Although the simulation model shows differences compared to the actual measurements, the accuracy of the model and the calculation are sufficiently precise for further investigations. Furthermore the total energy consumption and the process time as main criteria are not affected considerable by the deviation. Nevertheless an optimized tunnel model should be constructed to improve the predictions that can be made.

Table 1 gives values for the coefficient of performance of the two-stage ammonia system and other parameters at an evaporation temperature of -38°C as a result of further simulations that were conducted in (1). These values were used later on as a reference case for the cascade system model where improvements were expected.

Table 1: Reference values of the two-stage ammonia system

	Tevap [$^{\circ}\text{C}$]	Tcond [$^{\circ}\text{C}$]	η_{compr} [-]	COP [-]
Two-stage ammonia	-38	20	0.6	1.89
Cascade (R744/R717)	-38	17	?	?

Last but not least it should be noticed that the work within this thesis is mainly focused on the system efficiency enhancement with investigations on the compressors, cascade heat exchanger as well as the condensing process. A profound investigation of the air velocity distribution in the freezing tunnel is not discussed. Changes of the tunnel design or the evaporator and the effects will be examined in further reports.

2.4 Compressor

Industrial plants always contain more compressors of different sizes of a piston and screw type to get higher flexibility and a more efficient operation. Instead of running a compressor at part load it is more efficient to shut down one compressor and run only a small unit at low required capacities. In big pelagic fish production plants with up to 10 or more compressors the energy consuming part-load for the cooling capacity regulation becomes even more important. Especially in times of part load outside the season in between October till November the plants are highly inefficient why a higher flexibility is desired. A study, specified in (4), showed that an optimized model for a system with 11 compressors could increase the COP up to 6.1% as an average value of 9 days and from 1.6% - 11.8% during the days by switching of few compressors at low heat loads. The speed regulation with a slide valve regulation is less energy efficient since some power is lost due to the loop-controlled operation. A controlled flow volume of 10% requires around 60% of the energy consumed at high speed and at 100% capacity. Energy losses are caused by the change of lower volume ratio and the higher partial friction at low rotational speeds.

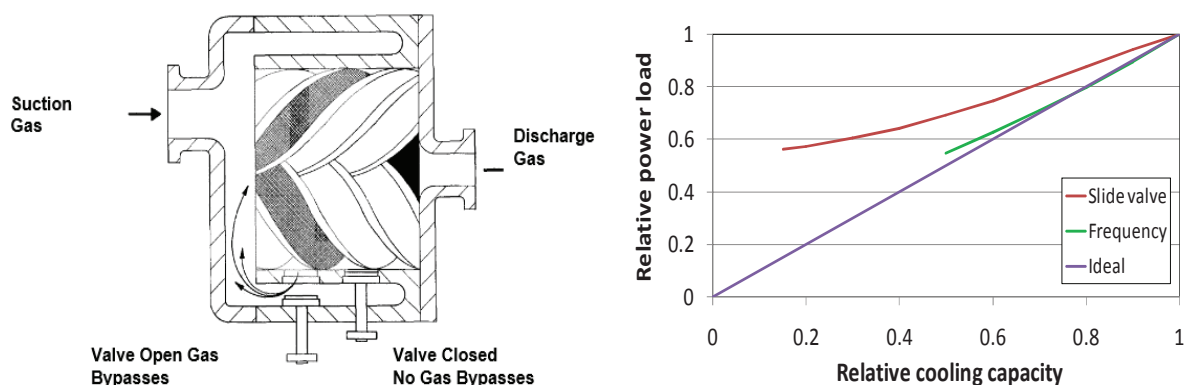


Figure 4: Speed regulation of a screw compressor (6), (1)

Regulations by a frequency drive are also common and more efficiency than the slide valve operation (Figure 4). Screw compressors with a variable speed regulation are more efficient due to adaption of the rotation speed to the load of the evaporator. The higher the cooling capacity, the faster the rotations speed of the screws. No energy is lost by venting already compressed gas back to the suction side. Especially scroll and reciprocating compressors are regulated by variable speed drive but the frequency of compression should be conducted in a certain range to prevent vibrations resulting in high noise or mechanical damage.

2.5 Maintenance of cooling fan

The freezing speed and the production quality are – beside the product box heat transfer and the air flow – mainly dependent on the heat exchange of the cold air in the freezing tunnel and the evaporator coils. Additional to the compressor the evaporator fans require also high amount of energy why the fan regulation management plays also an important role in the reduction of the energy consumption. The faster the fish is frozen, the better its quality after defrosting. This process can be speeded up for example by raising the evaporator fan speed to elevate the convective heat transport between the cooling air and the carton boxes. The total energy consumption of the fans in current plants is around 25% of the total energy use (7). In addition, at the end of the freezing period the heat emission by the fans into the tunnel can exceed the cooling load given by the products. In this case the fans are oversized and need to be slowed down. Usually the rotational speed is reduced to half of its start value after 9 – 10 hours of freezing. Investigations by switching of certain fans to avoid part load has been conducted and showed a high impact on the energy consumption. Also fan regulations of 33%, 66% respectively were performed (1).

3. Fundamentals of refrigeration systems

3.1 Thermodynamic fundamentals

3.1.1 Physical Process

Refrigeration is defined as a process of maintain desired temperatures, either the way of achieving low ambient temperatures or to freeze or cool a certain product. In both ways the diversity of application is extensively high.

However, all the refrigeration applications refer to one basic cycle realized by 4 main parts, as illustrated in Figure 5. The basic idea of a refrigeration cycle is to absorb heat from a low temperature level and to release it to a higher level, commonly the ambient pressure level. The phase change of the refrigerant and the latent heat exchange during that process is thereby utilized and brings great benefit in system efficiency.

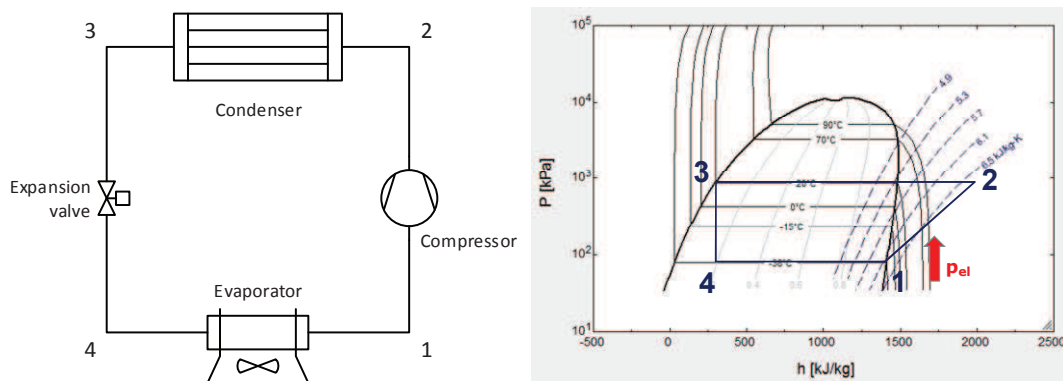


Figure 5: Simple refrigeration cycle with main components

As the only moving part the compressor provides the energy to raise the pressure up from point 1 to 2. He plays a major role in the efficiency enhancement due to its friction and volumetric losses during compression. The heat is furthermore released in the heat exchanger, isobaric cooled down and usually subcooled to increase the cooling capacity and to ensure a proper expansion from 3 to 4. The evaporator absorbs the heat, also isobaric and the cycle is closed by the compressor again. The highlighted cycle can be extended almost unlimited, related to its application form. Refrigeration systems like a gas compression followed by expansion and unrestrained expansion to the desired temperature or thermoelectric methods are differ-

ent in their design and execution. As the most common practice only the vapor compression refrigeration cycle will be described in detail within this report (8).

The pressure ratio has a direct influence on the isentropic efficiency of the compressor and their discharge temperature level. However the efficiency enhancement is limited to some restrictions, on the high pressure side by the cooling media (commonly the atmospheric temperature) and the application temperature level on the evaporator side. The volumetric and isentropic efficiency is dependent on the construction and the type of compressor. Thus the thermodynamic efficiency improving is finite for a one stage refrigeration cycle. A two stage system as shown in Figure 6 is divided into two loops, the low temperature (LT) and high temperature (HT) side. A benefit can be generated due to the lower pressure ratio for both compressors. The discharge temperature is thereby reduced what gives lower entropic energy losses and a lower thermal as well as mechanical strain on the compressor. The liquid collector serves as a separator for the vapor and liquid refrigerant.

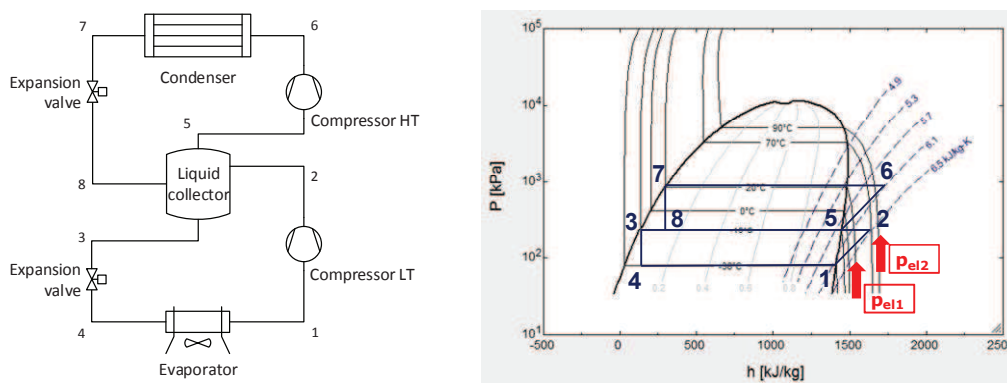


Figure 6: Two-stage refrigeration system

The LT and HT loops are physically connected together why only one refrigerant is used in that two-stage solution – resulting in a restrictive application field where deep temperatures cannot be obtained or an economic operation would not be possible. Therefore a cascade system is predestined. By separating the LT and HT cycle two different refrigerants with adequate pressure curves can be utilized and a deeper evaporation temperature can be reached. Cascade systems are e.g. applied in cryogenics where deep temperatures below -150°C compared with an economic operation are needed. Also for higher temperature levels a cascade structure can be beneficial because the cooling media can be selected specifically to its finest range of application.

For the heat transport from the LT to the HT cycle, a certain temperature difference must be realized. A higher difference would result in a higher heat flow but the work for the higher temperature elevation has a negative effect on the pressure ratio and thus the energy consumed by the compressors.

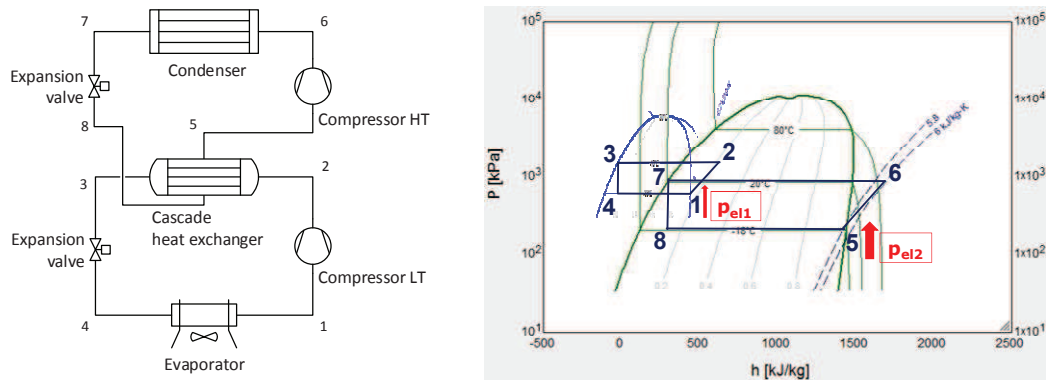


Figure 7: R717/R744 cascade system

In the next chapter the energetic and exergetic analysis for both systems – the two-stage and the cascade – are conducted to get a first impression of their potential. The results are attached at the end of the thesis in Table 1. For a comprehensive comparison also an economic appraisal must be performed since some components also differ from type, size and materials. Moreover the volumetric efficiency of the refrigerants and the resulting, reduced dimension must be considered.

3.1.2 Basic considerations and energy saving potentials

The complexity and the interaction between all components and occurring forces in a thermodynamic circuit necessitate a different design with individual parameters for each system. However there are general aspects which can be seen as basic energy enhancement strategies for every field of application.

First of all it is necessary to adjust the compressor size to the cooling needs. They should not to be oversized to avoid part-load operation at any time. A smaller compressor runs at a high rotational speed where its best efficiency is expected. Restrictions are made by the limited compressor speed for oil separation and the limitation of the condenser fan speed at high ambient temperatures. During hot seasons attention should be given on the critical point of the refrigerant to ensure an operation below the critical temperature to take advantage of the latent heat exchange. A Floating head pressure control on the condenser side brings energy savings during cold sea-

sons what keeps the pressure ratio low and thus the COP at a high level. Efficient condensing by variable fan speed should be also considered. Apart from a floating head pressure control the excess pressure within colder days could be used to defrost the evaporators by installing a blow-off valve to the compressors. Thereby the compressor runs at full-load and its highest efficiency point. The compressor efficiency is strongly depended on the pressure ratio between the suction and discharge line and also the evaporation temperature. At low temperatures the specific volume of hot gas increases and the volumetric efficiency drops. For that reason an economizer is often installed what aim to produce part of the refrigeration work on high pressure conditions. Besides lower obtained power consumptions a smaller compressor for the same cooling capacity or higher capacities for the same size can be realized. The oil recirculation management is also important: while a low oil level in the compressor can lead to mechanical damages, the physical and thermodynamic properties of the refrigerant are influenced negatively. When oil is carried into the heat exchangers, it leads to losses up to 30% in the heat transfer. Oil also accumulates in parts of low velocity and can be dragged away abruptly by the refrigerant. That can lead to fluid slugging in the compressors with irreversible damage (9).

Regular defrosting and cleaning of the heat exchangers during all seasons must also be part of an efficient operation to ensure a sufficient heat intake and output. Conventional defrosting with electrical heating devices are time and energy consuming while nowadays hot gas defrosting is state of the art. In current pelagic freezing plants where sea water is used as coolant the condensers are installed at 150 – 170 m depth in the ocean where a dark environment lowers the bacteria growth and cleaning of the fins is usually not required.

Besides the internal energy recovery of the compressor waste heat for superheating or defrosting purposes the thermal discharge of the condensers could also be used for heating as an elevation of the ambient temperature to increase the exergetic use of a thermal heat pump by increasing the COP defined by $\epsilon_{HP} = \frac{T_h}{T_h - T_{amb}}$ or for the air preheating used in an Organic Rankine Cycle.

3.1.2.1 Superheating

Superheating is conducted to prevent damage of the compressors due to liquid drops or cavitation and to increase the cooling capacity if happened in the evaporator. An internal heat exchanger affects the superheating and the subcooling positively. Longer pipes of the compressor suction line also bring a higher superheating rate. Removing the insulation of the piping must not be performed since humidity would condense on the outer pipe radius and freeze what impairs the effects of superheating. Superheating suppression is a way to increase the condensing efficiency by 6 – 12% by injection liquid refrigerant of the liquid evaporator suction line into the discharge line of the compressor. The superheated vapour is pre-cooled and the available condenser volume is increased (10).

3.1.2.2 Subcooling

Subcooling not only affects the cooling capacity but is also used for preventing vapour flash gas in the liquid line and a damage of the expansion valve. Therefore also pressure drops and resulting pre-flashing in the filter dryer, sight glasses, valves and the pipe systems need to be avoided. An installed liquid receiver holds the liquid-vapour mixture back and prevents a capacity and efficiency drop. Subcooling methods can be internal heat exchanger or a slight pressure increase of the liquid line by installing a small circulation pump. Sensible ambient subcooling and a higher refrigeration load are not common since less condenser volume is available for the latent heat exchange and an efficiency drop must be expected (10).

3.1.3 Energetic analysis

Based on the **Firs Law of Thermodynamics** the entire refrigeration process can be seen as one control volume. The mathematical expression is given with:

$$\frac{dE}{dt} = \sum_j^n \left[\left(z * g + \frac{w^2}{2} + h \right)_j * \dot{m}_i \right] + \sum_k^n \left[\left(z * g + \frac{w^2}{2} + h \right)_k * \dot{m}_o \right] + \dot{Q} - \dot{W}$$

For vapor compressor refrigeration processes the kinetic and potential energy can be neglected ($z = 0$; $w = 0$). Moreover the process can be assumed as Steady State ($\frac{dE}{dt} = 0$). Thus the equation becomes

$$\dot{Q} - \dot{W} = \sum_k^n h_k * \dot{m}_o - \sum_j^n h_j * \dot{m}_i$$

for each component of the system as a single control volume. As a closed cycle, the input and output mass flow off each component remains constant and the equation results to

$$\dot{Q} - \dot{W} = \dot{m} * \left(\sum_k^n h_k - \sum_j^n h_j \right)$$

1] Compressor (including the non adiabatic heat loss):

$$\dot{W}_{12} = \dot{m} * (h_2 - h_1) + \dot{Q}_s$$

$$\dot{Q}_s = \dot{m} * (h_2 - h_{2s})$$

2] Condenser:

$$\dot{Q}_{23} = \dot{m} * (h_3 - h_2)$$

3] Expansion unit (isenthalpic process):

$$\dot{m} * h_2 = \dot{m} * h_3$$

4] Evaporator:

$$\dot{Q}_{41} = \dot{m} * (h_1 - h_4)$$

(11).

Considering the **Second Law of Thermodynamics**, the entropy generation within the system can be determined.

$$\dot{S} = \frac{dS}{dt} + \sum_k^n (s_k * \dot{m}_i) - \sum_j^n (s_j * \dot{m}_i) - \sum_l^n \left(\frac{\dot{Q}_l}{T_l} \right)$$

Where in a steady state process the term $\frac{dS}{dt} = 0$.

1] Compressor:

$$\dot{S}_{12} = \dot{m} * (s_2 - s_1) + \frac{|\dot{Q}_{12}|}{T_{\text{amb}}}$$

2] Condenser:

$$\dot{S}_{23} = \dot{m} * (s_3 - s_2) + \frac{|\dot{Q}_{23}|}{T_{\text{amb}}}$$

3] Expansion unit:

$$\dot{S}_{34} = \dot{m} * (s_4 - s_3)$$

4] Evaporator:

$$\dot{S}_{41} = \dot{m} * (s_1 - s_4) + \frac{|\dot{Q}_{41}|}{T_0}$$

(11)

3.1.4 Exergetic analysis

To determine the losses and the effective work that is achieved by the system, it is more accurate to use the exergetic analysis as a further approach. As an established equation the **exergetic balance equation** of a control volume is:

$$\frac{dE_x}{dt} = \sum_m \dot{E}_{x,m} - \left(\sum_k \dot{W}_k - p_o * \frac{dV}{dt} \right) + \sum_j (e_{x,j} * \dot{m}_j) - \sum_l (e_{x,l} * \dot{m}_l) - \Delta \dot{E}_{xv}$$

As the system is in steady state, the equation becomes $\frac{dE_x}{dt} = 0$, as well as the term that describes the interaction with the ambient pressure $p_o * \frac{dV}{dt} = 0$, for a closed system.

$$\Delta \dot{E}_{xv} = \sum_m \dot{E}_{x,m} - \sum_k \dot{W}_k + \sum_j (e_{x,j} * \dot{m}_j) - \sum_l (e_{x,l} * \dot{m}_l)$$

With the specific exergy of the refrigerant,

$$e_x = (h - h_0) - T_0 * (s - s_0)$$

The equation can be adjusted to each element of the process, considering $\dot{m}_o = \dot{m}_i$.

1] Compressor

Exergy refrigerant:

$$\Delta \dot{E}_{x,12} = \dot{m} * [h_2 - h_1 - T_a * (s_2 - s_1)]$$

Exergy loss total:

$$\Delta \dot{E}_{x,comp} = |P_{el}| - \Delta \dot{E}_{x,12}$$

2] Condenser

Exergy refrigerant:

$$\Delta \dot{E}_{x,23} = \dot{m} * [h_3 - h_2 - T_a * (s_3 - s_2)]$$

Exergy output:

$$\Delta \dot{E}_{x,NH3} = \dot{m}_{NH3} * c_{p,NH3} * \left[T_{NH3,o} - T_{NH3,i} - T_a * \ln \left(\frac{T_{NH3,o}}{T_{NH3,i}} \right) \right]$$

Exergy loss condenser:

$$\Delta \dot{E}_{x,cond} = |\Delta \dot{E}_{x,23}| - \Delta \dot{E}_{x,NH3}$$

3] Expansion valve loss:

$$\Delta \dot{E}_{x,34} = \dot{m} * [h_3 - h_2 - T_a * (s_3 - s_2)]$$

4] Evaporator

Exergy refrigerant:

$$\Delta \dot{E}_{x,41} = \dot{m} * [h_1 - h_4 - T_a * (s_1 - s_4)]$$

Exergy input freezing tunnel:

$$\Delta \dot{E}_{x,ft} = \dot{m}_l * c_{p,l} * \left[T_{l,o} - T_{l,i} - T_a * \ln \left(\frac{T_{l,o}}{T_{l,i}} \right) \right]$$

Exergy loss evaporator:

$$\Delta \dot{E}_{x,evap} = |\Delta \dot{E}_{x,41}| - \Delta \dot{E}_{x,ft}$$

5] Exergy balance of the total refrigeration cycle (steady state):

$$\sum_i \dot{E}_x = \Delta \dot{E}_{x,12} + \Delta \dot{E}_{x,23} + \Delta \dot{E}_{x,34} + \Delta \dot{E}_{x,41} = 0$$

The conducted calculations include some simplifications that are listed beneath. Anyway the equations are valid for each particular cycle and emphasize the energetic and exergetic difference between the systems more explicit.

1. The pressure losses of the pipes, connection fittings and the principal components are neglected
2. Ambient temperature is assumed with $T_{\text{amb}} = 10^\circ\text{C}$
3. The calculations are made for a subcooling of 3K
4. Overheating of the refrigerant in the high temperature cycle is given with 3K
5. Other conditions are set as saturated gas
6. Expansion valves are assumed as isenthalpic components ($\Delta h = 0$)
7. A perfect insulation off all pipes and connection parts is assumed
8. The temperature difference of the heat exchange is given with 7K for the condensing unit to ambient air and 3K in the cascade heat exchanger and the evaporator, respectively (11)

3.2 Refrigerants

Increasingly stringent environmental standards require even higher efforts on developing new refrigeration systems. After limiting ozone depleting substances as Chlorofluorocarbons (CFCs) by the Montreal Protocol in the 1987, the Kyoto Protocol of 1997 sets new standards in the policy against the global warming. Greenhouse gases, especially the strong Hydro fluorocarbons (HFCs) were reduced (12). Subsequent new refrigerants were tested and introduced into the refrigeration industry. Particularly the natural refrigerants as hydrocarbons, ammonia (R717), CO₂ (R744), water (R718) and air has increased over time.

The indirect emissions of refrigeration systems that cause the global warming are stated with over 80% while only 20% are due to direct emission as leakages or losses while filling or refilling of systems. Besides 15% of the world-wide energy consume is used for refrigeration. Although the leakage rate is limited e.g. in the Euro-

pean F-gas regulation of 2007 and the direct emissions caused by coolants is comparatively low, the growth of natural refrigerants is still increasing in large scale applications as well as for the private use in refrigerators and air conditioners. Not only the low global warming potential (GWP) and ozone depletion potential (ODP) but also the high efficiency, the good availability and the low costs contribute to a wide range of utilization. However a refrigerant does not match all the requirements of a cooling device and its use must fit to the physical properties (13).

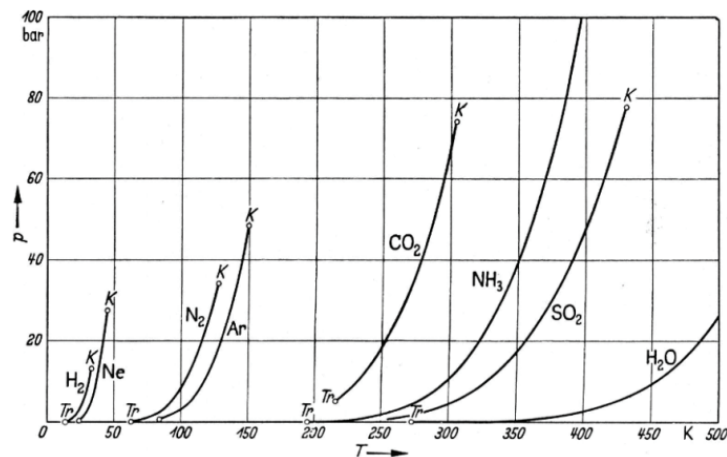


Figure 8: Pressure curve of different refrigerants (14)

Figure 8 shows different pressure curves for different natural refrigerants. Ammonia has a wide field of application but is not applicable at low temperature where carbon dioxide can be used. Water is predestined for higher temperatures above its freezing point of 0°C. Nowadays mainly ammonia and CO₂ are used for cooling purposes in the food industry like supermarket, big freezing plants or ware houses.

3.2.1 Ammonia

Ammonia, also known as R717, is worldwide used mainly in big refrigeration systems. First of all ammonia is extensively available and thus cheap to obtain. The second point is its wide pressure curve what makes it attractive for many industrial applications. Moreover ammonia has no bad influence on the environment; the global warming potential (GWP) and the ozone depletion potential (ODP) is zero. It is known that R717 has the highest efficiency above all natural refrigerants because of its high evaporation enthalpy of 1359 kJ/kg at -30°C. Since ammonia is toxic and can cause irritations of respiratory passages up to respiratory arrest or death in very high concentrations, there are crucial safety aspects that must be considered. In addition

ammonia is also flammable and explosive in highly concentrations in air. In case of critical overpressure or an accidental release a surge tank can absorb a certain amount of ammonia to provide reasonable assurance. Limitations in the material selection are given by the corrosive properties of ammonia and copper or copper alloys (14).

3.2.2 Carbon dioxide

Carbon dioxide is a promising alternative to volatile refrigerants especially in two-stage systems as low temperature fluid. Two considerable advantages can be adduced as reasons for the prevalence of CO₂ (R744) in supermarkets and many different applications. First of all the volumetric cooling capacity or the high specific volume of vapour is 5 to 8 times higher than other common refrigerants what leads to smaller system components – in particular the compressor and frequency inverter are expensive. Also the insulation of the pipe system can be realized smaller with the same heat transfer coefficient due to the reduced pipe diameter. The heat exchangers can be constructed smaller because of the high heat transfer or the temperature difference can be minimized, respectively (15). Moreover the refrigeration charge can be reduced due to better heat transfer. This brings great benefit in the energy use of the compressor – up to 5% of the energy needed at a high pressure ratio in different cooling systems (16). On the other side CO₂ is operated at high pressures why components must be designed more solid what reduces the benefit of the good specific volume. The reason of a high pressure operation makes the system less susceptible for pressure losses and high temperature drops. Carbon dioxide is harmless and no product spoilage in case of an outcome into the cooling occurs. At low temperatures at -40°C and even lower CO₂ involves a greater ease of operation and it is more efficient than ammonia. Below -33°C ammonia is operated down ambient pressures and thus air and humidity enters into the refrigeration system. At high ambient temperatures systems are operated transcritical in reason of the low critical point of CO₂. what decreases the system efficiency. Certainly CO₂ forms acid in contact with water why the installation of dry filters is very important. Dry ice formation and resulting clogging must be avoided in any case. Especially in big refrigeration systems with high cooling capacities dry ice formation in the liquid receiver can be caused by big compressors at low cooling loads. Accordingly small compressor units are required for a high flexibility. Also an idle state unit for temperatures around -25°C is compulsory because of

the occurring high pressures. Besides, R744 can be easily evacuated by a blow off valve as it is non hazardous, has an ozone depletion potential of zero and a global warming potential of 1 (15).

4. Refrigeration systems within the pelagic industry

The world-wide increasing demand of fish in a wide range, either fresh or frozen, necessitates also different production processes matching the requirements of high quality and a high uptime combined with fish species of different shape and ingredients. While in the past the main demand on fish products was on fish oil and fish meal, nowadays more high quality filets are desired and exported. Whereas in 1992 270.000 tons of pelagic fish was delivered, the demand increased within one year to 300.000 tons in 1993 and further increased to around 830.000 t in 2013 only by *Norway Pelagic AS*. Besides Mackerel or Capelin the main caught fish is herring with 42% (28% White Herring, 14% North Sea Herring), followed by the Blue Whiting with 24% (3). Pelagic fish is usually caught by purse seining to prevent cell damage. Further vacuum pumped to cause less strain to fish surface. It is furthermore chilled in refrigerated sea water tanks. The time from catching to the final onshore freezing is usually between 1 – 2 days and is kept as low as possible. After catching and storing in big vessels the fish is either processed entirely offshore or only gutted and packed and afterwards brought onshore directly into the freezing tunnels. Although consumer habits changed to a desired best quality, more efficient freezing processes needs to be established to generate competitive prices. Not only the product size varies but also the cell structure and composition of the fish are unique and the freezing and storing conditions need to be different for each fish to avoid a quality loss.

4.1 Considerations of freezing fish

Due to its specific environment fish in general has different muscles and cell structures compared to mammals. Their muscle fibers are not strongly linked together what results in low muscle strength and therefore fish must be handled with care. By applying to much pressure or mechanical stress, the fish cells break apart – so called “gapping” (17) – and the quality and the taste suffer. A fast freezing and low storing temperatures of -35°C to -40°C are desired to avoid rancidity what can occur even at common temperature levels of -25°C to -30°C (18). The primary fish temperature is around 4°C . At first, the freezing point of meat or fish is reduced due to the containing salts, proteins and solutes. After the initial freezing point of (-2.2° for mackerel), the

freezing speed slows down in result of solutes that agglomerate in the fresh parts of the fish.

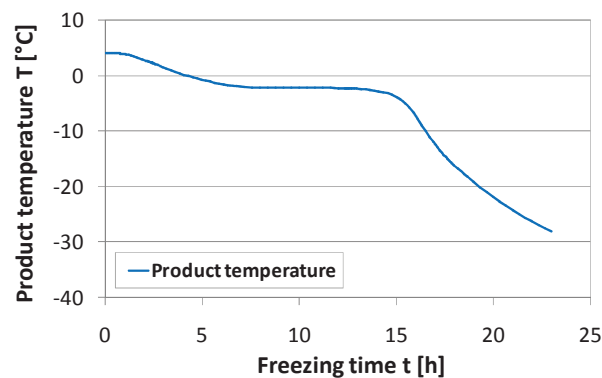


Figure 9: Product cooling curve

A procedure of freezing mackerels is given in Figure 9. The beginning freezing period is followed by a lower temperature drop. The product temperature remains constant in theory due to the latent heat removal of water. However there are many parameters that influence the cooling curve as the thermal conductivity, diffusivity, the specific heat or the enthalpy. These time and location-dependent values make it difficult to calculate the exact freezing procedure and Plank's equation only considers the phase change period and also the modifications can only give limited statements (18). In addition to the product properties the packing is highly important for a fast freezing rate. Especially the air gap between the fish and the package containing the packaging film and the carton box slow down the procedure. The air temperature and the humidity also make a contribution. In contrast to the refrigeration system that supplies the cooling medium and is discussed explicitly within this report, the mentioned considerations are described extensively by others and will be not included in the following work. Conclusively it can be said that the faster the fish is frozen and stored at deeper temperature levels, the better the quality after thawing the fish. The quick-freezing results in a slower ice crystal growth with many small crystals and a lower damage of the fish cells. As a result the vitamins and minerals are trapped so that the fish shall be considered as fresh fish (19).

4.2 Application and usage in contemporary industry

As so far, there are different freezing methods based on different refrigerants or physical processes and the selection of the one that matches the desired application

the best way is complicated. Beside the cooling load, the freezing time and the final state temperate, the process needs to be investigated for its investment and variable costs such as laboring, energy consumption and the shrinkage – due to structure damage or dry-out – during the process. Also the feasibility for a certain location must be checked (20). The major processes used in industry are:

- Contact freezer
- Blast freezer
- Immersion freezer

For this work only the blast freezer is relevant and described later in more detail. However the results discussed in Chapter 6 can be also applied for contact and immersion freezers since the background of the refrigeration system is the same.

4.2.1 Contact freezer

As the name implies, the principle of contact freezing is the direct contact of freezing plates that contain the primary refrigerant and the product. A second refrigerant as air is not used. For a better heat transfer between the pates and the fish, the plates are compressed hydraulically. In case of a proper proceeding, the contact freezing brings great benefits in the freezing time due to the high heat removal rate. High energy efficiency is given from the missing secondary refrigerant and the additional fans and circulation devices that are redundant.

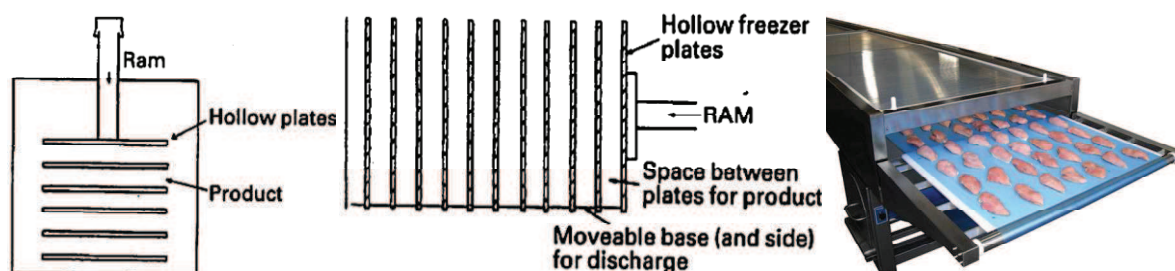


Figure 10: Horizontal (left) and vertical (right) contact freezing (21)

A part from the efficient freezing procedure, the laboring for the loading and unloading of the freezer is costly and time consuming. To keep the heat transfer as high as possible, air gaps between the fish filets or the plates must be avoided. If the air is trapped it serves as a good insulation parameter. In some cases the fish batches are filled with water or are vacuum-packed. A way to improve the laboring time is given with a polythene lined paper to prevent the frozen package from sticking on the

plates what makes the reloading process more difficult and lasting. Furthermore, after each freezing period it is necessary to clean the plates that are usually made of aluminum or stainless steel, from ice particles and residuals to maintain the advantages of a fast freezing process. This operation meets all the food sanitation requirements since no additive is used and is suitable for freezing aquatic, food, vegetable and fruit, meat, etc. (17). While the vertical plate freezer is used in offshore applications the horizontal concept can be found in onshore plants where more space is available.

4.2.2 Blast freezing

As companies like Northern Pelagic catches and provide many different kind of fish, a flexible process method that can also handle huge capacities in a short period are required. Packed in boxes for 20 or 25 kg the products are therefore frozen in big air blast freezing tunnels where the air is recirculated by installed fans. Easy to stack in rackets the tunnel is refilled once a day and frozen in 16 – 20 hours. Current one stage and two-stage ammonia systems are designed for batches of 200 t and an installed total cooling capacity of 1.200 kW. Usually divided into 4 blast freezing tunnels each tunnel can store between 45 – 70 t of fish. The batch process takes one day where the logistic work for maintaining, reloading with fresh fish and the startup time take between 4 and 6 hours. A typical evaporation temperature is -42°C . Lower temperatures are not applicable since the pressure on the evaporator side decreases too much and the pressure ratio and thereby the isentropic compressor efficiency would drop significantly (2). Due to the uneven freezing process of the products on different shelves and rackets, the frozen state of fish needs to be checked before taking out of the tunnel. That is done by random sampling according to empiric values where the longest freezing rate is expected.



Figure 11: Product box, freezing tunnel and air flow simulation with Airpak (1), (17)

The disadvantage of a lower heat transfer coefficient due to the package is one big issue that must be mastered in future. Especially the heat transfer through the lid of the boxes what represents the highest thermal resistance must be improved to fasten the freezing process. Tests with varied perforation in the box lid were performed and showed great impact in the freezing time reduction but were not realized yet since the stability of the carton boxes was reduced. As a consequence the storage was more laborious and the desiccation during freezing increased. Additionally simulations and practical tests with higher air velocities were also performed. An elevation from 2 – 9 m/s resulted in a 4 hours faster freezing what is one way to enhance the efficiency and capacity of an air blast freezer. Nonetheless new methods must be investigated and tested for the future trends of a demand on a high quality product in numerous amounts (7).

4.2.3 Immersion freezing

Rather unconventional freezing methods like the immersion freezing are less well-established in the pelagic fish industry and moreover used for small products like prawn or shrimps. Tuna is also completely frozen in salt brine since it only absorbs a less amount of salt what is unproblematic with regards on taste or quality (21). Brines like propylene glycol, glycerol or sugar are also used in some applications but it is difficult to find a cooling agent that matches the properties of the product. A big advantage of immersion freezing is the rapid freezing rate since no air is used as coolant and the heat transfer is increased (20). As an application with an R12 immersion sprayer the product surface is first hardened, afterwards frozen completely in the refrigerant tank and transported to further production steps (Figure 12). Excess refrigerant is lead back to the tank and keeps the losses at a minimum. A more costly process method is the immersion with liquid N₂ at temperatures around -196°C for prawns or small products. Pre-cooled it is conveyed into the freezing section where it gets in direct contact with the liquid N₂. The nitrogen is evaporated and the heat removed completely in the tempering zone.

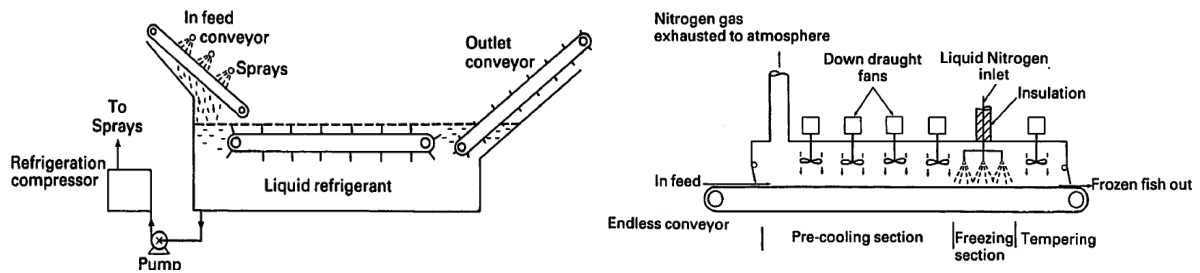


Figure 12: Immersion spray – and liquid N₂ immersion freezer (21)

Since the liquid nitrogen evaporates and is released into the atmosphere after pre-cooling of the fresh products, the refrigerant losses are high what results in high running costs. Contrary to that, the investment and maintaining costs are low as the only moving part is the conveyor and the circulation fans. The low temperatures and fast freezing make that method furthermore attractive. Glazing with water after freezing is a usual way to increase the quality during storage.

4.3 Development and future trends

An example of a highly developed one-stage ammonia system design for storing purposes was built by *Portland General Electric (PGE)* as a “Super-efficient refrigerated warehouse”. With a ground surface of 135.000 m² and 950 kWh cooling capacity the location shows relevance to the size of the pelagic fish industry. Besides enhancement strategies as a variable speed screw compressors or a floating suction device, the condensing unit was equipped with a floating head pressure that reduces the condensing pressure during cold seasons. Variable speed regulation of the fans and an efficient hot gas defrosting were installed and also contribute to lower energy consumption. Those wide-spread improvements are combined with installed LED-lighting equipped with motion sensors that uses 80% less energy. The screw compressor-unit with variable speed drive is supported by Photovoltaic panels that cover the power consumption up to 70%. In total the annual energy savings of the industrial plant are 3.4 GWh what brings a 60% higher efficiency than the base case in 2013 (22). This instance shows that it is also necessary to focus on the entire plant and not only the actual freezing or storing process but also on unconventional methods to reach a state of a high developed industrial plant what should be today’s state of the art.

Consume is rising and vessels getting bigger and are planned for capacities up to 1.200 tons. Therefore higher storing capacities must be realized and new concepts investigated and tested for future projects. The enhancement of current refrigeration systems is limited so that is only a short-term solution. The limiting space available on big trawlers and vessel as well as current on-shore plants also needs higher efforts on more compact solutions with higher production capacities.

A/S Dybvad Stål Industri is a supplier of manually-operated and automatic plate freezers for onshore and offshore applications. The first CO₂/NH₃ cascade system for plate freezers has been established on the large fishing vessel *MS Kvannøy* in 2002 with a total capacity of 1350 kW (23). Thereby the freezing capacity could be increased by 4 – 8% at -40°C and up to 30-40% at temperatures around -50°C, resulting in reduced fuel costs. Due to the high volumetric efficiency of CO₂ the plate freezer volume was reduced and higher production rates were obtained. After all that cascade system was implemented in offshore applications by different manufacturers like *NORSK KULDE*, *GEA Refrigeration* or *Johnson Control* (24).

Where such systems running with CO₂/NH₃ are nowadays used in huge trawlers, an on-shore application for the pelagic fish industry has not been realized in Norway till now (2). However many cascade systems have been established in the industry in supermarkets in the US, Japan and whole Europe and on a poultry plant in Denmark and can be seen as state of the art for those applications (15). It is also discussed to use CO₂ as brine what becomes interesting with its good food compatibility as a natural, non hazardous coolant. The lower achievable temperature compared to brines with sodium chloride or glycol also contributes to that fact. Using CO₂ in an indirect hot gas defrosting system was also considered and realized on the *MS Kvannøy*. As offshore freezing brings restrictions in the product quality, offshore catching and on-shore freezing should be always considered. Therefore a cascade system using CO₂/NH₃ is predestined for those applications.

5. Material and methods

The aim of this thesis was the dimensioning of a high efficient refrigeration system for a given freezing tunnel by *Northern Pelagic AS*. Within the calculations of Chapter 3, the CO₂/NH₃ cascade system was predetermined and showed the highest system efficiency. However this is only a rough theoretical approach for a steady state with many simplifications and restrictions and must be still confirmed by simulations for transient processes. The system was designed by the following boundary conditions:

Table 2: Specified boundary conditions by *Northern Pelagic AS*

Freezing tunnel capacity	100.000 kg
Installed cooling capacity	500 kW
Evaporation temperature	-38°C
Freezing process time	18 h
Sea water inlet temperature	10°C

As a tool for the simulations the objective-oriented, declarative language *Modelica* was used. Applied with the simulation environment *Dymola (Dassault Systemes AB)* the cascade model was an enlarged cycle of the set-up by Walnum H. and Andresen T. which was also used for the simulations of Chapter 2 (5). The freezing tunnel, primary realized for a 375 kW plant was scaled up to a bigger capacity. The draft of the rackets was accepted. Two refrigeration concepts were investigated and both results will be compared later on in this report. While the cascade system investigation was also part of this work, the two-stage ammonia system with an open intercooler (1) was analyzed by Stavset O.. These examination results are shown below in Table 3.

Table 3: Reference values, two-stage ammonia system

Parameter	Symbol	Unit	Value
Energy consumption	E	MWh	4.124
Freezing time	t	h	18
Cooling capacity	\dot{Q}	kW	600
HT compressor size	V	cm ³	6533.43
LT compressor size	V	cm ³	19454.9
Coefficient of Performane	COO	-	1.85

The freezing time of 18 hours is defined by daily production process and the 4 – 6 hours of labor time for refilling the tunnel with fresh products. The demanded cooling capacity of 500 kW could not ensure the frozen state of all products within 18 hours so a bigger system had to be designed with a 600 kW capacity. A corresponding adjustment of the compressor sizes for a maximum rotational speed of 1450 min^{-1} for the low and high temperature cycle was also conducted by Stavset O.. The energy consumption of around 4.1 MWh includes also the cooling fan of the evaporator and the sea water cooling pump with a mass flow rate of 12 kg/s and a pressure head of 2.2 bar (22 m).

5.1 NH_3/CO_2 cascade system

The idea is to implement a two-stage-system using NH_3/CO_2 instead of a regular one-stage-system with NH_3 as refrigerant. That system can take advantage of ammonia and its environmental qualities, combined with the good preferences of CO_2 at low temperatures (25). Two main advantages of using CO_2 as a refrigerant at low temperatures are described as followed:

5.1.1 Simulation model

The cascade refrigeration cycle was realized as followed, see Figure 13. On the basis of the model, described in 2.3 and set up by Walnum H., Andresen T., Widell K. (5), the cycle was extended and tailor-made to the pre-calculated R744/R717 cascade system. To get a common platform for a better understanding and comparability to the reference model of 2.3 most parts remain unchanged. The evaporator design was given by the tunnel dimensions and the space available for the evaporator installation. Since the evaporation pressure was defined by the desired evaporation temperature of -38°C the only degree of freedom was the refrigeration mass flow given by the refrigeration pump. The model for the freezing tunnel cycle including the fish and fan component was part of the demanded specifications and was not modified.

The liquid receiver of the ammonia cycle as well as the liquid separator of the low temperature cycle was designed according to experience values. The heat exchanger for the condensing unit and the cascade heat exchanger were considered as a shell and tube type while the evaporator was typically a flooded fin and tube heat exchanger design. A refrigeration pump ensured the liquid refrigerant state in all times.

Moreover the product boxes were design as a 100 kg fish box, one for each shelf. Differentiated into 5 layers included the heat transfer coefficients values for the fish, vacuum package, air gap between the fish and the box and the casing, the design is still simplified compared to the 5 times 20 kg boxes used in the plant.

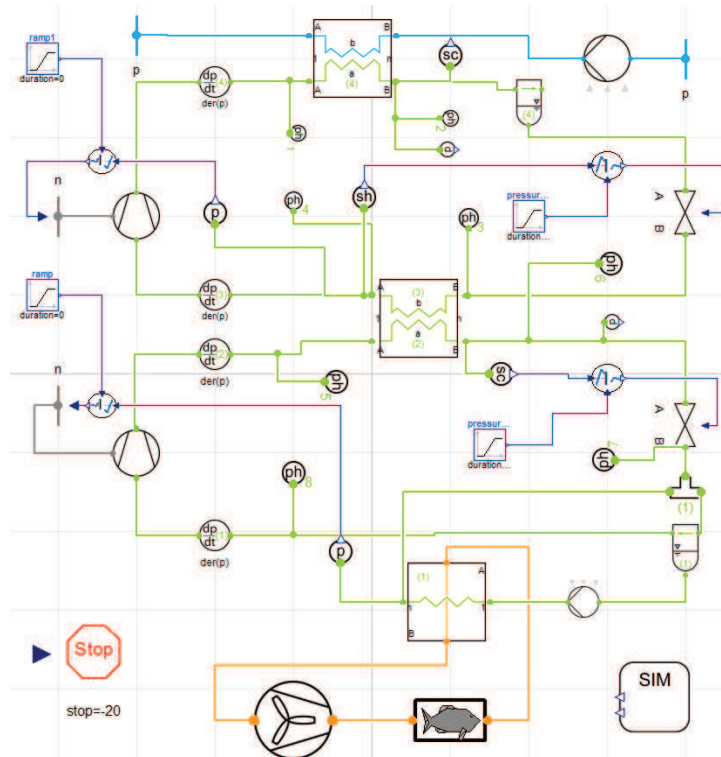


Figure 13: Dymola, NH_3/CO_2 cascade model

A static head for the sea water cooling pump was assumed with 22 m or a 2.2 bar pressure loss as commonly prevalent in refrigeration systems (2). It should be taken into account that the additional power consumption of these pumps must not exceed the positive impact on the condensing pressure and thereby the reduced power consumption of the ammonia compressor and total benefit in the energy consumption. As mentioned previously, only few changes of the cycle parameters were changed and listed in Table 4. Also attached are a simulation schedule and a list of the input parameters that were varied during the simulations to examine their influence on the output results (especially the freezing time). The main focus of the cascade performance was given on the improvement of the power consumption and the energy consumption, respectively, along with the time reduction of the freezing process. Since the freezing process is meant for a certain batch proceeding the latter gets only important if the time can be cut at least half. Whereas that did not appear to sound

practice the importance of a lower energy consume become more important in the result discussion.

Table 4: Variable simulation parameters

Parameter	Symbol
Heat exchanger size	L
NH ₃ superheating	K
CO ₂ subcooling	K
Suction volume	
CO ₂ /NH ₃ compressor	m ³
Heat exchanger size	L
Sea water mass flow	kg/s
Refrigeration mass flow	kg/s
Suction volume	m ³

5.1.1.1 Modifications

In reason of a significant long simulation time, the cascade model was modified by the following progress:

- The heat exchanger nodes were reduced from $n = 15$ to 5.
- The pressure loss according to Konakov was changed to constant pressure model with $\Delta p = 0$ bar
- A boundary element included in the freezing tunnel for a constant pressure of 1.013 bar, a humidity of 60% and a constant enthalpy of 350 kJ/kg was removed
- The compressor regulation time was extended from $\tau = 10$ to $\tau = 100$
- The integration tolerance for the simulation process was increased from 0.0001 to a value of 0.001

After setting these new values the output of the new model was verified with the reference model to ensure a proper functionality. Since the cascade model was established without a pressure loss boundary element in the evaporator the results showed a variation of around 1% compared to the reference of the two-stage ammonia system. After all this deviation due to the model changes had to be considered in the result discussion and the evaluation of both systems.

5.1.1.2 Components

The components were chosen as followed:

- 1) Evaporator: flooded fin and tube heat exchanger model, cross flow
- 2) Cascade heat exchanger: Tube and tube heat exchanger, cross flow. The evaporation temperature for ammonia was chosen with -18°C and a correlating CO_2 condensing pressure of -15°C according to (26) what was determined for the highest system efficiency.
- 3) Condenser: Tube and tube heat exchanger: cross flow
- 4) HT compressor efficiency is calculated by the pressure difference in each time step
- 5) LT compressor is given with a constant isentropic efficiency of 0.7
- 6) Circulation pumps with constant efficiencies according to KSB data sheets (see attachments)

5.1.2 Problem definition of the air and water intake

As mentioned in chapter 3.2.1, ammonia as a natural refrigerant brings many benefits to a refrigeration system. However, there are some restrictions that should be considered in using ammonia especially at low temperatures. When used at temperatures below -33.44°C the working fluid pressure exceeds the atmospheric pressure of 1,013 bar. Operated as a vacuumized evaporator the low pressure side must be sealed hermetically to avoid the entry of air and water vapor into the system. While the water sets in the evaporator unit, the air accumulates in the high pressure side in the condenser and leads to a lower heat transfer coefficient k and thus to a decreasing heat dissipation. To ensure a proper heat removal according to the equation $\dot{Q} = k * A * \theta_{ml}$ the logarithmic temperature difference must be raised for a constant heat exchanger surface A . Resulting in a higher condensing pressure, the pressure ratio is increased and the system efficiency is drops substantially. In practical applications ammonia operation under vacuum are performed but a certain energy loss cannot be avoided completely what necessitates certain arrangements to ensure a high efficiency at temperatures below -33°C . As a well known problem, different solutions have been discussed and tested like an air separator or a pressure release valve. Since the air accumulates at the highest points of the system, the placing of those installations is of crucial importance. The intake of water into the low pressure

side of the system is not a big issue and is removed occasionally by a drainage system (27).

5.1.3 Pressure loss and hydraulic adjustment of the evaporator

A second advantage of using CO₂ as primary refrigerant is linked with the high pressure state at low temperatures. Considering the pressure loss in the evaporator only a low temperature drop can be expected. For a comparison of both refrigerants the pressure drop within the heat exchanger need to be calculated. Therefore a common fin and tube heat exchanger of FINCOIL/Alfa Laval and the illustration of the occurring pressure losses in the piping are shown in Figure 14. The evaporator is divided into a low and high section where the refrigerant flow is shown in blue and red respectively. The length of 6.53 m and a total height of 5 m are suited to the freezing tunnel dimensions of Northern Pelagic and thus the static head comes to 1.75 m. The two-phase flow as occurring in the evaporator is dependent on three different factors: the static pressure Δp_G due to the gravity, the hydraulic pressure Δp_f due to the friction of the wall and the pressure loss due to the change in momentum of both states, the liquid and gas phase, what is not considered in the following, simplified pressure drop calculations (28).

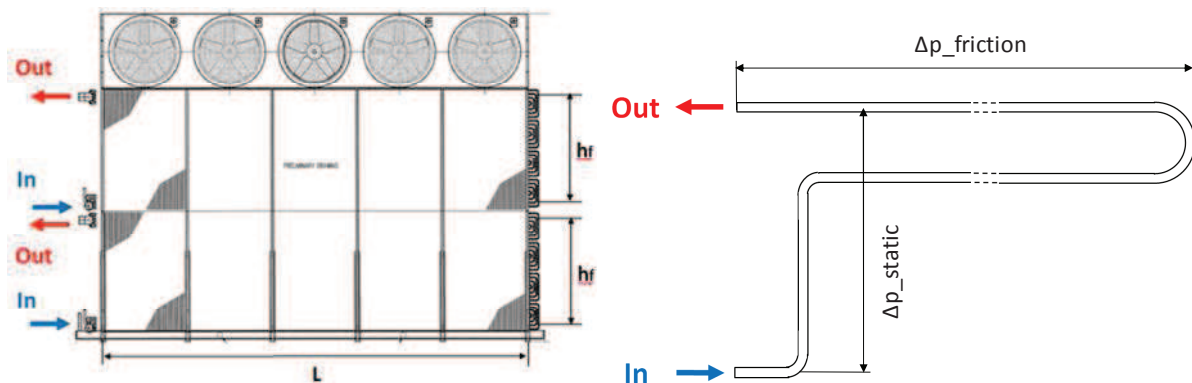


Figure 14: Fin and tube evaporator (FINCOIL/Alfa Laval) and evaporator pipeline

First of all the pressure loss due to the static refrigerant column, described by Darcy's Law, is given with $\Delta p = \rho * g * h_f$. For a certain fluid column height h_f and the density ρ the static pressure loss is dependent on the construction and the refrigerant itself. The pressure loss resulting from the friction between the two-phase refrigerant and the pipe wall was calculated with a fin and tube heat exchanger model in Dymola Control according to the Konakov pressure drop correlation for a two-phase turbulent

flow in smooth pipes. The results can be seen in Figure 15. Taken into account that ammonia shows a high temperature dependency on the pressure especially at low temperatures around -40°C , the evaporation temperature for CO_2 is much less susceptible to a pressure drop. Thus the flexibility of the system can be advanced and the temperature distribution over the heat exchange surface is more constant what results in a more even freezing process in the product boxes of all height.

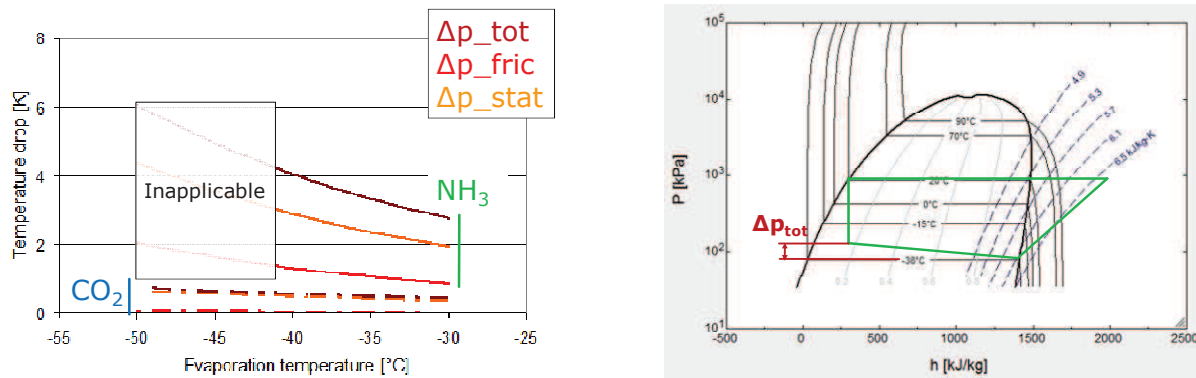


Figure 15: Temperature drop calculations and resulting pressure drop

The lower the evaporation temperature of the system the higher is the effect of the pressure drop for ammonia. Since there are inescapable head losses in the pipes and connection fittings due to friction between the fluid and the walls, the temperature loss also increases with a higher mass flow rate and the resulting higher friction. As it can be seen, the temperature drop of CO_2 remains almost constant with the evaporation temperature what is beneficial in the field of application. The evaporation temperature is meant by the temperature of the saturated vapor and the suction volume before the compression. Under this approach, the Inlet temperature of the evaporator drops pursuant to Figure 15 and cooling capacity is lost what affects the cooling capacity as well as the freezing time for the whole process negatively.

An explicit calculation of the temperature losses and distribution in the evaporator piping was conducted for the specified evaporation temperature of -38°C and the results are highlighted in Figure 16 for an ammonia system and in Figure 17 for a cascade system using CO_2 . For each temperature a new simulation in Dymola were run and the new freezing time of the biggest temperature differences were noted down, what can be seen on the right side.

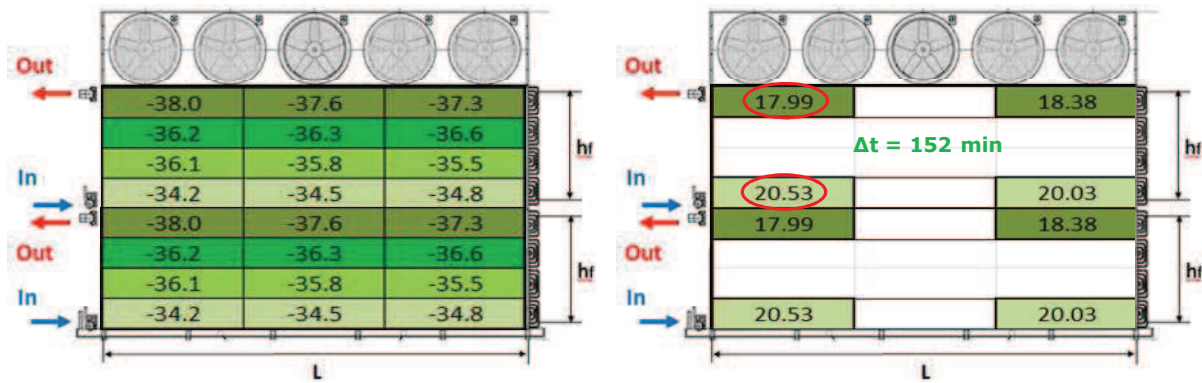


Figure 16: Temperature and resulting freezing time (right) with R717

While the uneven distribution in the ammonia system leads to differences in the freezing time of 152 min, the freezing process in a cascade system decelerate only by 25 min. As a consequence a better and more even product quality can be reached in a shorter time what also lowers the total energy consumption.

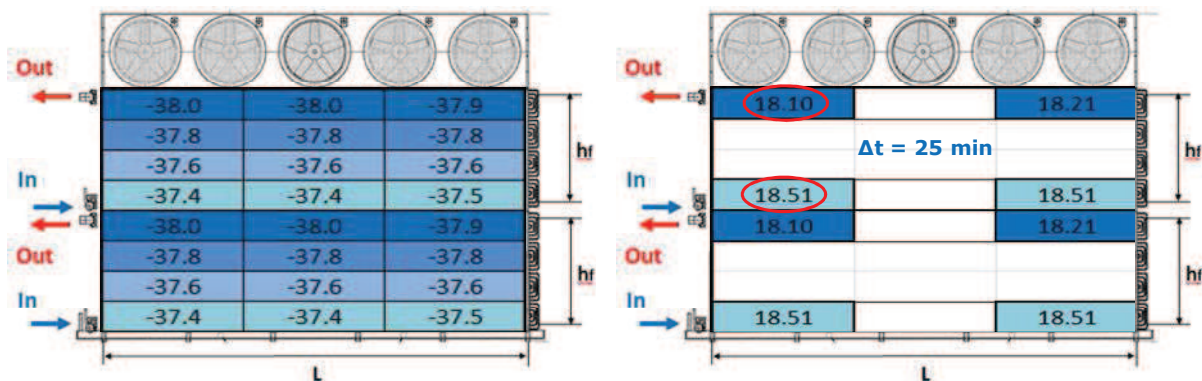


Figure 17: Temperature and resulting freezing time (right) with R744

Moreover the deceleration of the fish freezing at the bottom of the piping leads to another aspect that is beneficial for using CO₂ as primary refrigerant. While the fish at the bottom still needs to be cooled for additional 152 min to reach the required -20°C, the fish in the top shelves is cooled down further and cooling capacity is wasted. This big issue of an uneven temperature distribution was confirmed by measurements, evaluated and described by Magnussen, Nordtvedt, Stavset and Gullsvåg (29).

5.2 Cold thermal energy storage

A further approach of improving the energy efficiency is based on the basic idea of a compressor full-load operation during the whole process (30). The compressor is thereby operated at its highest efficiency point to achieve a higher economy. The surplus energy of the last freezing stage can be stored in a latent heat storage tank and the total efficiency is increased. Afterwards the energy is brought back into the next freezing process, especially in the beginning where high cooling capacities are desired and the highest load is expected. The quality of the fish and the freezing time strongly depends on the first period of the process and storing the energy is thus an utterly interesting method. Figure 18 clarifies the concept that will be further reviewed.

The heat input progression curve was taken out of (31) and matched to the desired tunnel capacity for 100 t of mackerel. Calculated by Magnussen O. the equation was confirmed by various measurements and simulations. Not only the fish but other sources as the heat emitted by the evaporator fans lead to the total heat input. It is common to slow them down after 9 hours of operation to 50% of their maximum rotational speed (dark blue). Minor thermal conduction by the diabatic tunnel wall is negligible and only added for completion. The installed cooling capacity of 500 kW is provided by the compressors and constant for the full-load operation.

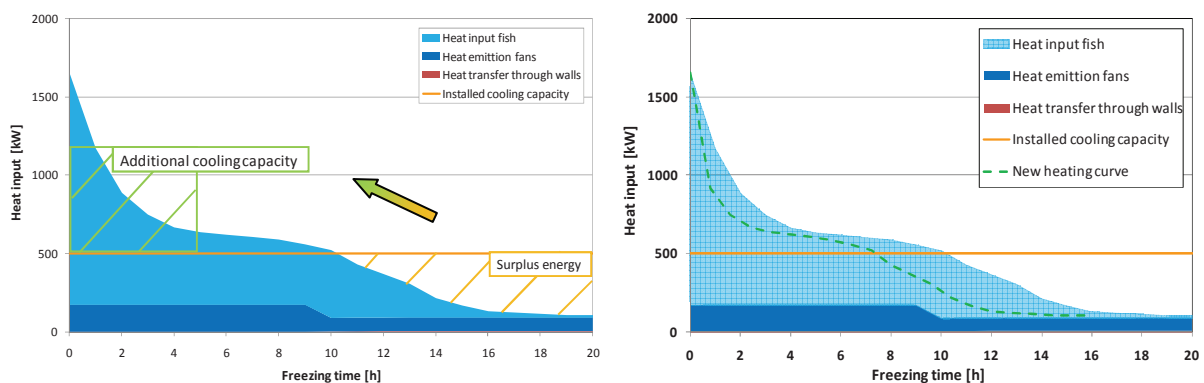


Figure 18: Enhancement of the efficiency by an energy storage system

As the heat load at the onset is higher than the installed capacity, the freezing process decelerates noticeably, also highlighted with the dotted line of (Figure 18). To increase the cooling capacity by installing bigger compressors would not be economically feasible. At first sight just the investment costs increase but moreover the compressor efficiency drops significantly due to the longer part-load operation (see

also Chapter 2.4) and the running costs rise as well. The idea of adding an energy storage system to the refrigeration cycle is simple: Run at its highest efficiency, a high COP can be achieved throughout the whole process. The higher cooling rate in the beginning brings also benefit in the process time and the quality of the product either by increasing the mass flow or by decreasing the evaporation temperature.

The Cold thermal energy storage is designed as an add-on to the cascade refrigeration system (Figure 19). As a consequence a subsequent adjustment of the storage system is possible to match full system requirements. Built with a shell and heat tube exchanger, the storage tank contains a phase change material in the shell side that stores provided heat by the refrigerant cycle. To get advantage not only of the sensible but the latent heat, the total thermal capacity is enhanced considerably.

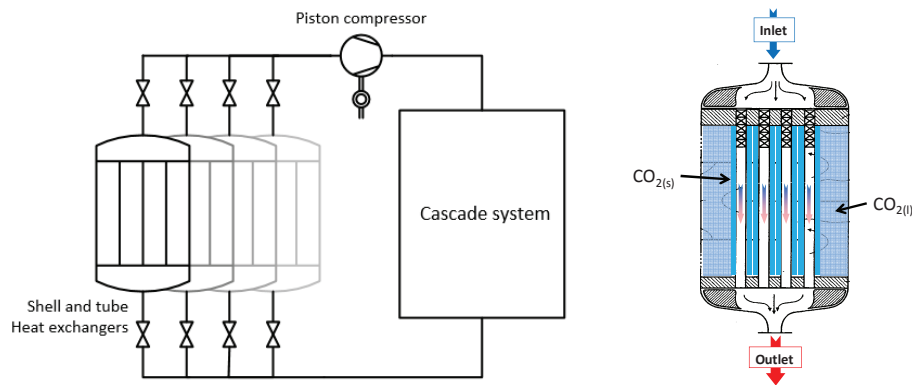


Figure 19: Outline of the storage system

Absorbing the surplus energy after around 10 hours (Figure 18) the full energy content to be stored is calculated with 2915 kWh what leads to a total tank volume of around 28 m³, considering a total temperature difference ΔT of 15 K and using the latent heat energy. Yet that rough estimation is given for water around the freezing point why the actual volume will furthermore increase for a particular phase change material. The heat capacity coefficients are declared with $c_{p,l} = 4.18 \frac{\text{kJ}}{\text{kg} \cdot \text{K}}$ and $c_{p,s} = 1.695 \frac{\text{kJ}}{\text{kg} \cdot \text{K}}$ for the liquid and solid phase, respectively. The latent heat is given with $\Delta h_m = 330 \text{ kJ/kg}$.

5.2.1 Physical basics of the storing process

Although the latent heat storage system has a long history and was patented in the mid-forties, i.a. by John A C Bowies (32), there are still many issues to master. Par-

ticularly the intended high capacity \dot{Q} (specified with 600 kW) that mainly depends on the storage material and its thermal conductivity limits the heat input in the freezing process. As Equation 1 shows, the heat transfer coefficient k depends on the thermal conductivity coefficient λ and the thickness s_n of the solid ice layer.

Equation 1

$$\frac{1}{k} = \frac{1}{\alpha_i} + \sum \frac{s_n}{\lambda_n} + \frac{1}{\alpha_a}$$

With Equation 2 it comes clear that besides the temperature difference ΔT of the process, only the construction parameter A gives a real degree of freedom.

Equation 2

$$\dot{Q} = k * A * \Delta T$$

Moreover two different cases needs to be differentiated: the charging and discharging process that point out the restriction of a high cooling capacity rate in more detail. During the charging process of the system, the liquid storage media absorbs the energy provided by the cool refrigerant flowing through the tube side of the heat exchanger. Also highlighted in Figure 20, the CO₂ molecules freeze next to the pipe wall and the ice layer grows slowly. The pipe geometry thereby leads to a hyperbolic deceleration of the heat transfer and the ice growth process over time, calculated with the heat transfer coefficient of Equation 3 with the shape coefficient $F^*_n = \frac{2 * \pi * L}{\ln \frac{r_a}{r_i}}$

for a coaxial pipe. The fundamental statement is the strongly limited capacity even at a thin ice layer.

Equation 3

$$k = \frac{1}{\frac{A_b * 1}{A_i * \alpha_i} + \sum \frac{1}{\lambda_n * \frac{A_b}{F^*_n}} + \frac{A_b * 1}{A_a * \alpha_a}}$$

In view of the additional heat transfer layer during the discharging process, the heat transfer coefficient is reduced several times compared to the charging process and the ice layer growth (Figure 21).

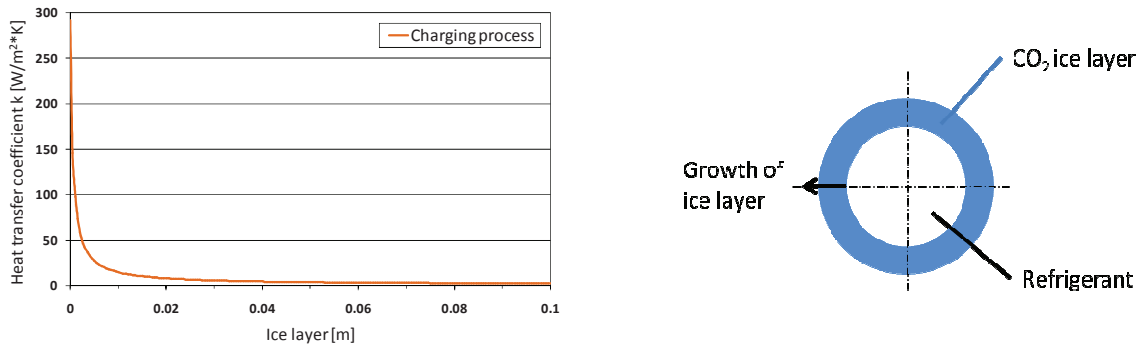


Figure 20: Heat transfer coefficient of the charging process

Beginning from the pipe outer radius, the ice layer is melted by the convective refrigerant in the tube side. The water layer of the melted ice propagates by time and the influence of water and its lower heat transfer coefficient increases (solid phase = $2.33 \text{ W/m}^2\cdot\text{K}$ compared to $0.5562 \text{ W/m}^2\cdot\text{K}$ of the liquid phase). The total heat transfer coefficient approaches a limiting value when the ice is melted completely and only the remaining water affects the heat flow.

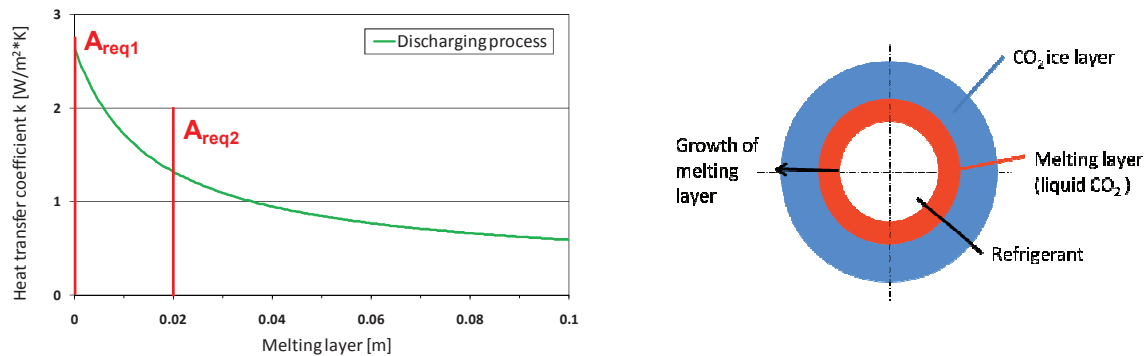


Figure 21: Heat transfer coefficient of the discharge process

Since discharging is the dominating process (values of the heat transfer are much lower than for the charging process) only this heat transfer coefficient was used for further calculations. It should be noticed, that the calculations in 5.2.1 are conducted with the values for water in the liquid and solid phase. The specific heat capacity as well as the values for heat transfer coefficient and the thermal conductivity are assumed as constant and not time dependent. Additionally the natural convection within the melting layer and the convection of the refrigerant are also considered in this heat capacity calculations. The required heat exchange surface A_{req1} at the beginning of the discharge is calculated to 15.000 m^2 which is increased significantly over the time by the decreasing heat transfer coefficient. After 0.02 m of the ice is melted the

required surface $A_{\text{req}2}$ equals to 30.300 m². Based on that assumptions using the shell and tube heat exchanger of *Skala fabrikk* and the certain dimensions (specifications see appendix) the total volume of the storage facility comes to $V = 606 \text{ m}^3$ what is around 20 times higher than the pre-calculated value of 28 m³. Since the design of such facility is limited by the construction size and thus the investment costs as well as the available space in a refrigerant plant, the realization of a big heat exchange surface needs to be discussed from the economical point of view and with deploying that technology.

5.2.2 CO₂ used as phase change material

As a reference the energy storage device should extend the cascade system; hence it needs to be designed for temperatures even lower than the actual refrigeration process to enable an adequate heat exchange. Considering the reference two-stage-ammonia system with an evaporation temperature of -38°C and the required temperature for a proper heat exchange, the system should be operated around -40°C or even lower. Though a high cooling capacity is also realized by a bigger temperature difference (Equation 2), the cold thermal storage is defined for a phase change around -55°C. This will give a higher cooling capacity and the Cold thermal energy storage system could be also applied for lower evaporation temperatures as -50°C.

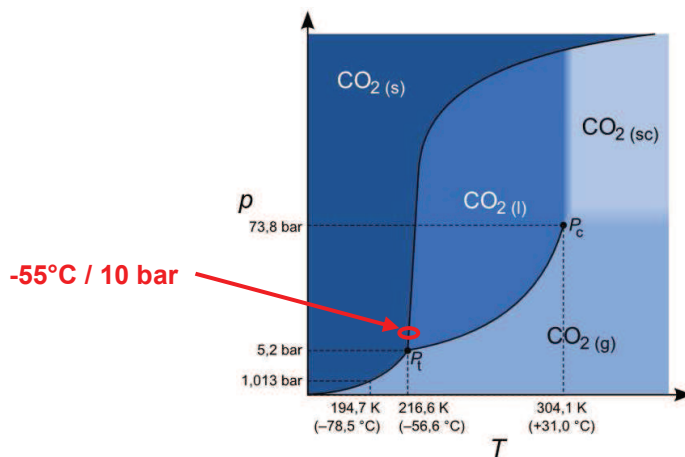


Figure 22: Phase diagram of CO₂

Due to its physical properties (Figure 22), CO₂ is predestinated for such application. Besides the advantages (also see 3.2.2) carbon dioxide is used in the refrigeration process itself and a loss of storage capacity or within the refrigerant cycle can be balanced easily. Nevertheless some facts need to be taken account of. Based on safe-

ty-relevant aspects the storage pressure must not exceed the triple point pressure of 5.2 bar. During the sublimation, the frozen CO₂ would expand to a volume 800 times of the solid phase and as a result the storage tank would burst. That case must be prevented by all means. Blowing off the vaporized CO₂ does not match the requirements of a thermal storage tank since the system would need to get refilled after every phase change process. An application below an evaporation temperature of -50°C is not recommended since the pressure difference in the fish and its surface would lead to cracks or a burst of the fish products (2). Also the exergetic losses should be minimized when the cooled refrigerant is lead back into the separator (outline is attached in the appendix) and mixed with the refrigerant of the common process. The higher the temperature difference is the higher the exergetic losses.

5.2.3 Laboratory setup

To gain expertise in the field of energy storage using CO₂ as storage media, a small system was designed (Figure 23). The main storage tank is a shell and tube heat exchanger (1) where the storage media will be filled in the shell side. The tube side is connected to the low temperature side of the cascade system. In a laboratory setup CO₂ gas bottles provide the proper amount of coolant. The regular heat exchanger is equipped with some additions. Welded joints (2) and gauge glasses (3) ensure the observation of the ice layer propagation during the charging and the melting process during the discharge, respectively. Considering the comparatively high dew point temperature of water in the environment and the low temperatures occurring during the storing process within the heat exchanger, air humidity would freeze on the surface of the gauge glasses and would make an observation of the process laborious. Therefore two connection fittings (4) are attached to the welded joints. An installed vacuum pump can reduce to pressure within the joints and the heat transfer coefficient of the air (26.2 mW/m²*K at RT) drops significantly to a value of around 0 mW/m²*K for vacuum. By heating the air inside the joints the humidity can also be lowered to obtain an even lower heat transfer.

A connected liquid storage tank (5) acts as a compensation unit for liquid CO₂ when the density increases due to the ice propagation. A fluid indicator (6) shows the level of CO₂ remaining in the storage device and gives an answer to the speed of ice propagation and the CO₂ evaporation near to the walls due to the diathermic insula-

tion what appear as bubbles. An attached safety valve prevents the worst case scenario of a facility burst.

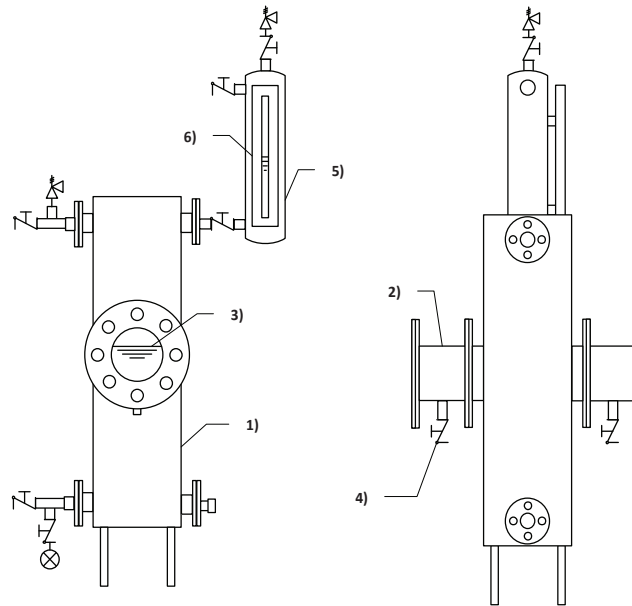


Figure 23: Laboratory setup of a Cold thermal energy storage system

All the components required for the laboratory setup highlighted in Figure 23, including contact information of different suppliers, are attached with a pre-calculated price list and few alternatives for flexibility in the execution of the construction. This primary design will give first impressions of handling such a Cold thermal energy storage system at that low temperatures as well as the rate of CO₂ ice growth. As part of the investigations a laboratory setup can be the first step of inventing new thermal storage devices as an add-on for refrigeration system at temperatures around -40°C or even lower. Anyhow, in addition to a cascade system as described in it can be an important step to enhance the energy efficiency.

5.2.4 Pipe geometry simulation

The extension of the heat exchange surface has been discussed and that option is limited. Anyhow the heat transfer coefficient k can be also optimized by the heat conduction and not only the heat convection. Decisively is the storage medium side and the outer pipe surface can be enlarged by different geometry designs by adding fins or blades. Different supplier offer tubes with a three times higher heat transfer that usual coaxial pipes. This phenomenon can also be seen in (Figure 24) where besides a coaxial pipe; two different fin designs were simulated. The Boundary conditions for water were described and were used for all three cases. The blue color indi-

cates the lowest and initial temperature of the solid phase ($T_0 = 213.15$ K). Deep orange and red indicate the highest occurring temperature of the refrigerant that need to get cooled ($T_1 = 228.15$ K).

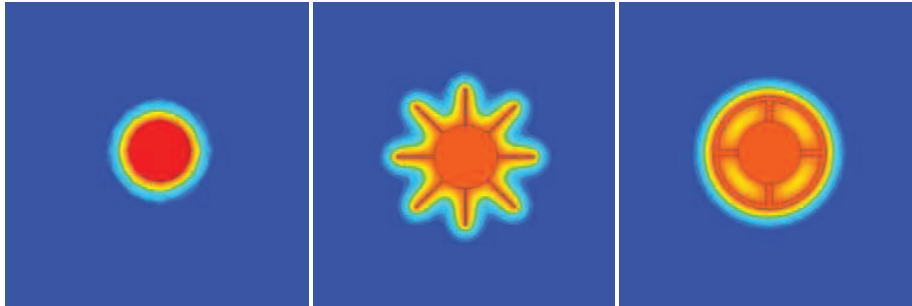


Figure 24: Heat flow simulation, QuickField

While the heat transfer in the beginning of the discharging process is quite low with the standard pipe and only a small area is heated, the other pipe geometries can heat immediately a much higher space what is also beneficial for the further melting process. However, it must be said that these pipe geometries are standard parts but not available for common shell and tube heat exchanger.

Nevertheless it shows a good way to increase the total heat transfer and considerations should be also given to that approach. Since the company *Skala fabrikk* is specialized for individual and customized heat exchanger, the design offer, also attached, could be extended with such pipe geometries.

5.2.5 Ice Slurry system

Apart from the static CO₂ storage system other solutions should be proved for their applicability with a refrigeration process in terms of a CTES as an add-on. Especially the limited cooling capacity as a major challenge of such energy storing facilities requires different approaches.

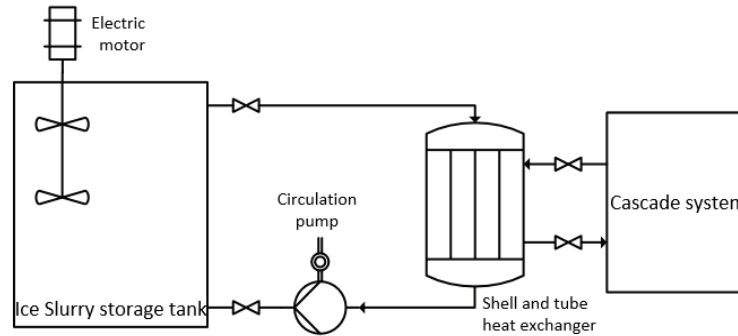


Figure 25: Outline of an Ice Slurry storage system added to the cascade system

One solution for realizing a high capacity is a dynamic Ice Slurry system as shown in Figure 25 where the freezing point of water is decreased by an additive comparable to brine freezing. The main difference in operation is the moving storage media and that only one shell and tube heat exchanger is used for the heat exchange during charging and discharging. Additional parts that raise the investment costs are the depressurized conventional storage tank where the Ice Slurry is stored and an installed stirrer which prevents agglomeration during the standstill phase. The heat emission of the stirrer is with 2 – 3% of total heat capacity comparatively low and an equation for a calculation is given with $\dot{Q} = Ne * \rho * n_s^3 * d_s^5$ (33). Dependent on the additive media and its flow behavior ($Ne =$ Newton-number, $\rho =$ density) also the rotational speed n_s of the stirrer and the screw propeller diameter d_s affects the result. The biggest advantage of an Ice Slurry system is the substantially higher heat transfer in reason of the higher thermal convection and conduction than for stagnant processes without artificial convection as in the CO₂ storage design. Beyond the convection, the phase change process during the heat exchange is beneficial for a high heat transfer coefficient k . By using the phase change enthalpy of the frozen water the amount of heat capacity for a certain temperature difference can be enhanced consequential – dependent on the Ice content in the Ice Slurry solution. Ice up to 30 – 35 vol-% can be pumped easily with regular circulation pumps (34). The Ice particles are melted almost entirely during the discharging period. Only small particles

remain at the outlet as precipitations for a faster crystal growth and a higher homogeneous Ice Slurry in the next charging period is reached. The enthalpy –phase diagram of Figure 26 illustrates the enthalpy of ethyl alcohol-water mixtures with different content of ice particles c_i . Ethyl alcohol as an additive was chosen because of its capable use at very low temperatures. Since the diagram is taken out of EES (Engineering Equation Solver) as a tool for solving equation systems, the data of the progression curves for different mixtures was confined. Nevertheless the isothermal line for -50 and -60°C is assumed and also integrated in. Supposed that the storage system is operated in the temperature range between -45 and -60°C the energy storing capability of a 54 -mass% mixture amounts to around $\Delta h = 40$ kJ/kg.

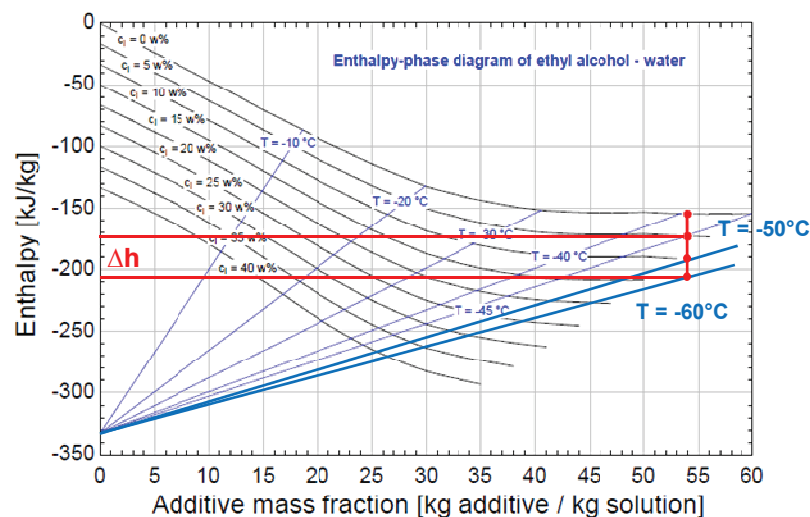


Figure 26: Enthalpy-phase diagram of different ethyl alcohol-water compounds

Calculated with the surplus energy of 2915 kWh that can be stored during one freezing period (see chapter 5.2) and the equation $Q = m * \Delta h_s = V * \rho * \Delta h_s$ with the enthalpy of fusion Δh_s , the required volume of the storage tank comes to approximately 264.5 m^3 . Yet the radius r for a sphere would be around 4 m what sounds feasible for an application in a huge industrial plant. Despite this fact of a high storage volume the construction can be designed simple and the investment costs can be reduced as the stirrer including the electric drive device are standard components. Since the fish freezing process should be supported by the energy storage system in the beginning of the next period a high heat transfer coefficient k needs to be obtained. Therefore, k is highlighted in Figure 27 and shows the heat transfer coefficient for an ethanol-water solution with different ice contents and different flow velocities.

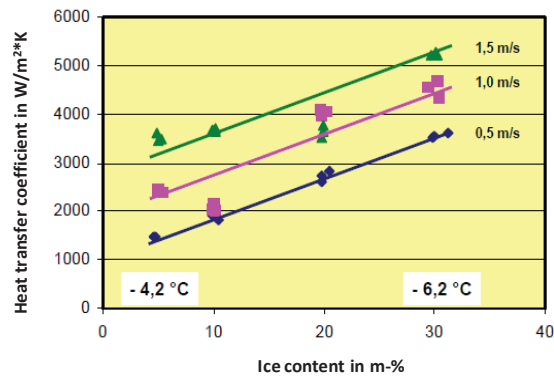


Figure 27: Heat transfer coefficient, solutions with different ice contents (35)

In fact the stated temperatures are different compared to the desired application, the statement is clear: the higher the ice content the higher the heat transfer because a higher melting process occurs and the total enthalpy increases (35). In addition the heat transfer coefficient k increases significantly with a higher flow velocity of the Ice Slurry. The extensive heat transfer coefficient can be compared to a one-phase refrigerant and can reach even higher values (35). Considering that the physical process is equal for charging and discharging, the heat transfer coefficient can be assumed as the same.

In general it can be said that the application of Ice Slurry as CTES system can be a huge achievement in the efficiency enhancement strategy but need to get analyzed thoroughly. There are many different additives that can be used for Ice Slurry applications but only few are suitable for the low temperature range around -50°C .

6. Experimental results

The Dymola simulation model set up by Walnum H. and Andresen T. (5) was the basis and further extended to the cascade model by Banasiak K. To compare both cycles the substructure and the freezing tunnel model including the evaporator were retained unchanged in all simulations. Although an environment for comparable structure is desired, restrictions had to be made for the cascade system and some parameters were adjusted within this work. To get a first indication for the cascade system, the cycle was pre-calculated based on the boundary conditions given in Chapter 5. These initial simulation parameters were used as a basis for the next simulation steps what made them more practicable. The parameters are therefore listed in Table 6, attached in the appendix.

6.1 *Modelica simulation of NH₃/CO₂ cascade system*

For the efficiency analysis the cascade system running with R717 and R744 different parameters and their influence of the entire system operation were investigated and compared to the reference conditions and the reference model of Table 3. In the following discussions the outcome of the basic cascade system is shown in dark orange. Besides the evaporation pressure and the condensing pressure, the refrigeration circulation pump as well as subcooling of the liquid and superheating of the vapor phase show an effect on the system performance. For further implementation steps the selection of proper compressors is also essential to change and optimize the cooling capacity to the freezing tunnel capacity. Each parameter was simulated with the Dymola model of Figure 13 and discussed in this chapter.

6.1.1 Cooling capacity adjustment

An evaporation temperature of -38°C was predetermined by *Northern Pelagic*. However it is also a matter of installed capacity that is necessary to reach the specified 18 hours for freezing the 100 t of fish. The bigger the compressors are the higher the installed cooling capacity and the faster a desired temperature is reached. Particularly the inertia and the slow start-up phase should be investigated and improved to gain additionally capacity and thus a higher freezing rate what results in a better product quality as well as in cost savings. The basic setup that was pre-defined pro-

vides a cooling capacity of approximately 550 kW at a freezing rate of 18.11 hours. For reproducibility the installed capacity had to be adjusted to the 600 kW of the two-stage ammonia system.

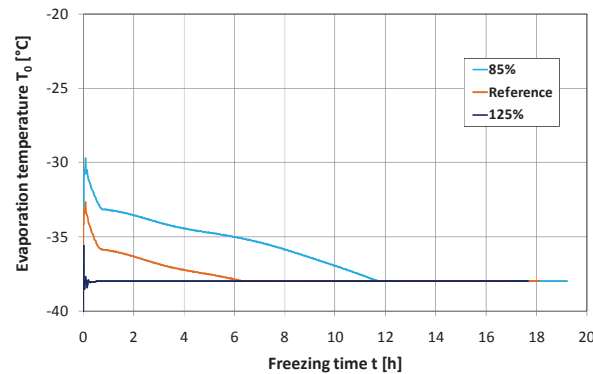


Figure 28: Evaporation temperature curve

As mentioned the defined evaporation temperature of -38°C is reached faster with a larger system. As a consequence the freezing process time is reduced. A system enlargement to 125% of the basis case leads almost immediately to low temperatures and the fastest start-up. A larger system would be oversized for this temperature. With that knowledge the compressor size was changed by 2.5% of the basis case at each step of its suction volume what was also performed at the same rule for the heat exchanger sizes, the sea water mass flow and the refrigeration mass flow to ensure a proper heat removal and a constant temperature difference of the heat exchange. The simulation results show that an exact relationship between the freezing time and the energy consumption at high capacities is difficult to define for such a complex system. At capacities of 500 kW the freezing time is comparatively slow and small changes of the components result in a high improvement of the process. At a certain size the maximum cooling capacity for the given evaporator design is reached with around 615 kW.

It can be seen that a desired freezing period of 18 hours for a tunnel capacity of 100 t of fresh fish can only be obtained by installing a 570 kW capacity what is 14% higher than the specified 500 kW by *Northern Pelagic AS*.

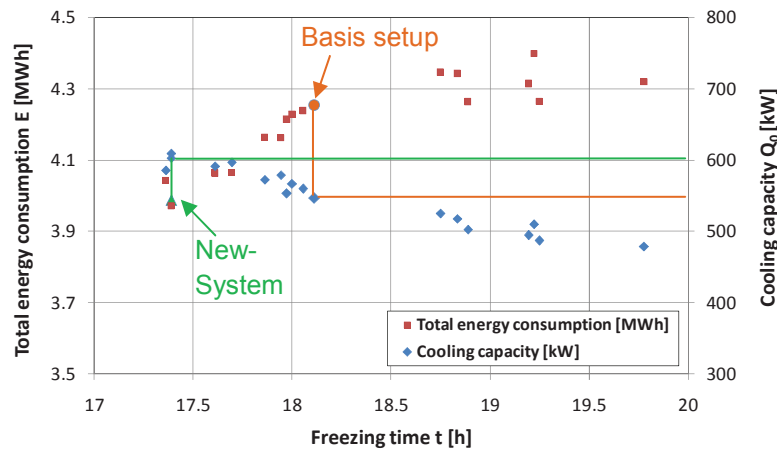


Figure 29: Cooling capacity adjustment

Nevertheless the same finding was spotted for the two-stage ammonia system where a capacity of 600 kW was needed. This value was now also used for the cascade system, what made them comparable. The “new system” with 600 kW uses 3.97 MWh in total what results in a lower energy consumption (compared to the basis setup) of around 6.3% (-268 kWh per freezing period) and the freezing time is reduced about 4% or 43 min. The parameters are:

- CO₂ compressor: 3675 cm³
- NH₃ compressor: 15313 cm³
- Cascade heat exchanger length: 2.45 m
- Sea water mass flow: 14.7 kg/s
- Condenser length: 5.5 m
- Refrigeration mass flow: 3.7 kg/s

This “new system” was the concept for the comparison to the two-stage ammonia setup. A main target of further investigations was to figure out the influence of the essential components as the circulation pumps, the compressors or the heat exchanger. Later on the cascade system was further optimized unrestricted to the two-stage ammonia cycle

6.1.2 Cascade heat exchanger optimization

The cascade heat exchanger, designed as tube and tube, is the connection part between the low and high temperature cycle. It is important to minimize the temperature difference between the ammonia and the CO₂ temperature profile to optimize the pressure ratio and thus the isentropic compressor efficiency. The additional work that

must be provided for a necessary heat exchange between the low and high temperature stage affects the benefits of a cascade system adversely compared to a two-stage ammonia system with an open intercooler. Two strategies must be considered: At first the subcooling of CO₂ and superheating of the ammonia was investigated to find the best configuration for the use of latent phase change. At a constant mass flow the total heat flow can be increased according to $\dot{Q} = \dot{m} * \Delta h$. Pursuant to the equation $\dot{Q} = k * A * \theta_m$ with a constant heat transfer coefficient k a better heat exchange in the cascade heat exchanger is only obtained by a bigger exchange surface since the logarithmic temperature difference should be constant or as low as possible for a good pressure ratio. The simulations were conducted with a the temperature difference of 0, 3 and 5 K whereas the heat exchanger surface was varied in 5% steps to utilize the higher enthalpy difference and thus a better heat exchange between the cycles. It can be seen that the superheating of ammonia leads in average to a lower energy consumption and combined with a temperature difference $\Delta T = 3$ K for the CO₂ subcooling the lowest energy consumption can be achieved. For further simulations the values for the superheating and the subcooling were chosen with 3 K.

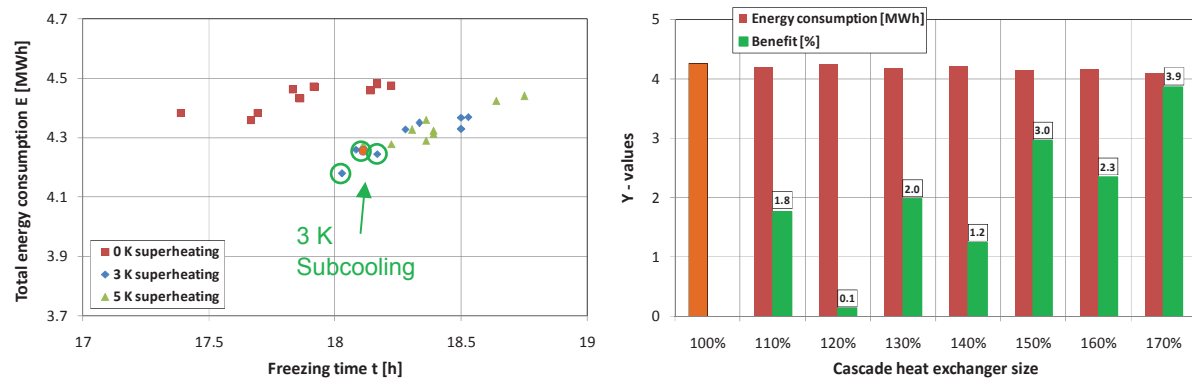


Figure 30: Parameter regulation of the cascade heat exchanger

The second approach is the enlargement of the cascade heat exchanger surface (Figure 30, right) while keeping the subcooling and superheating constant at the same level. The bigger the heat exchange surface A the lower the temperature difference and total energy consumption E and the benefit increases. The decision for a certain heat exchanger size is relevant for further economic consideration. Fluctuant and inconsistent results cannot be interpreted simply due the model complexity but the general statement is clear.

6.1.3 Condensing pressure investigation

One big challenge of a refrigeration system is to keep the pressure ratio as low as possible. The evaporation pressure is a parameter that can influence the energy consumption in a serious manner (Figure 31). As usually controlled by a floating head pressure to minimize the temperature difference also in cold seasons, the freezing plant is cooled with a sea water pump at a constant inlet temperature of 10°C over the whole season. To reduce the condensing pressure either the sea water cooling pump mass flow ($\dot{Q} = \dot{m} * c_p * \Delta T$) or the condenser surface can be increased ($\dot{Q} = k * A * \theta_m$) what results in a lower logarithmic temperature difference. It should be noticed that the latter is limited for a given mass of the sea water. First the general mass flow on the condensing pressure was determined and later on the simulations were conducted. (Figure 31, right):

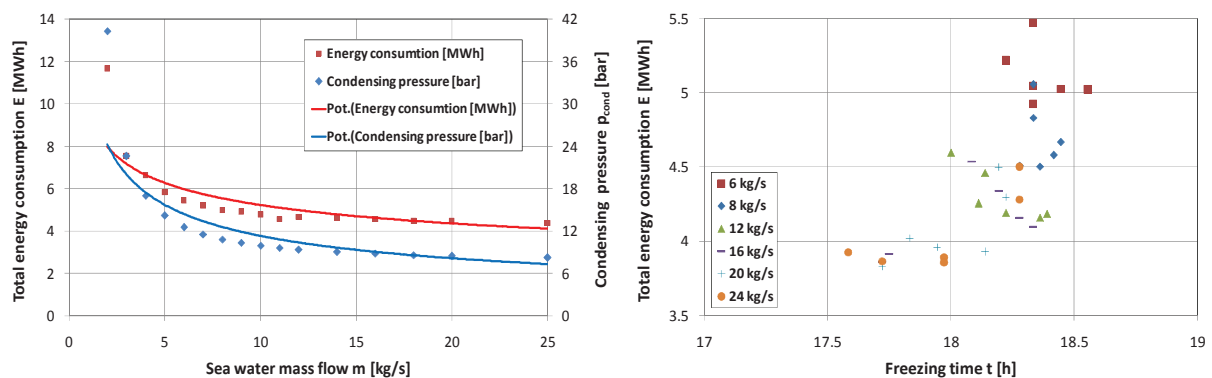


Figure 31: Condensing pressure investigation

The strong dependency comes clear in both illustrations. It is essential to provide a certain mass flow for a proper heat removal to keep the compression temperature and the condensing pressure and consequently the compressor work low. At a high mass flow rate of around 20 kg/s the condensing pressure is not reduced further since the heat flow of the condenser gets dominant. In current plants the circulation pumps are not equipped with a frequency drive because of the low power consumption and the free available cooling media. But still the selection of pumps should be done in an economic and ecologic way. For this purpose two circulation pumps, offered by KSB, were chosen as a realistic value for the volume flow. Considering that, the cascade system was readjusted with a total sea water mass flow of 27.8 kg/s ($\approx 2 \times 50 \text{ m}^3/\text{h}$).

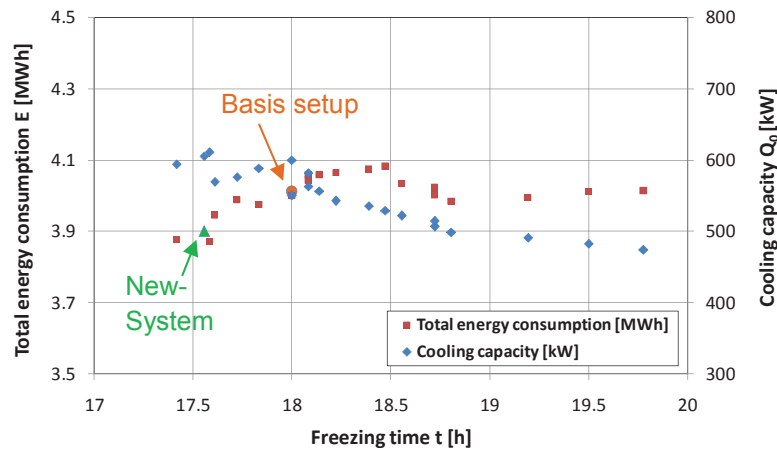


Figure 32: New system with adjusted parameters

This mass flow is given by the selected cooling pump of KSB, attached in the Appendix. A 10k NOK higher investment for two pumps are justified with the decreasing total energy consumption of 2.2% (-87 kWh) and the payoff time is calculated with 2.3 years.

6.1.4 Refrigeration pump

As prevalent in large refrigeration systems, the evaporator is operated under flooded conditions and a superheating is omitted. Therefore a refrigeration pump was installed providing a proper liquid CO₂ flow from the liquid receiver of the low temperature side. The liquid state is important that a good heat transfer and the use of the phase change enthalpy can be ensured. Investigations showed that only a the freezing time t is influenced remarkably at refrigeration flows lower than 2 kg/s for the basic case at an evaporation temperature of -38°C. Since the amount of liquid is not sufficient for the high cooling load in the beginning, the CO₂ is overheated and the heat removal process is slowed down. Despite that a higher mass flow only leads to a higher power consumption of the circulation pump. The cooling capacity is dependent on the installed compressor power and cannot be increased why the freezing rate remains constant for higher mass flows. However the refrigeration pump is the component that ensures the heat exchange in the evaporator and should not be undersized. For the investigated system two refrigeration pumps of KSB were chosen with a total mass flow rate of 3.3 kg/s (See attachments).

6.2 System comparison

6.2.1 Total energy consumption

When both systems are compared it must be considered that the new cascade system is designed with 22.5% bigger heat exchanger and circulation pumps that increase the investment costs and the final decision for a certain system needs to be viewed also from the economical side. Nevertheless the focus is hereby given on the variable plant costs and illustrated in Figure 33. Including the calculated pressure drop of Chapter 5.1.3, the benefit in the energy consumption increases from 3.3% (-138 kWh) to 4.2% (-179 kWh).

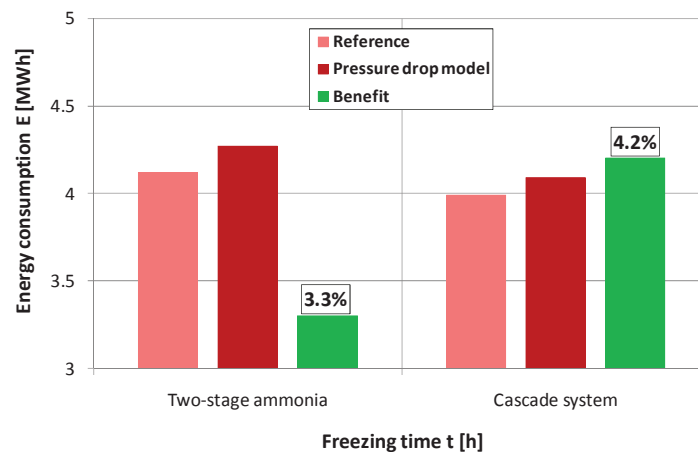


Figure 33: Energy consumption, system comparison

Calculated for a seasonal operation of 100 days and specific energy costs of 0.5 NOK/kWh the benefit can be calculated to around 9000 NOK/a. After that first impression it is of utmost interest to weight up the costs and opportunities of a certain investment.. If both systems are compared by the same freezing time of 18 hours, the cascade system consumption is calculated with 4.23 MWh what is even higher than for the ammonia system. The percentage composition of the energy used by the individual parts is shown beneath. Although both high temperature compressors use the same amount of energy, the ammonia compressor for the cascade system is over 2 times bigger for the same cooling capacity. By a downsizing of the compressor, the CO₂compressor power increases noticeably since the heat is agglomerated in the heat cascade heat exchanger and the discharge temperature is raised significantly (A 2) what affects the total energy consumption negatively. The sea water cooling pump uses just 7% of the total energy but affects the other components strongly

as discussed before. As a last point it comes clear that the selection of an appropriate compressor to the defined capacity must of utmost interest.

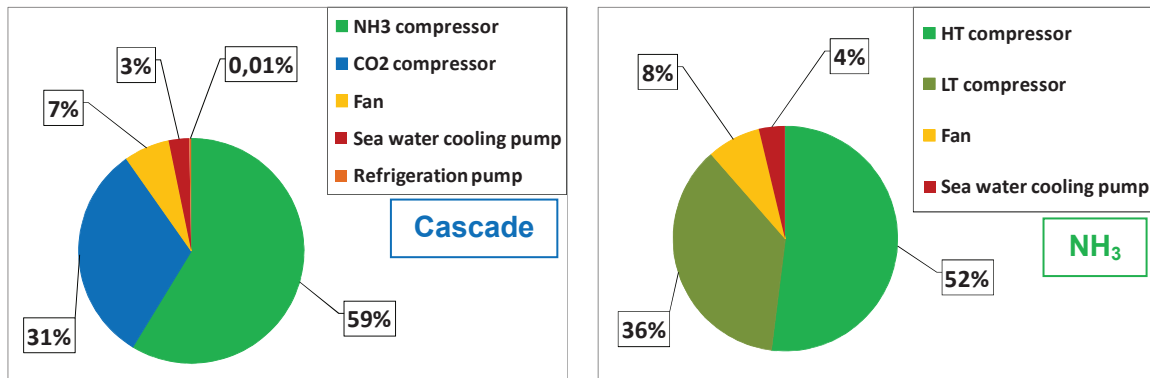


Figure 34: Percentage composition of the total energy consumption

6.2.2 Coefficient of Performance

As a value for the thermodynamic efficiency in a certain operation point, the Coefficient of Performance (COP) is calculated with the cooling capacity divided by the total energy consumption of the plant, also including ancillary units as fans and the sea water cooling pump.

$$COP = \frac{\dot{Q}_0}{P_{el,ges}} = \frac{\dot{Q}_0}{P_{Fan} + P_{Pump} + P_{Compression}}$$

The refrigeration pump is not included. Its value is defined by $P_{el} = \frac{\dot{m}_{CO2} \cdot \Delta p_{loss}}{\rho_{CO2} \cdot \eta_{ges}}$ and with a total efficiency of 21.4% (36) the consumed power is 0.7 kW what equals to around 0.2% at the start up and 0.6% in the end of the total power consumption. These results are given for a static head of 0.5 bar (5 m) and the density of 1109 kg/m³ at -38°C. Despite expectations the COP of the cascade system is lower than for the two-stage ammonia system. The temperature difference of the cascade heat exchanger and the resulting higher condensing pressure needs to be provided by the compressors what might be a reason for the slightly lower system efficiency.

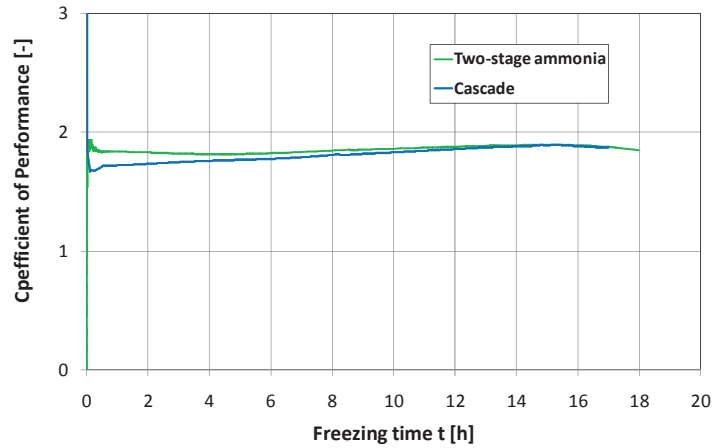


Figure 35: COP, system comparison

A fan regulation management according to Chapter 2.5 was not included in the cascade model what could enhance the efficiency additionally. More simulations were also conducted for different evaporation temperatures and system sizes.

6.2.3 Tunnel capacity

Simulation results showed the positive impact in lower an energy consumption as well as faster freezing rate. As opposed to the higher efficiency the shorter freezing time does not bring valuable benefit since the tunnel is refilled once a day in the batching process and only a two times faster freezing could result in a second batch freezing rate. Hence the tunnel capacity was increased and adjusted to the specified freezing time of 18 hours for different evaporation temperatures. Also attached are the basis setup of the cascade model before the sea water and refrigerant pump adjustment

Table 5: Cooling capacity enhancement due to a cascade system

System	Energy consumption [MWh]	Additional consumption [%]	Capacity enhancement [%]	COP
Two-stage ammonia -38°C	4.12	-	-	1.86
550 kW cascade	4.25	3.2	-	1.81
600 kW cascade	3.9	-5.3	-	1.86
Cascade -38°C	5.10	23.8	20	1.75
Cascade -50°C	6.36	54.5	31	1.64
Cascade -55°C	6.43	56	34	1.62

The comparison shows clearly the high flexibility of a cascade system in times of production shortages where the energy consumption is subordinated. Plus the pressure drop model is not included in these calculations what would result in further a decrease of the energy consumption related to the ammonia system. However the dimensions of the freezing tunnel were not adjusted to the higher capacities. A higher amount of fish that is frozen could thereby lead to an overload where the air could accumulate between the rackets and shelves. Thus the proper air flow and the desired even air velocity distribution would be obstructed and as Chapter 2 showed, good flow conditions are crucial for a high heat transfer and heat exchange of the product boxes. This tunnel design issue is also temporary discussed.

Nevertheless the results showed that the NH_3/CO_2 cascade system is a good way to increase the capacity for a certain system size and a given tunnel layout in times of high production rates.

6.2.4 Economical view

An economical assessment of the cascade system was not part of this work but has to be considered in the decision-making. The total investment for a common one-stage ammonia plant is around 15 – 20 million NOK dependent on the installed cooling capacity and the freezing tunnel size. 8 – 10% of the costs account for the insulation of pipes and the heat exchanger. Since carbon dioxide pipes can be designed smaller due to its low specific volume the insulation can be minimized for a constant heat transfer coefficient what brings a great potential. Also savings in the pipe material can be obtained. Around 10% of the investment is for piping and minor parts like expansion and valves. CO_2 compressors are smaller but needs to be built more robust than ammonia compressors at pressures for around 9 bar. The major costs are also expended for the liquid separator and the liquid receiver. How far the higher pressure operation affects these advantage must be calculated in further design steps.

7. Conclusion

The objective of this work was to investigate and evaluate different energy saving strategies. Many cascade systems using NH_3/CO_2 have been established successfully for different applications. However this approach is still not applied within the pelagic fish industry in Norway. One-stage or two-stage ammonia systems show good efficiencies and a high reliability especially in large plants with high cooling capacity requirements. A *Dymola* model was examined including a specified air blast freezing tunnel designed by *Norway Pelagic AS*. Simulation results showed a reduced energy consumption compared to a two-stage ammonia system but the overall system efficiency was slightly lower. Investigations also showed that at temperatures of -40°C the impact of the temperature reduction due to pressure losses on the low pressure side increases in ammonia systems. As a result, the freezing process lengthens significantly. To compensate for this disadvantage, a higher cooling capacity must be installed and the energy consumptions will increase. Moreover, the air intake resulting of the operation below ambient pressures rises dramatically at evaporation temperatures lower than -40°C . Owing to the poor pressure ratio and isentropic compressor efficiency, ammonia systems are therefore not suitable at such low temperatures. A major advantage of a cascade system using CO_2 is its high flexibility. The high pressure operation makes the system less vulnerable to pressure reductions and thus a constant quality of batches even at low temperatures up to -55°C can be achieved. In addition, the capacity is increased which shortens the freezing procedure and improves the product quality. A specified refrigeration system with 500 kW installed cooling capacity is undersized for the given freezing tunnel and the 100.000 kg of fish. For a cascade system an appropriate capacity is 14% higher (570 kW) and 20% for the ammonia system (600 kW). Furthermore, the tunnel capacity could be increased by 20% at a 24% higher energy consumption at an evaporation temperature of -38°C . In case of potential production shortages, the evaporation temperature can be lowered to -55°C where the capacity was increased by 34% at a higher energy consumption of approximately 55%. When using CO_2 as refrigerant, smaller pipes and equipment (compressor, valves, and insulation) can be utilized due to lower volume flows. However the high pressure operation needs sturdier and more durable equipment with an increased piping wall thickness and a compressor

designed for higher pressure operation. How much the smaller parts and thus the greater specific loads will affect the durability of the system is unclear so far and will require further research. Higher strength materials may be necessitated to meet the durability criteria and influence the investment costs. A further topic of investigation was the impact of the sea water cooling mass flow on the condensing pressure. In addition, the positive effect on the system efficiency was proven under economical preconditions. An energy recovery system is a good approach to increase the COP and to shorten the freezing process remarkably. It is less known about the dry ice formation at temperatures around -50°C to -60°C and no papers have been published yet about the usage of Carbon dioxide as a phase change material. The shown construction and the realization of the storage facility can bring fundamental facts about a latent heat storage tank at low temperatures. Also an *ICE SLURRY* system could be deployed for an energy improvement either by using glycol-ethanol mixtures or CO_2 Slurry in view of new storage systems processes.

8. Further work

The findings of this work demonstrated the economic viability of a NH_3/CO_2 cascade system for an application in the pelagic fish industry for specified boundary conditions. However, there is a need to further expand the investigations regarding the issue of high energy consumptions and a fast freezing process to improve the product quality sustainably. The following considerations give ideas to fulfill these requirements and list rudiments for further working approaches:

- 1) Economic evaluation of the investment costs for the cascade system in comparison to the state-of the art equipment of ammonia refrigeration plants. With that knowledge the final selection of the system components can be generated.
- 2) Establishment of the Cold thermal energy storage facility, designed in 5.2. The facility will give first impressions of the dry ice propagation and an achievable low temperature storing level. It will also answer questions about the energy storing capacity potential, the required dimensioning and the applicability in the pelagic fish industry.
- 3) Creating a Cold thermal energy storage model using *Dymola Control* and later on the integration into the refrigerant model to simulate the effect on the thermodynamic efficiency and the freezing rate.
- 4) Improving of the air flow by a certain freezing tunnel design to enable higher tunnel capacities for a selected cascade system to obtain a higher flexibility.
- 5) Strategies to determine the influence of the water and air intake in ammonia systems at operations below ambient pressures.

Since the positive effects of a NH_3/CO_2 cascade system is not well known in the pelagic fish industry in Norway, a further profound literature review on the economical and ecological side of view should be conducted.

9. References

1. *Refrigeration and Freezing of Foods*. s.l. : McGraw-Hill Education, 2013.
2. **Widell, Kristina Norne**. *Energy efficiency of freezing tunnels - towards an optimal operation of compressors and air fan*. Trondheim, Norway : NTNU Norwegian University of Science and Technology, 2011.
3. **K.N. Widell, T.Eikevik**. *Reducing Power Load in Multi-Compressor Refrigeration Systems by limiting Part-Load Operation*. Trondheim, Norway : NTNU Norwegian University of Science and Technology, 2008.
4. **Harald Taxt Walnum, Trond Andresen, Kristina Widell**. *Dynamic simulation of batch freezing tunnels for fish using Modelica*. Trondheim, Norway : SINTEF Energy Research, 2011.
5. **J.W.Pillis**. *Basic of Operation, Application & troubleshooting of Screw Compressors*. Milwaukee, United States : Johnson Controls, 1998.
6. **Arora, Ramesh Chandra**. *Refrigeration and Air Conditioning*. New Delhi : PHI Learning Private Limited, 2012.
7. Carly - International experienced expert for refrigeration equipment. [Online] CARLY GmbH, 2013. [Cited: October 15th, 2013.] <http://www.carly-sa.de/-Olmanagement-im-Kaltekreislauf.html>.
8. *HVAC Systems and Equipment*. Atlanta, United States : ASHRAE Inc., 2008.
9. **Camelia STANCIU, Adina GHEORGHIAN, Dorin STANCIU, Alexandru DOBROVICESCU**. *Exergy Analysis and Refrigerant Effect on the Operation and Performance limits of a one Stage Vapor Compression Refrigeration System*. Bucharest, Romania : Universit Politehnica of Bucharest, 2011.
10. **Portland General Electric Company** . *Intro to Ammonia Refrigeration Webinar*. <http://www.youtube.com/watch?v=Qt7M7TjuZM8> : s.n., April 2013.
11. **Prof. Dr.-Ing Klaus Langeheinecke, Prof.Dr.-Ing. Peter Jany, Prof.Dr.-Ing Gerd Thieleke**. *Thermodynamik für Ingenieure*. Wiesbaden, Germany : Friedr. Vieweg & Sohn Verlag / GWV Fachverlag GmbH, May 2006.

12. **Witt, Monika.** *Natürliche Kältemittel - aktuelle Entwicklung und Trends.* Linz, Austria : Eurammon - refrigerants delivered by mother nature.
13. **S.Forbes Pearson, Ph.D.** *Using CO₂ to reduce Refrigerant Charge.* Milwaukee, United States : ASHRAE Journal, 2012.
14. **Magnussen, Ola M.** *Freezing of mackerel in carton boxes - heat flow and freezing time.* Trondheim, Norway : The Norwegian Institute of Technology, 1993.
15. **Ola M. Magnussen, Anne K. T. Hemmingsen, Vidar Hardarsson, Tom S. Nordtvedt, Trygve M. Eikevik.** *Frozen Foods, Current and Future Technologies.* Trondheim, Norway : SINTEF Energy Research, NTNU Trondheim.
16. **Unknown.** *FREEZING METHODS AND QUALITY LOSS AT FREEZING TEMPERATURES.* unknown : United Nations Industrial Development Organization, unknown.
17. **Garthwaite, Tony.** *The frozen fish chain.* London, England : Seafish, 1986.
18. **Moen, Per A.** Equipment of current refrigeration systems within the pelagic fish industry. Trondheim, Norway : Pam Refrigeration, March 14, 2014.
19. **David Wylie, P. E.** *Intro to Ammonia Webinar .* Portland General Electric , 2013.
20. **Nielsen P., Lund T.** *Introducing a new Ammonia/CO₂ Cascade Concept for large Fishing Vessels.* Albuquerque, New Mexiko : YORK Refrigeration, Marine & Controls, 2003.
21. **Industri, AIS Dybvad Stål.** *Plate Freezers aboard Fishing Vessels using CO₂ and ammonia.* Brussels, Belgium : EU ATMOSphere , 2013.
22. **H. Liu, Z. Gu, Y. Li.** *Simulation of NH₃/CO₂ Two-Stage Low Temperature Refrigeration System.* West Lafayette, India : Purdue University Libraries, 2002.
23. **Ola Magnussen, Ola Jonassen, Tom.S.Nordtvedt.** *Undersøkelse av kondensatorsystem for kuldeanlegget.* Trondheim, Norway : SINTEF Energiforskning AS, 2006.
24. **Köhler, Jürgen.** *Wärme- und Stoffübertragung in Zweiphasenströmungen.* Wiesbaden, Germany : Springer Fachmedien, 1996.
25. **Magnussen O., Nordtvedt T., Stavset O., Gullsvåg P.** *Norway Pelagic Selje AS, Anleggsgjennomgangogmålinger.* Trondheim, Norway : SINTEF Energi AS, 2013.

26. **Armin Hafner, Tom Ståle Nordtvedt, Ingrid Rumpf.** *Energy saving potential in freezing applications by applying cold thermal energy storage with solid carbon dioxide.* Trondheim, Norway : SINTEF Energy Research, 2011.
27. **Magnussen, Ola M.** *Norsk Kjøleteknisk Møte, Industrielle Frysetunneler - Praktiske forhold ved utforming og drift.* Trondheim, Norway : NTNU Trondheim, Institutt for klima- og kuldeteknikk, 1995.
28. **John A C Bowies, Mcfarlan Ronald Lyman, Neck Marblehead.** *Heating Pad.* US2114396A December 18, 1938. Latent heat storage system.
29. **Melinder, Åke.** *Handbook on indirect refrigeration and heat pump systems.* Kullavik, Sweden : Svenska Kyltekniska Föreningen,.
30. **Michael Kauffeld, Masahiro Kawaji, Peter W. Egolf.** *Ice Slurries - Fundamentals and Engineering.* Paris, France : International Institute of Refrigeration (IIR), 2005.
31. **Kauffeld, Pof. Dr.-Ing. habil. Michael.** *ICE SLURRY - Heat transfer.* Karlsruhe, Germany : Danish Technological Institute, 2010.
32. **Stavset, Ole.** *Modelica-simuleringer.* Trondheim, Norway : SINTEF Energi AS, 2013.
33. **Fenton, John D.** *Calculating resistance to flow in open channels.* Vienna, Austria : John D. Fenton / Alternativ-Hydraulics, 2000.

10. Appenix

Table 6: Values of basis cascade system, re-calculated with 500 kW

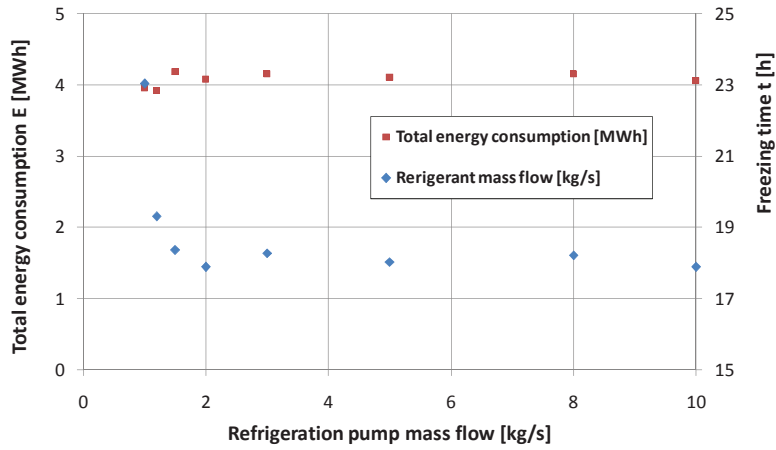
Parameter	Symbol	Unit	Value
Sea water cooling pump	\dot{m}	kg/s	12
Condenser length	L	m	4.5
NH ₃ compressor	V_{NH_3}	cm ³	12500
NH ₃ mass flow rate	\dot{m}	kg/s	0.533
Superheating NH ₃	ΔT	K	3
Cascade heat exchanger length	L	m	2
Subcooling CO ₂	ΔT	K	3
CO ₂ compressor	V_{CO_2}	cm ³	3000
Refrigeration pump	\dot{m}	kg/s	3

Table 7: Values for cascade heat exchange study

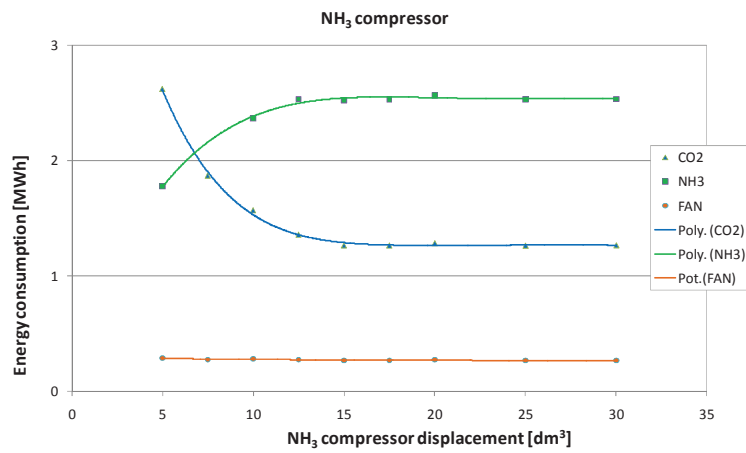
	Unit	Parameter values		
Superheating NH ₃	K	0	3	5
Subcooling CO ₂	K	0	3	5
Heat exchange length	m	2	2.1	2.2

Table 8: Condensing pressure investigation, parameters

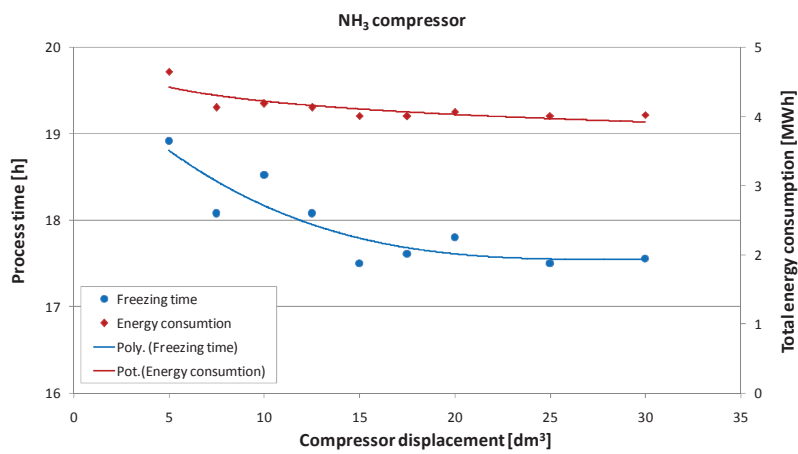
	Unit	Parameter values						
Sea water mass flow	kg/s	6	8	10	12	16	20	24
Heat exchanger length	m	2.25	3	3.75	4.5	6	7.5	9



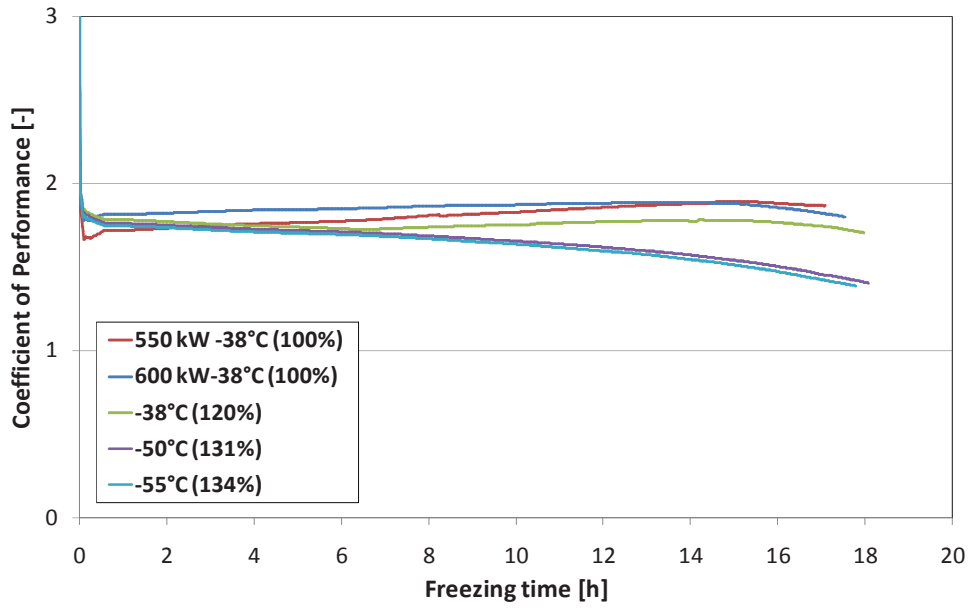
A 1: Refrigeration pump investigations



A 2: Downsizing of the HT ammonia compressor



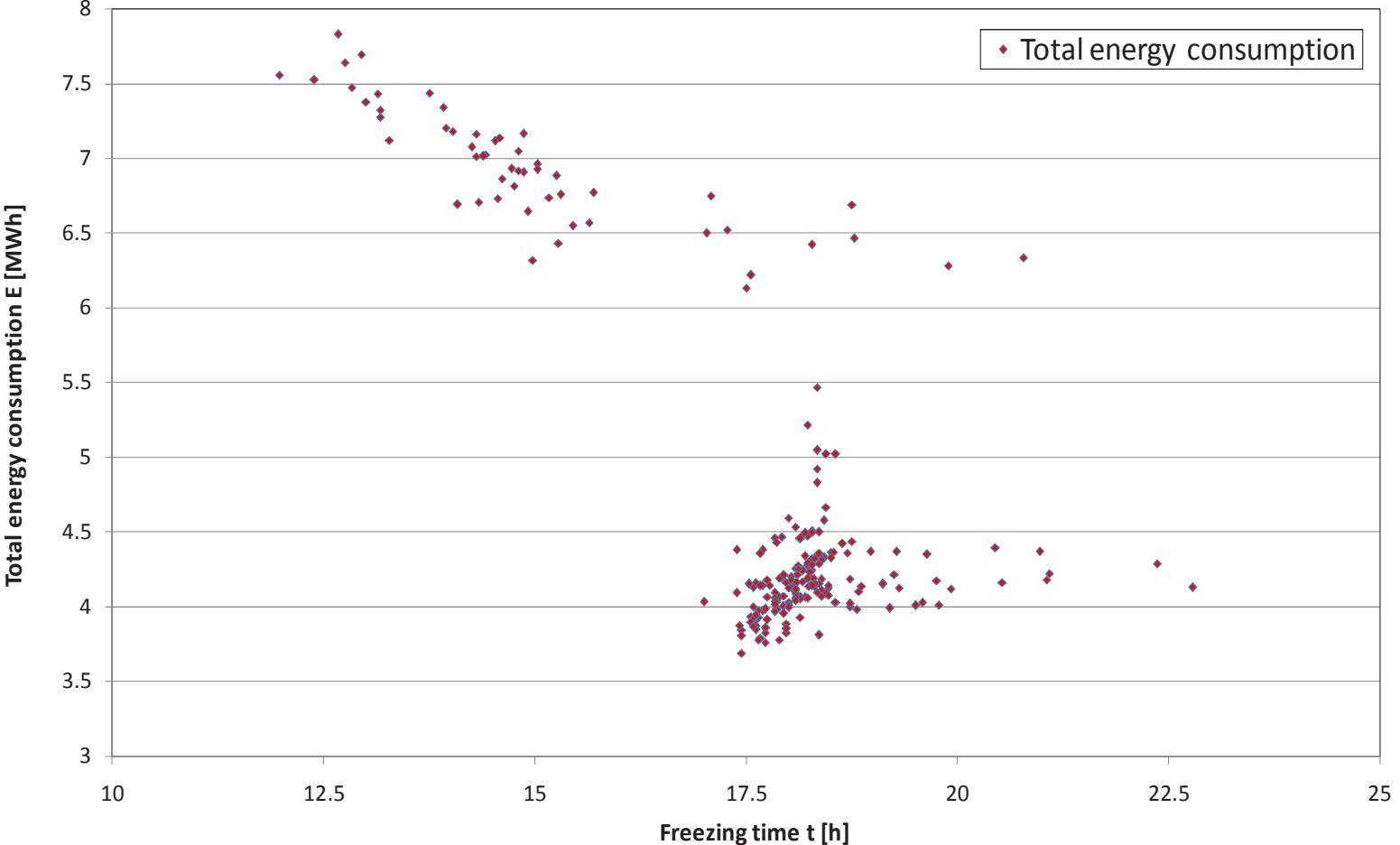
A 3: Downsizing of the HT ammonia compressor



A 4: Cascade COP, different tunnel capacities

Table 9: Simulation parameters and selected values

Parameter	CO2 comp- ressor size	NH3 comp- ressor size	Cascade heat exchanger length	NH3 superheating	CO2 subcooling	Evaporation pressure	Condenser length	Sea water mass flow	Refrigeration mass flow
Symbol	V	V	L	ΔT	ΔT	p	L	m	m
Unit	m ³	m ³	m ³	K	K	Pa	m	kg/s	kg/s
Value	0.0015	0.00625	1	0	0	1081000	2.25	6	1
	0.00165	0.006875	1.1	3	3	1050000	2.475	8	2
	0.0018	0.0075	1.2	5	5	915500	2.7	12	3
	0.00195	0.008125	1.3			832350	2.925	14	3.33
	0.0021	0.00875	1.4			739500	3.15	16	6
	0.00225	0.009375	1.5			684200	3.375	18	8
	0.0024	0.01	1.6			554300	3.6	20	10
	0.00255	0.010625	1.7				3.825	27.8	
	0.0027	0.01125	1.8				4.05		
	0.00285	0.011875	1.9				4.275		
	0.003	0.0125	2				4.5		
	0.00315	0.013125	2.1				4.725		
	0.0033	0.01375	2.2				4.95		
	0.00345	0.014375	2.3				5.175		
	0.0036	0.015	2.4				5.4		
	0.00375	0.015625	2.5				5.625		
	0.0039	0.01625	2.6				5.85		
	0.00405	0.016875	2.7				6.075		
	0.0042	0.0175	2.8				6.3		
	0.00435	0.018125	2.9				6.525		
	0.0045	0.01875	3				6.75		
	0.00465	0.019375	3.1				6.975		
	0.0048	0.02	3.2				7.2		
	0.00495	0.020625	3.3				7.425		
	0.0051	0.02125	3.4				7.65		
	0.00525	0.021875	3.5				7.875		
	0.0054	0.0225	3.6				8.1		
	0.00555	0.023125	3.7				8.325		
	0.0057	0.02375	3.8				8.55		
	0.00585	0.024375	3.9				8.775		
	0.006	0.025	4				9		



A 5 Cascade model simulation for table 9, in all combinations

11. Paper



Design of a R717/R744 cascade system for the pelagic fish industry

Armin Hafner, Ephraim Gukelberger, Krzysztof Banasiak,

Dr. Armin Hafner Senior Research Scientist
SINTEF Energy Research, Kolbjørn Hejes vei 1D, 7465 Trondheim, Norway
Armin.Hafner@sintef.no

Tel. (+47) 92 85 77 30

Abstract

Design of a R717/R744 cascade system for the pelagic fish industry

Possible energy efficiency enhancement strategies and energy saving potentials for an air blast freezing tunnel system were presented. Therefore a R717/R744 cascade model was designed with the declarative modeling language *Modelica* and implemented in the simulation environment *Dymola Control*. Various simulations were performed for a specified freezing tunnel design given by *Norway Pelagic AS*. The total efficiency enhancement was compared to a two-stage ammonia system as state of the art. Also the temperature drop vulnerability of an ammonia system at low temperatures was investigated and included. The integration of an energy recovery system as an add-on solution was discussed.

Keywords: R744/CO₂, R717/NH₃, refrigeration, efficiency enhancement

1. Introduction

Fish, after oil, gas and metals, is the third largest export good of Norway. Mainly sold to Russia, Japan and Denmark, the demand on fresh, dried and especially frozen fish is constantly increasing. This growth requires increasing cooling capacities to ensure a good and steady quality of the frozen fish during the long transport routes. To cope with those challenges larger fishing vessels, refrigeration plants and warehouses are being built. To offset the additional electricity costs, the energy efficiency must be improved either by



inventing and investigating new and highly efficient industrial processes. Furthermore, increasingly stringent environmental standards impose even higher efforts on developing refrigeration systems with natural refrigerants. The limiting space available on trawlers and vessels as well as current on-shore plants also need higher efforts on more compact solutions with higher production capacities. In total the amount of pelagic fish caught by *Norway Pelagic AS* was 828.000 t in 2013 [1]. Due to the different sizes and cell structures, it is of utmost interest to find a freezing process that can ensure a constant quality for all products. As a result, the air blast freezing process is commonly used in industrial plants for pelagic fish.

Ammonia is known as the thermodynamic most efficient refrigerant and is nowadays used for many applications. Introduced in a cascade system with R744 it brings many benefits in the efficiency and the installed capacity. Although many NH_3/CO_2 cascade systems have proven to be highly efficient in various applications all over the world, this technology has not yet been established for onshore plants within the pelagic fish industry in Norway [2].

A/S Dybvad Stål Industri is a supplier of manually-operated and automatic plate freezers for onshore and offshore applications. The first CO_2/NH_3 cascade system for plate freezers has been established on the large fishing vessel *MS Kvannøy* in 2002 with a total capacity of 1350 kW. Thereby the freezing capacity could be increased by 4 – 8% at -40°C and up to 30-40% at temperatures around -50°C , resulting in reduced fuel costs. Due to the high volumetric efficiency of CO_2 the plate freezer volume was reduced and higher production rates were obtained. After all that cascade system was implemented in offshore applications by different manufacturers like *NORSK KULDE*, *GEA Refrigeration* or *Johnson Control* [3].

Furthermore, political discussions about the climate change; the results and possible control approaches are nowadays hold and will also lead to a change of the energy policies. The Kyoto and the Montreal Protocol already limited the emissions and the application for certain refrigerants and the use of natural refrigerants will further increase. Ammonia and CO_2 are already established in the US, Japan, and Europe and the objective must be the introduction in the Norwegian onshore industry. Lower energy consumption also reduces the negative impact on the environment. Additionally, the greenhouse gas emissions are declined, leading to an improvement of the greenhouse effect

While the applicability of ammonia is limited below -42°C and the efficiency drops significantly, carbon dioxide with its high volumetric efficiency brings great benefits in the temperature range between -40°C and -50°C . The main tool for this work was simulation environment Dymola Control. Besides the investigation of various system parameters that mainly affected the freezing process time and the energy consumption, considerations of an energy recovery system (ERS) were made and a solution as an add-on was investigated.

2. Simulation model

As an objective-oriented, equation based language, modelica is provided for complex, component-orientated systems. Modeled in the simulation environment Dymola (Dassault Systems AB, Sweden) the cascade refrigeration cycle was based on the model set up by Walnum H., Andresen T., Widell K. [3]. This cycle was extended and tailor-made to a pre-calculated R744/R717 cascade system. In case of simplicity the pressure loss in the heat exchanger as well as the condenser was not included. The freezing tunnel including the fans was remained unchanged.

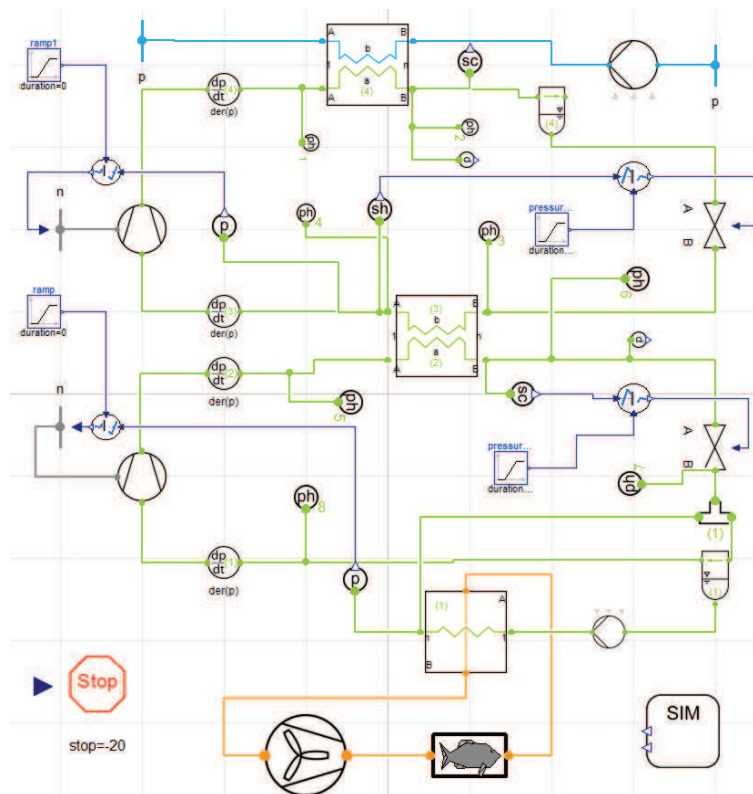


Figure 1: R717/R744 cascade model, Dymola Control

Following assumptions were made for the simulations:

- Freezing tunnel capacity 100.000 kg
- Evaporation temperature -38°C
- Sea water inlet temperature 10°C
- Pressure head of the cooling pump 22 m
- Cascade condensing temperature -15°C
- Maximum compressor speed 1450 min⁻¹
- R717 compressor: efficiencies according to the pressure difference
- R744 compressor: constant isentropic and volumetric efficiency of 0.7

The refrigeration pump was not involved in the simulations since the power consumption was negligible compared to other components.

3. Pressure drop and resulting temperature differences

A big advantage of using CO₂ as refrigerant is the high pressure state even at low temperatures. Considering the pressure loss in the evaporator only a low temperature drop can be expected. For a comparison to ammonia the pressure drop within the heat exchanger was calculated according to Darcy and the Konakov pressure drop correlation for a two-phase turbulent flow in smooth pipes [4].

Therefore the dimensions of a fin and tube heat exchanger of FINCOIL/Alfa Laval which is assembled in current freezing tunnels of Norway Pelagic were used. Including the frictional and static losses ammonia shows high temperature drops at low temperatures around -40°C whereas the CO₂ is much less susceptible even at lower evaporation temperatures. Thus the flexibility of the system can be advanced and the temperature distribution is more constant what results in an even freezing process for all products. Calculated for a mass flow of a 500 kW system, the temperature loss would also increase with higher capacities and respectively higher mass flow rates due to the higher friction. As it can be seen, the temperature drop of CO₂ remains almost constant with the evaporation temperature what is beneficial in the field of application. The saturated vapor of the suction volume before the compression is given with -38°C. Under this approach, the inlet temperature of the evaporator drops pursuant to Figure 3 and cooling capacity is lost what affects the freezing time for the whole process negatively.

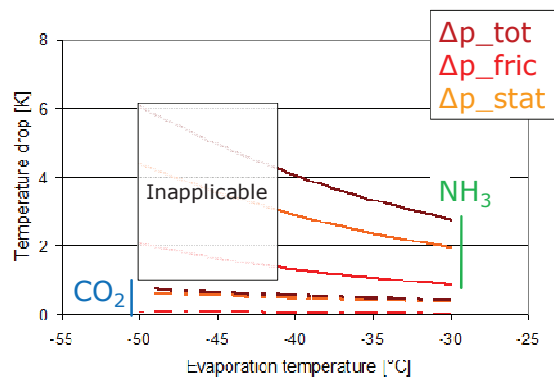


Figure 2: Temperature drop calculations

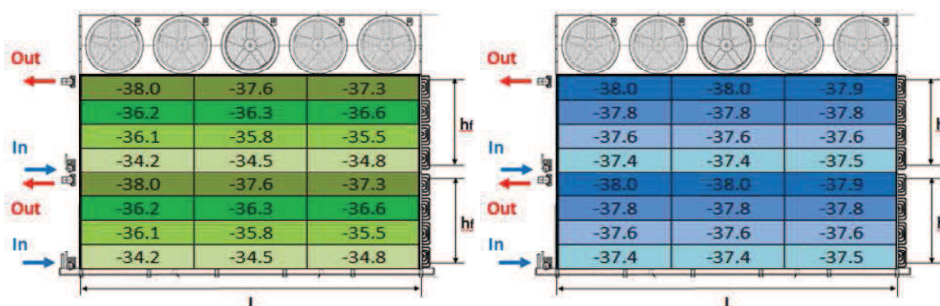


Figure 3: Temperature distribution in an evaporator commonly used within the pelagic fish industry

While the uneven distribution in the ammonia system leads to differences in the freezing time of 152 min between the top and bottom side, the desired product temperature of -20°C in a

CO₂ system varies only by 25 min. As a consequence a better and more even product quality can be reached in a shorter time what also lowers the total energy consumption.

4. Simulation results

The basic setup for the R717/R744 system was pre-defined and provides a cooling capacity of approximately 550 kW at a freezing rate of 18.11 hours. For reproducibility the installed capacity had to be adjusted to the 600 kW of the ammonia model in [3]. It can be seen that a desired freezing period of 18 hours for a tunnel capacity of 100 t of fresh fish can only be obtained by installing a 570 kW capacity what is 14% higher than the specified 500 kW by *Northern Pelagic AS*.

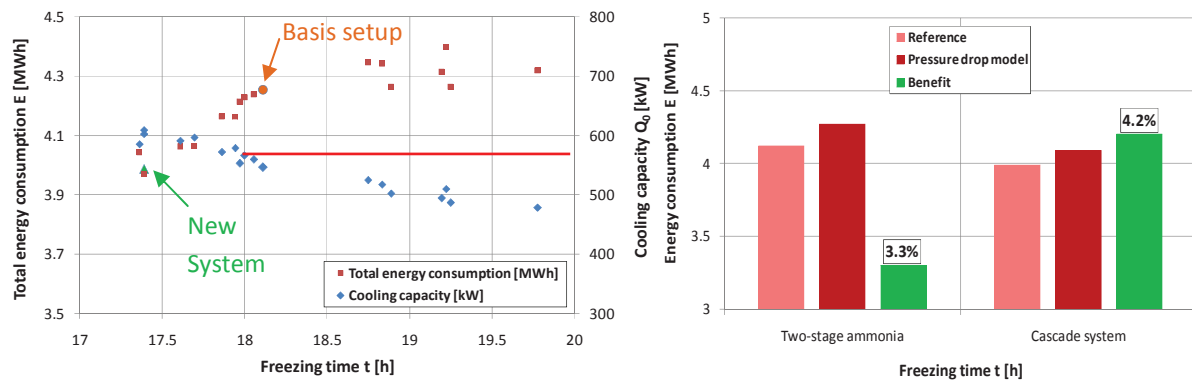


Figure 4: Cascade cooling capacity adjustment and the resulting energy consumption

Nevertheless the same finding was spotted for the two-stage ammonia system where a capacity of 600 kW was needed. This value was now also used for the cascade system, what made them comparable. The “new system” with 600 kW uses 3.97 MWh in total what results in a lower energy consumption of around 4.2% (-179 kWh per freezing period) and the freezing time is reduced about 4% or 43 min. This new system that was determined was 22.5% larger than the basic setup. For a seasonal operation of 100 days and specific energy costs of 0.5 NOK the savings were calculated to 9.000 NOK/a.

To take advantage of the low temperature application of CO₂ up to -55°C simulations were also conducted with different evaporation levels. Simulation results showed the positive impact in a lower energy consumption as well as faster freezing rate. As opposed to the higher efficiency the shorter freezing time does not bring valuable benefit since the tunnel is refilled once a day in the batching process and only a two times faster freezing could result in a second batch freezing rate. Hence the tunnel capacity was increased and adjusted to the specified freezing time of 18 hours for different evaporation temperatures.

The comparison shows clearly the high flexibility of a cascade system in times of production shortages where the energy consumption is subordinated. Plus the pressure drop model is not included in these calculations what would result in a further decrease of the energy consume. The results showed that the NH₃/CO₂ cascade system is a good way to increase

the capacity for a certain system size and a given tunnel layout in times of high production rates.

Table 1: Cooling capacity enhancement due to a cascade system

System	Energy consumption [MWh]	Additional consumption [%]	Capacity enhancement [%]	COP
Two-stage ammonia -38°C	4.12	-	-	1.86
550 kW cascade	4.25	3.2	-	1.81
600 kW cascade	3.9	-5.3	-	1.86
Cascade -38°C	5.10	23.8	20	1.75
Cascade -50°C	6.36	54.5	31	1.64
Cascade -55°C	6.43	56	34	1.62

5. Energy recovery system

A further approach of improving the energy efficiency is based on the basic idea of a compressor full-load operation during the whole process, also investigated by Hafner A., Nordthvedt T. [5]. The compressor is thereby operated at its highest efficiency point to achieve a higher economy. The surplus energy of the last freezing stage can be stored in a latent CO₂ heat storage tank and the total efficiency is increased. Afterwards the energy is brought back into the next freezing process, especially in the beginning where high cooling capacities are desired and the highest load is expected. The quality of the fish and the freezing time strongly depends on the first period of the process and storing the energy is thus an utterly interesting method.

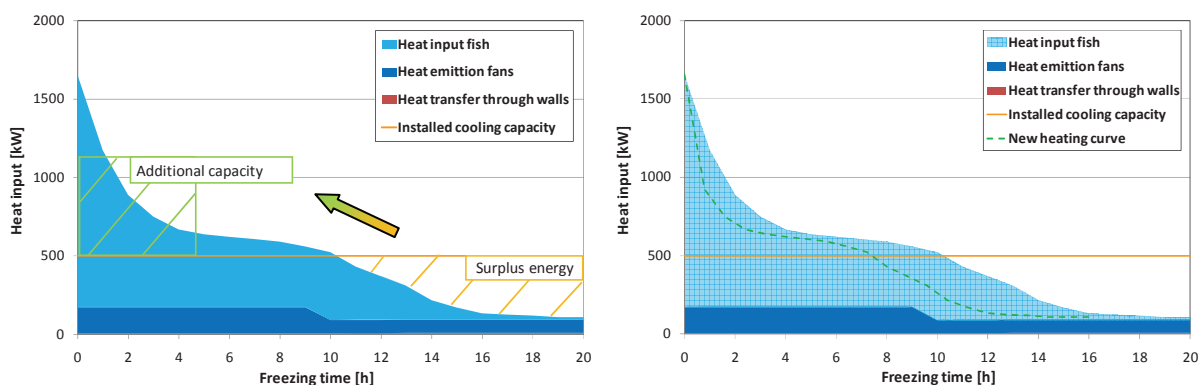


Figure 5: General idea of an energy recovery system

The heat input progression curve was taken out of [6] and matched to the desired tunnel capacity for 100 t of mackerel. Calculated by Magnussen O. the equation was confirmed by various measurements and simulations. The idea of adding an energy storage system to the

refrigeration cycle is simple: Run at its highest efficiency, a high COP can be achieved

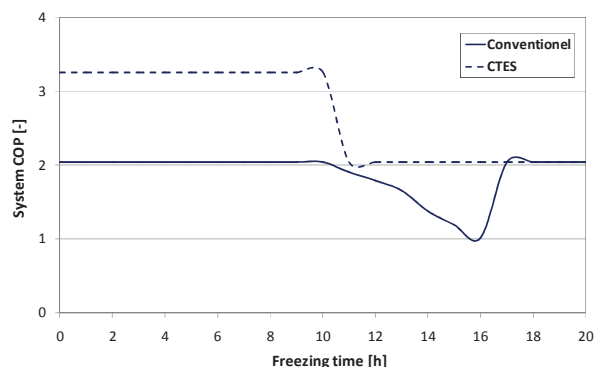


Figure 6: System efficiency enhancement by an ERS

throughout the whole process. The higher cooling rate in the beginning brings benefits in the process time and the quality of the product either by increasing the mass flow or by decreasing the evaporation temperature. For conventional systems the COP drops due to the part load operation but with an ERS the COP can be kept constant and raised remarkably in the start-up phase. The energy recovery system is designed as an add-on to the cascade refrigeration system.

As a consequence a subsequent adjustment of the storage system is possible to match full system requirements. Built with a shell and heat tube exchanger, the storage tank contains CO₂ as a phase change material in the shell side that stores provided heat by the refrigerant cycle; the investment can be kept at a minimum. Calculated with an excess energy of 2915 kWh and the specific values for CO₂ with a process temperature difference of $\Delta T=15$ K, the required volume of the system is calculated to 45.38 m³. However the high cooling capacity needs to be realized since the surface area is a limited factor. Especially the melting process is slowed down by the liquid CO₂ layer that forms around the tubes. A test facility will be built up to get a fundamental knowledge of using CO₂ as a latent phase change material at low temperatures.

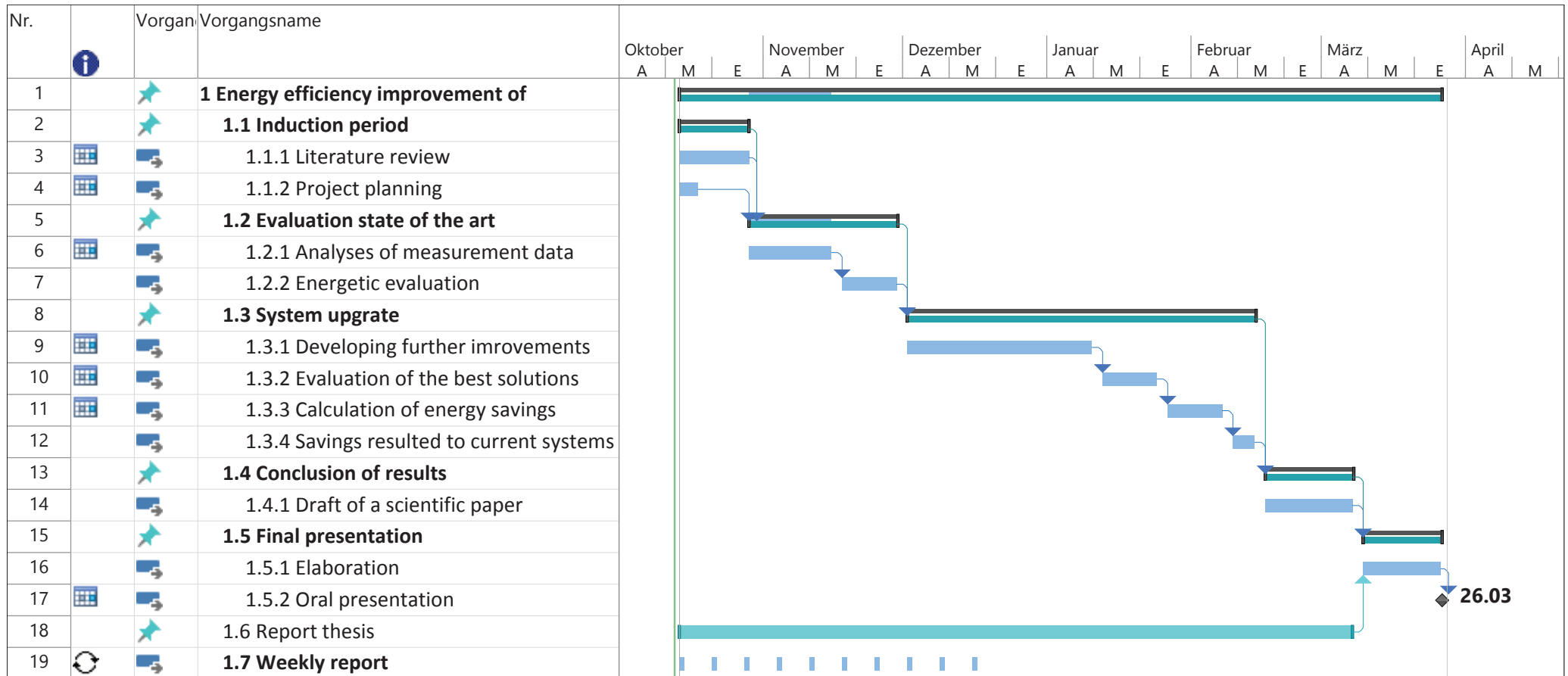
6. Conclusion

A Dymola model for a R717/R744 cascade system was examined including a specified air blast freezing tunnel designed by *Norway Pelagic AS*. Simulation results showed a reduced energy consumption compared to a two-stage ammonia system but the overall system efficiency was slightly lower. Investigations also showed that at temperatures around -40°C the impact of the temperature reduction due to pressure losses on the low pressure side increases in ammonia systems. As a result, the freezing process lengthens significantly. A major advantage of a cascade system, using CO₂, is its high flexibility. The high pressure operation makes the system less vulnerable to pressure reductions and thus a constant quality of batches even at low temperatures up to -55°C can be achieved. In addition, the capacity is increased which shortens the freezing procedure and improves the product quality. The installed capacity for a NH₃/CO₂ cascade system was 5% lower than for a two-stage ammonia system at a temperature level of 38°C. Furthermore, the tunnel capacity could be increased by 20% at a 24% higher energy consumption for an evaporation temperature of -50°C. In case of potential production shortages, the evaporation temperature can be lowered to -55°C where the capacity was increased by 34% at a higher energy consumption of approximately 55%. An energy recovery system is a good approach to increase the COP and to shorten the freezing process remarkably. A laboratory facility needs to be established to quantify the technical advantages and the practicable application.

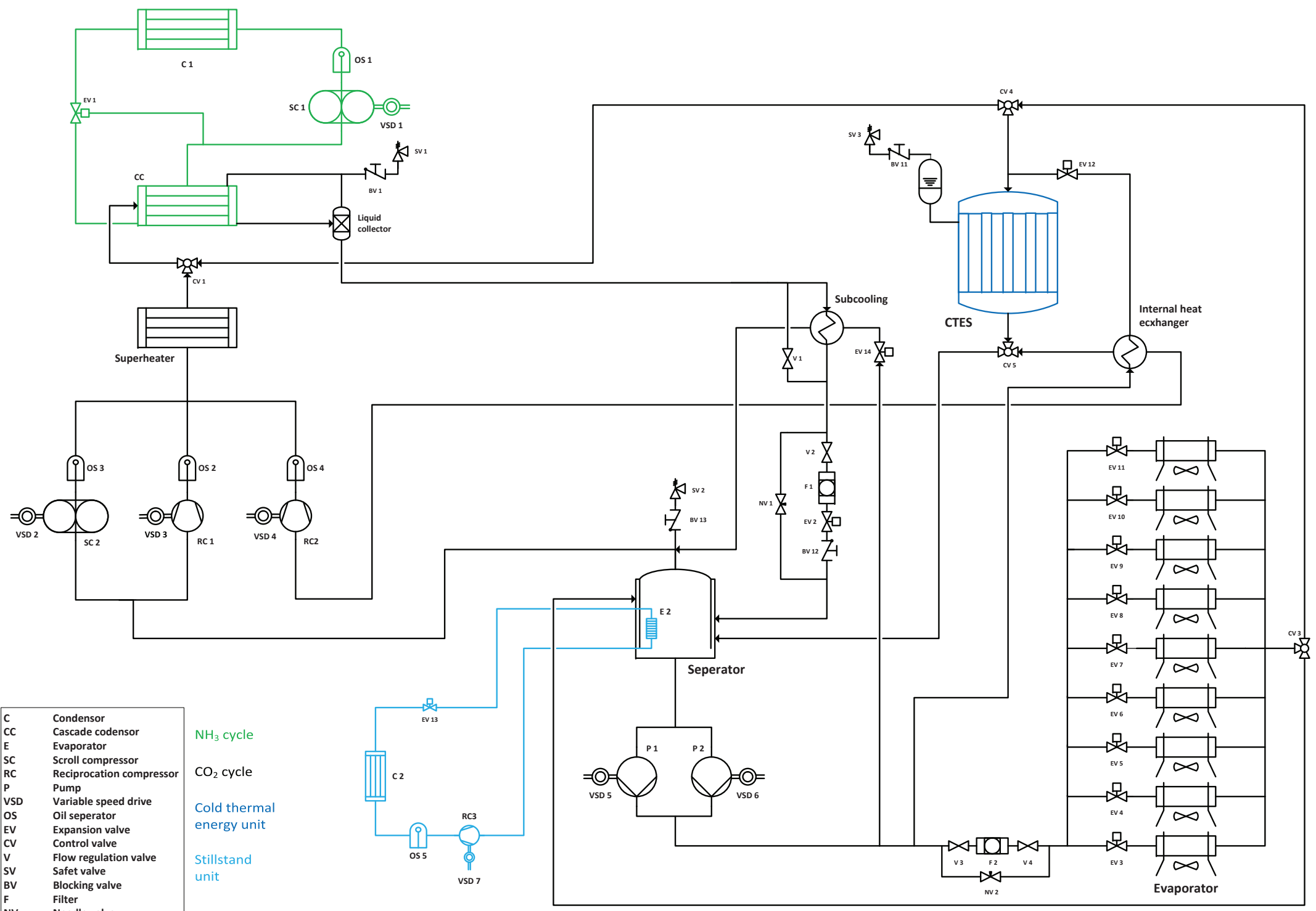


7. References

- [1] **www.norwaypelagic.no.** [Online] Norway Pelagic AS, April 05, 2014.
<http://www.norwaypelagic.no/index.asp?id=26267>.
- [2] **Industri, AIS Dybvad Stål.** *Plate Freezers aboard Fishing Vessels using CO₂ and ammonia*; Brussels, Belgium : EU ATMOSphere; 2013.
- [3] **Harald Taxt Walnum, Trond Andresen, Kristina Widell.** *Dynamic simulation of batch freezing tunnels for fish using Modelica.* Trondheim, Norway ; SINTEF Energy Research; 2011.
- [4] **Prof. John R. Thome;** *Engineering Data Book III – Chapter 13: two phase pressure drops*;
Swiss Federal Institute of Technology Lausanne (EPFL); Wolverine Tube; Inc.; 2006;
Lausanne Switzerland; <http://www.wlv.com/products/databook/db3/data/db3ch13.pdf>
- [5] **Armin Hafner, Tom Ståle Nordtvedt, Ingrid Rumpf.** *Energy saving potential in freezing applications by applying cold thermal energy storage with solid carbon dioxide.* Trondheim, Norway : SINTEF Energy Research, 2011.
- [6] **Magnussen, Ola M.** *Norsk Kjøleteknisk Møte, Industrielle Frysetunneler - Praktiske forhold ved utforming og drift.* Trondheim, Norway : NTNU Trondheim, Institutt for klima- og kuldeteknikk, 1995.



Projekt: Projekt_plan Datum: Son 13.10.13	Vorgang		Inaktiver Sammelvorgang		Externe Vorgänge	
	Unterbrechung		Manueller Vorgang		Externer Meilenstein	
	Meilenstein		Nur Dauer		Stichtag	
	Sammelvorgang		Manueller Sammelrollup		In Arbeit	
	Projektsammelvorgang		Manueller Sammelvorgang		Manueller Fortschritt	
	Inaktiver Vorgang		Nur Anfang			
	Inaktiver Meilenstein		Nur Ende			



C	Condenser
CC	Cascade condenser
E	Evaporator
SC	Scroll compressor
RC	Reciprocation compressor
P	Pump
VSD	Variable speed drive
OS	Oil separator
EV	Expansion valve
CV	Control valve
V	Flow regulation valve
SV	Safet valve
BV	Blocking valve
F	Filter
NV	Needle valve

NH₃ cycle
CO₂ cycle
Cold thermal energy unit
Stillstand unit

Material: Hot dip galvanized steel
Feuerverzinkter Stahl

Tubes/Rohre: Fe diam. (20 x 1.5)mm, 0.684 kg/m

Tube spacing/Rohrabstand: (50 x 57,74)mm (dxh/TxH), staggered/versetzte Anordnung

Tube weight/Gewicht der Rohre: mFe/AFr. x Z = 11.85 kg/m²

Tube volume/Volumen der Rohre: 0.227 L/m

Fins/Lamellen: Fe 0.4 mm; 0.56 after hot dip galvanizing nach Feuerverzinkung

La. -mm	Aä/ Ai	Apr./ Asek.	Aä/ AFr.Z	Aä/ m	Weight of fins Gewicht der Lam. mL/AFr. x Z kg/m ²	Total weight Gesamtgewicht m.ges./AFr.x Z kg/m ²	
						without Zn/ ohne Zn	with Zn/ mit Zn
4.5	22.8	0.055	21.1	1.218	32.7	44.6	55.2
6	17.5	0.066	16.2	0.935	24.6	36.5	45.0
8	13.5	0.098	12.4	0.716	18.4	30.3	37.3
10	11.0	0.122	10.2	0.589	14.7	26.6	32.7
12	9.4	0.147	8.7	0.502	12.3	24.2	29.7
15	7.8	0.183	7.2	0.416	9.82	21.7	26.5
18	6.8	0.220	6.3	0.364	8.19	20.2	24.4

La	= fin spacing	Lamellenabstand
Aä	= external surface area	äussere Fläche
Ai	= internal surface area	innere Fläche
Aprim.	= external surface area of tubes	äussere Oberfläche der Rohre
Asek.	= surface area of fins	Oberfläche der Lamellen
AFr.	= face area	Frontoberfläche
Z	= number of tube rows in depth direction	Anzahl der Rohrreihen in Tiefenrichtung
mL	= fin weight	Gewicht der Lamellen
mges.	= total weight	Gesamtgewicht

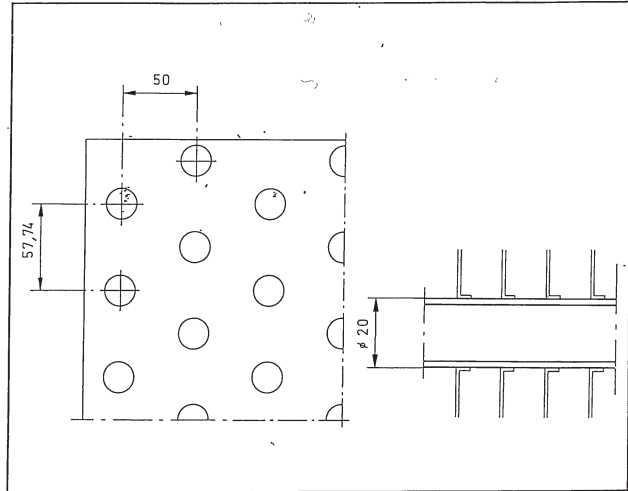
Galvanizing thickness/Verzinkungsstärke

Fins/Lamellen:	80 μ m
Tubes/Rohre:	80 μ m
Headers/Sammlerrohre	80 μ m
Casing of sendzimir-galvanized steel	20 μ m
Gehäuse aus sendzimirverzinktem Stahl	20 μ m

Lamellelement A1

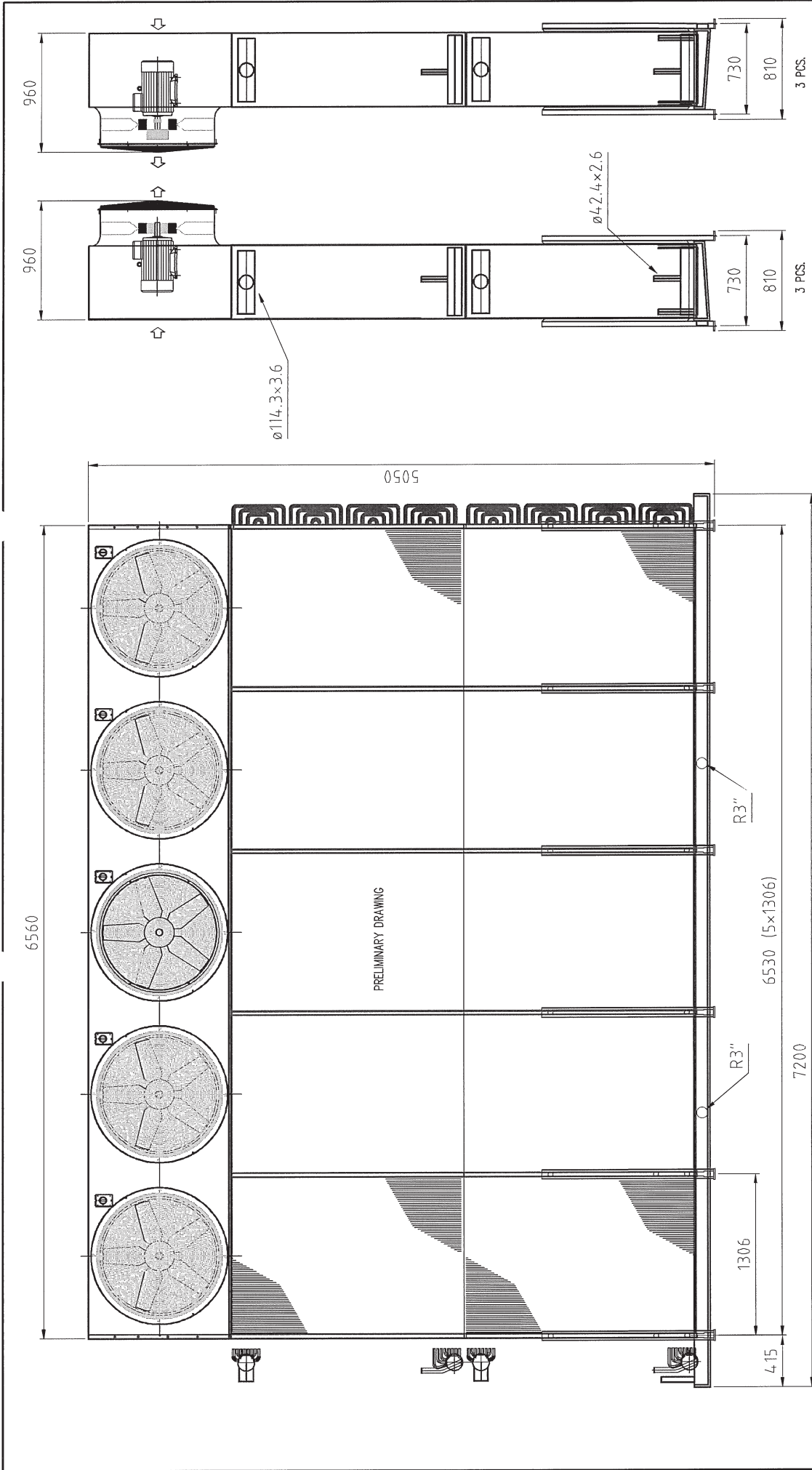
Material: Varmförzinkat stål



Rörets ytterdiameter 20 mm, rörplacering sick-sack och rördelning 57,74 x 50 mm. Standardlamelldelning 4,5, 6, 8, 10, 12, 15 och 18 mm. Största flänsad längd ca 6 m. Elementet varmgalvaniseras efter tillverkningen. Elavfrostningsstavar är placerade i rör mellan egentliga batterirör.



 **FINCOIL**

Ansatie 3, SF-01740 VANTAA, FINLAND
Tel. +358 0 89441, telefax +358 0 8944318,
teletex 1000456



0024628	<p>A1-ZZ-JXP-6500-2X1848-10-15-KK Refrigerant and system: NH3 / pumped Surface area: 833+833 m² Fin spacing: 15 mm Internal volume: 610 + 610 L Net weight: ~3000 + ~3300 kg</p>	<p>A1-ZZ-JXP-6500-2X1848-9-15-KK Refrigerant and system: NH3 / pumped Surface area: 750+750 m² Fin spacing: 15 mm Internal volume: 555 + 555 L Net weight: ~2700 + ~3000 kg</p>			<p>A1-ZZ-JXP-6500-2X1848-10-15-KK 3+3 PCS.</p>	<p>A1-ZZ-JXP-6500-2X1848-9-15-KK 3+3 PCS. Replaces</p>	<p>Associated</p>	<p>Drawn Date: H. Lintunen 23.11.2012 Checked Date: Tolerance class N EN 22768-1 22768-2</p>	<p>Frame: A3 Scale: 1:30 Job Id: Article number: 9460083246</p>
---------	---	--	--	---	--	---	-------------------	---	---

This document and its content is owned by Alfa Laval AB (publ) or its affiliates and protected by laws governing intellectual property and thereto related rights. Without limiting any rights related to this document, no part of this document may be copied, reproduced or transmitted in any form or by any means (electronic, mechanical, photocopying, recording, or otherwise), or for any purpose, without the express permission of Alfa Laval. No part of this document may be used in any other way than for the specific purpose for which it was prepared, or for any other purpose than expressly permitted by Alfa Laval. Alfa Laval will enforce its rights related to this document to the fullest extent of the law, including the seeking of criminal prosecution.

Sabroe SAB 157 HR high-pressure screw compressor units

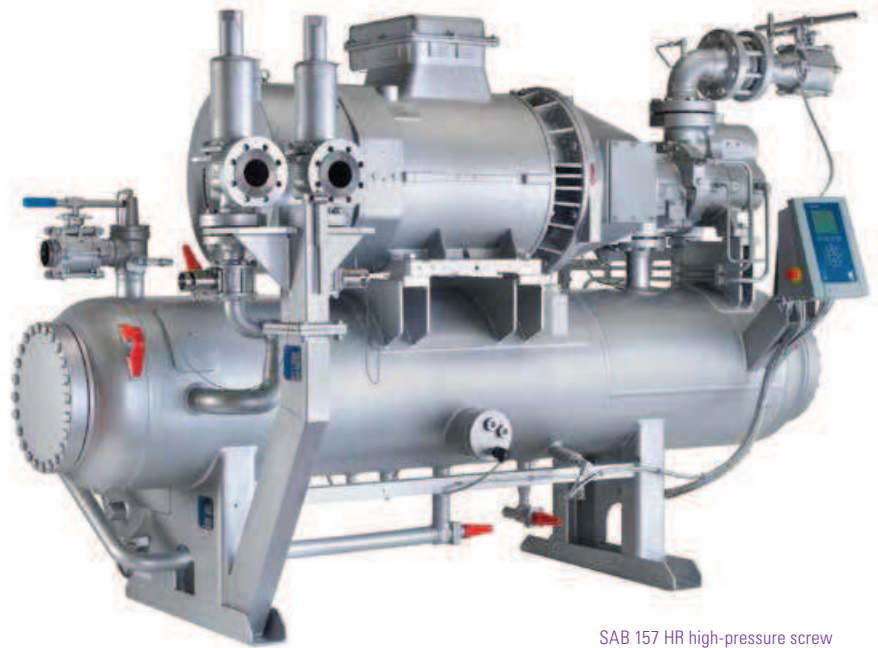
Variable-speed high-pressure screw compressor units with swept volumes of 100–600 m³/hour, for use with CO₂ as refrigerant

These unique high-pressure compressor units are ideal for low-temperature two-stage freezer installations, such as carbon dioxide–ammonia (R744–R717) cascade refrigeration systems. The 52 bar configuration makes it possible to undertake freezing and defrosting in one single stage with condensing temperatures up to 15°C.

The game-changer SAB 157 HR design radically shifts the boundaries between low-stage and high-stage refrigeration, by keeping the inter-stage temperature above 0°C so that the thermal energy in the discharge gas can be used to defrost the cooling element (hot gas defrosting).

This in turn makes it possible to make big saving on installation, piping and compressor costs because a single SAB 157 HR unit can replace multiple compressors using traditional refrigerants.

Right from the outset, SAB 157 HR units are designed for variable-speed operation and maximum flexibility, doing away with traditional capacity slide valves. Capacity range: 1000–6000 rpm.



SAB 157 HR high-pressure screw compressor unit

Significant advantages

Customer benefits

Stepless, skip-free capacity control ensures that output always matches requirements

Lowest possible operating costs and rapid return on investment

Consistently high performance at both full and part load

Maximum part-load efficiency and low life cycle costs ??

Unique 52 bar unit designed specifically for CO₂ applications

Makes it possible to undertake freezing and defrosting in one stage

Space-saving small footprint, with fewer moving parts and very low vibration

Exceptional reliability and low maintenance costs

Supports Condition Based Service (CBS) schedules and the Sabroe Block Swap Concept

Optimised service/maintenance intervals, with a minimum of unscheduled downtime



Range

One model is available to provide swept volumes of 600 m³/hour at 6000 rpm.

Options

- Thermosyphon and water-cooled oil coolers, with 3-way oil temperature control valve
- Dual external oil filters



SAB 157 HR high-pressure screw compressor block



Model	Swept volume at 6000 rpm m ³ /h	Capacities in kW at 6000 rpm R744			Dimensions in mm L x W x H	Weight excluding motor/oil kg	Sound pressure level dB(A)
		-35/+5°C	-45/-5°C	-50/-5°C			
SAB 157 HR	596	939	630	585	3300 x 1500 x 2100	2600	on request

Nominal capacities are based on 6000 rpm at 60 Hz.

Sound pressure levels in free field, over reflecting plane and one metre distance from the unit.

All information is subject to change without previous notice

Johnson Controls Denmark ApS · Sabroe Factory
Christian X's Vej 201 · 8270 Højbjerg · Denmark
Phone +45 87 36 70 00 · Fax +45 87 36 70 05
www.sabroe.com



° In touch with our products

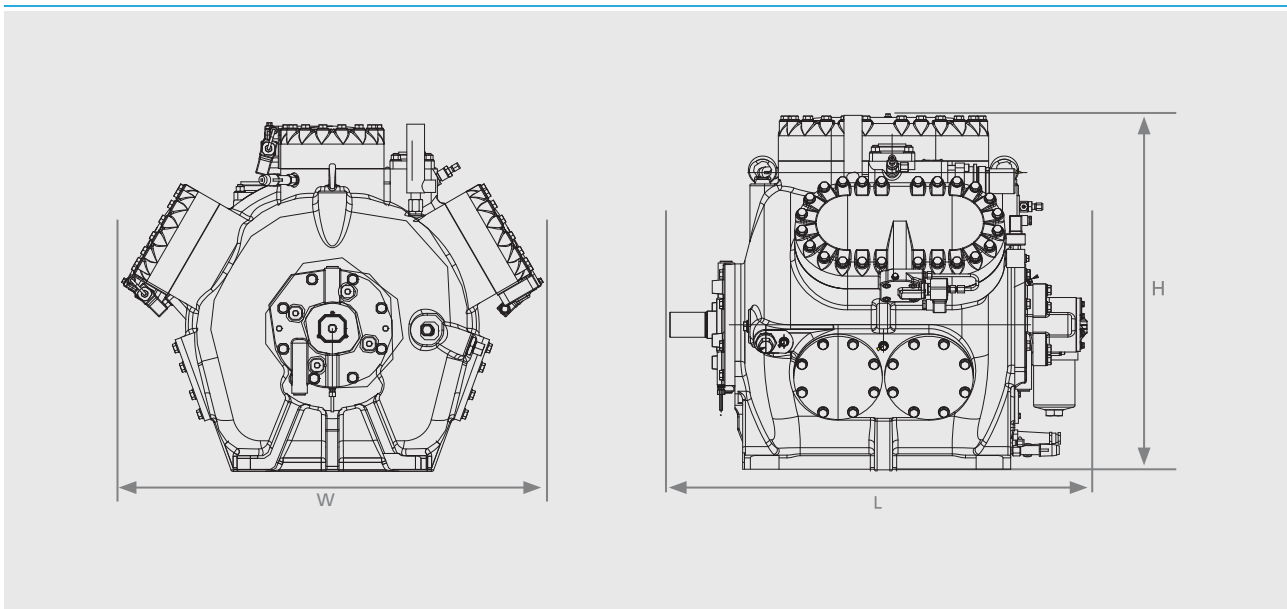
Technical data and features

Models	Swept Volume* (m ³ /h)	Cooling cap. (kW)**		Dimensions (mm)			Weight (kg)
		CO ₂		L	W	H	
Single stage		-50/0 °C	-40/-10 °C				
Grasso 35HP	101	88	152	883	861	718	552
Grasso 45HP	135	117	202	883	861	718	552
Grasso 55HP	168	147	252	919	943	768	633
Grasso 65HP	202	176	303	919	943	768	633

Models	Swept Volume* (m ³ /h)	Cooling cap. (kW)**		Dimensions (mm)			Weight (kg)
		NH ₃		L	W	H	
Single stage		35/82 °C	35/70 °C				
Grasso 35HP	101	260	276	883	861	718	552
Grasso 45HP	135	346	368	883	861	718	552
Grasso 55HP	168	433	460	919	943	768	633
Grasso 65HP	202	520	552	919	943	768	633

* Theoretical swept volume based on max. speed of N = 1500 min.⁻¹

** Capacity based on: 2K superheat, 0K subcooling



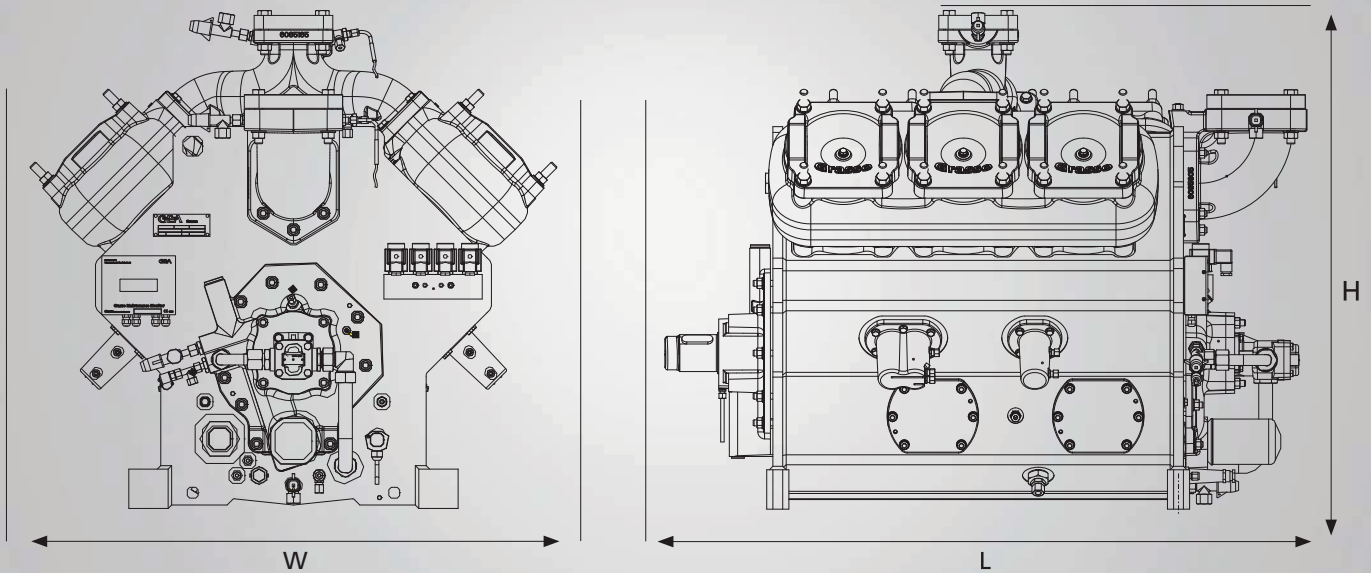
GEA Refrigeration Technologies

GEA Refrigeration Netherlands N.V.

P.O. Box 343 • 5201 AH 's-Hertogenbosch • The Netherlands • Phone +31 (0)73 6203 911 • info@grasso.nl • www.grasso.nl

Subject to modification • Copyright GEA • www.gearefrigeration.com





Models	Swept volume* (m³/h)	Number of cylinders	Speed min.-1	Cooling cap. (kW)** NH ₃		Dimensions (mm)			Weight (kg)
				-10/+35 °C	0/+40 °C	L	W	H	
Single stage									
GEA Grasso V 300	290	4	1500	155	237	882	933	922	575
GEA Grasso V 450	435	6	1500	233	355	1076	933	922	751
GEA Grasso V 600	580	8	1500	310	474	1363	933	922	1042
GEA Grasso V 700	637	4	1200	367	549	1062	1076	1013	794
GEA Grasso V 1100	955	6	1200	550	823	1306	1076	1013	1054
GEA Grasso V 1400	1274	8	1200	734	1098	1666	1076	1027	1495
GEA Grasso V 1800	1592	10	1200	917	1372	1909	1076	1027	1725

Models	Swept volume* (m³/h)	Number of cylinders Low/High stage	Speed min.-1	Cooling cap. (kW)** NH ₃ ***		Dimensions (mm)			Weight (kg)
				-35/+35 °C	-40/+35 °C	L	W	H	
Two stage									
GEA Grasso V 300T	217	3/1	1500	45	34	935	940	922	590
GEA Grasso V 450T	290	4/2	1500	67	52	1310	940	922	769
GEA Grasso V 600T	435	6/2	1500	90	68	1425	940	922	1062
GEA Grasso V 700T	478	3/1	1200	108	85	1060	1072	1013	814
GEA Grasso V1100T	637	4/2	1200	157	123	1304	1072	1013	1077
GEA Grasso V1400T	955	6/2	1200	217	170	1672	1072	1027	1520
GEA Grasso V1800T	1114	7/3	1200	262	203	1874	1072	1027	1755

* Theoretical swept volume based on low stage cylinders

** Based on: 0K subcooling, 2K superheat (non usefull)

*** Cooling capacity based on open flash interstage cooler system (GEA Grasso system "C")

GEA Grasso MC



The GEA Grasso MC series comes in four sizes with a swept volume ranging from 471 to 860 m³/h. It has a simple and compact design between the compressor and package. Some package components may come already integrated such as a suction side non-return valve, suction filter, an oil pump along with an oil and hydraulic system with the appropriate solenoid valve assemblies for Vi and capacity adjustment. The control lines for the solenoid valve for Vi and capacity control are connected directly to the compressor. The stepless capacity and Vi control enables high efficiency in part and full load.

Technical data

- Integration of package components
- Integrated oil distribution system
- Compact design
- Rotors completely equipped with roller bearings
- Stepless capacity and Vi control by parallel slide system

Technical data										
Series	Compressor type ¹⁾	Swept volume ²⁾ (m ³ /h)	Swept volume ³⁾ (cfm)	Max. design pressure (bar)	Dimensions (mm)			DN1 ⁴⁾ (mm)	DN2 ⁵⁾ (mm)	Weight (kg)
					L	W	H			
GEA Grasso MC	H	471	335	28 / 52	938	425	554	125	80	340
	L	544	387	28 / 52	974	425	554	125	80	365
	M	690	490	28 / 52	1090	480	610	150	100	580
	N	860	611	28 / 52	1135	480	610	150	100	640

1) regarding swept volume, 2) at 2940 min⁻¹, 3) at 3550 min⁻¹, 4) suction connection, 5) discharge connection

Capacity					
Series	Compressor type ¹⁾	28 bar compressor ²⁾ (kW)		52 bar compressor ²⁾ (kW)	
		Cooling capacity ³⁾ NH ₃ -35/+35 °C	Cooling capacity NH ₃ 0/+35 °C	Cooling capacity CO ₂ -50/-5 °C	Heating capacity NH ₃ +35/+80 °C
GEA Grasso MC	H	112	431	482	1.303
	L	129	498	556	1.285
	M	165	637	712	1.900
	N	206	795	888	-

1) regarding swept volume, 2) at 2940 min⁻¹ with 5 K superheat and 0 K subcooling, stated temperature values: evaporation/condensation, 3) with economizer

GEA Grasso SH



The GEA Grasso SH series comes in four sizes with a swept volume ranging from 231 to 372 m³/h. The simple design is owed by the integration of the complete oil management system with only one oil connection and important package elements in the compressor. The screw compressors come equipped with connections for monitoring pressure and temperature, position displays on the control screen, and controlling the integrated solenoid valve assembly for combined Vi and capacity adjustment. The direct assignment of the solenoid valves to Vi and capacity regulation and the connection of pressure and temperature sensors on the compressor ease assembly and service work on the package. The parallel slide system allows for Vi optimization and part load adaption to take place simultaneously and independently of one another. It means that even in part load operations a low-loss work process is possible for the screw compressor.

Technical data

- Integration of package components
- Integration of oil management system
- Compact design
- Rotors completely equipped with roller bearings
- Capacity and Vi control by parallel slide system
- Suitable for all standard DIN-flange motors

Technical data										
Series	Compressor type ¹⁾	Swept volume ²⁾ (m ³ /h)	Swept volume ³⁾ (cfm)	Max. design pressure (bar)	Dimensions (mm)			DN1 ⁴⁾ (mm)	DN2 ⁵⁾ (mm)	Weight ⁶⁾ (kg)
					L ⁶⁾	W	H			
GEA Grasso SH	C	231	164	28 / 52	888	585	560	80	50	313
	D	265	188	28 / 52	918	585	560	80	50	324
	E	321	228	28 / 52	975	675	670	100	65	460
	G	372	264	28 / 52	1004	675	670	100	65	471

1) regarding swept volume, 2) at 2940 min⁻¹, 3) at 3550 min⁻¹, 4) suction connection, 5) discharge connection, 6) length and weight depending on motor

Capacity					
Series	Compressor type ¹⁾	28 bar compressor ²⁾ (kW)		52 bar compressor ²⁾ (kW)	
		Cooling capacity ³⁾ NH ₃ -35/+35 °C	Cooling capacity NH ₃ 0/+35 °C	Cooling capacity CO ₂ -50/-5 °C	Heating capacity NH ₃ +35/+80 °C
GEA Grasso SH	C	50	194	226	587
	D	60	230	268	-
	E	72	279	312	839
	G	85	330	369	-

1) regarding swept volume, 2) at 2940 min⁻¹ with 5 K superheat and 0 K subcooling, stated temperature values: evaporation/condensation, 3) with economizer



Offer

Sintef Energi AS

Kolbjørns Hejes vei 1 A

Att.: Ephraim Gukelberger

Dato: 14.03.2014
Tilbud nr.: 11140131-S
Vår ref.: Håvard Næss
Deres ref.: Kjøleanlegg
Leveringstid: 6-7 working weeks
Leveringsmåte: Bring
Leveringsbetingelser: Ex W. KSB Norge, ex VAT
Kontraktsbetingelser: In accordance with NL09
Gyldig til: 30.04.2014
Betalingsbetingelser: Net 30 days
Valuta: NOK
Side: 1

We thank you for your inquiry and quote:

Varenr.	Beskrivelse	Antall	Pris	Rabatt %	Beløp
Budget offer					
111221000	Sea water feed pumps: <i>Alternativ 25m³/h @ 25m:</i> KSB MCPK065-040-165 CC See datasheet for further information	1	55 000,00		55 000,00
111221000	<i>Alternativ 50m³/h @ 25m:</i> KSB MCPK080-050-160 CC See datasheet for further information	1	60 000,00		60 000,00
111221000	<i>Alternativ 100m³/h @ 25m:</i> KSB MCPK100-065-160 CC See datasheet for further information	1	75 000,00		75 000,00
111830000	Refrigeration pump (CO2 / R744) KSB/Nikkiso HQ21A-A1 Pump can be optimized to 1m ³ /h, 2m ³ /h or 3m ³ /h. This will not affect price. See datasheet for further information NB! Delivery time for refrigiaton pump is 18 working weeks.	1	85 000,00		85 000,00

With kind regards

KSB NORGE AS

Totalbeløp:

275 000,00

Data sheet



Customer item no.: 50 m³/h@25m

Order dated:

Order no.:

Quantity: 1

Number: ES 2837045

Item no.: 100

Date: 12/03/2014

Page: 1 / 6

MCPK080-050-160 CC NA 00752A

Chemical pump to EN 22858/ISO 2858/ISO 5199

Version no.: 1

Operating data

Requested flow rate	50.00 m ³ /h	Actual flow rate	50.00 m ³ /h
Requested developed head	25.00 m	Actual developed head	25.00 m
Pumped medium	Water, sea and brackish water Brackish water Not containing chemical and mechanical substances which affect the materials	Efficiency	72.8 %
Ambient air temperature	20.0 °C	Power absorbed	4.82 kW
Fluid temperature	10.0 °C	Pump speed of rotation	2968 rpm
Fluid density	1030 kg/m ³	NPSH required	2.54 m
Fluid viscosity	1.37 mm ² /s	Permissible operating pressure	16.00 bar.g
Suction pressure max.	0.00 bar.g	Discharge press.	2.52 bar.g
Mass flow rate	14.30 kg/s	Min. allow. mass flow for continuous stable operation	2.83 kg/s
Max. power on curve	6.11 kW	Shutoff head	28.01 m
Min. allow. flow for continuous stable operation	9.89 m ³ /h	Max. allow. mass flow	23.23 kg/s Tolerances to ISO 9906 Class 3B; below 10 kW acc. to paragraph 4.4.2

Design

Pump standard	ISO 2858	Manufacturer	Burgmann
Design	Baseplate mounted, long-coupled	Type	MG1G6
Orientation	Horizontal	Material code	Q1Q1VGG
Shaft execution	Dry	Sealing plan	A Single-acting mechanical seal (A-type casing cover, taper bore)
Pump nominal pressure	PN 16	Seal chamber design	Conical seal chamber (A-type cover)
Suction nominal dia.	DN 80	Impeller diameter	137.0 mm
Suction nominal pressure	PN 16	Free passage size	11.6 mm
Suction position	axial	Direction of rotation from drive	Clockwise
Suction flange dimension according to standard	EN1092-1	Bearing bracket construction	Chemical standard economy
Suction flange drilled according to standard	EN1092-1	Bearing bracket size	CS40
Discharge nominal dia.	DN 50	Bearing seal	Lip seal
Discharge nominal pressure	PN 16	Bearing type	Anti-friction bearings
Discharge position	top (0°/360°)	Lubrication type	Oil
Discharge flange dimension according to standard.	EN1092-1	Lubrication monitoring	Constant level oiler
Discharge flange drilled according to standard	EN1092-1	Bearing bracket cooling	Uncooled
Surface type	Raised face form B1 (to EN 1092-1)	Color	Ultramarine blue (RAL 5002) KSB-blue
Shaft seal	Single acting mechanical seal		

Performance curve

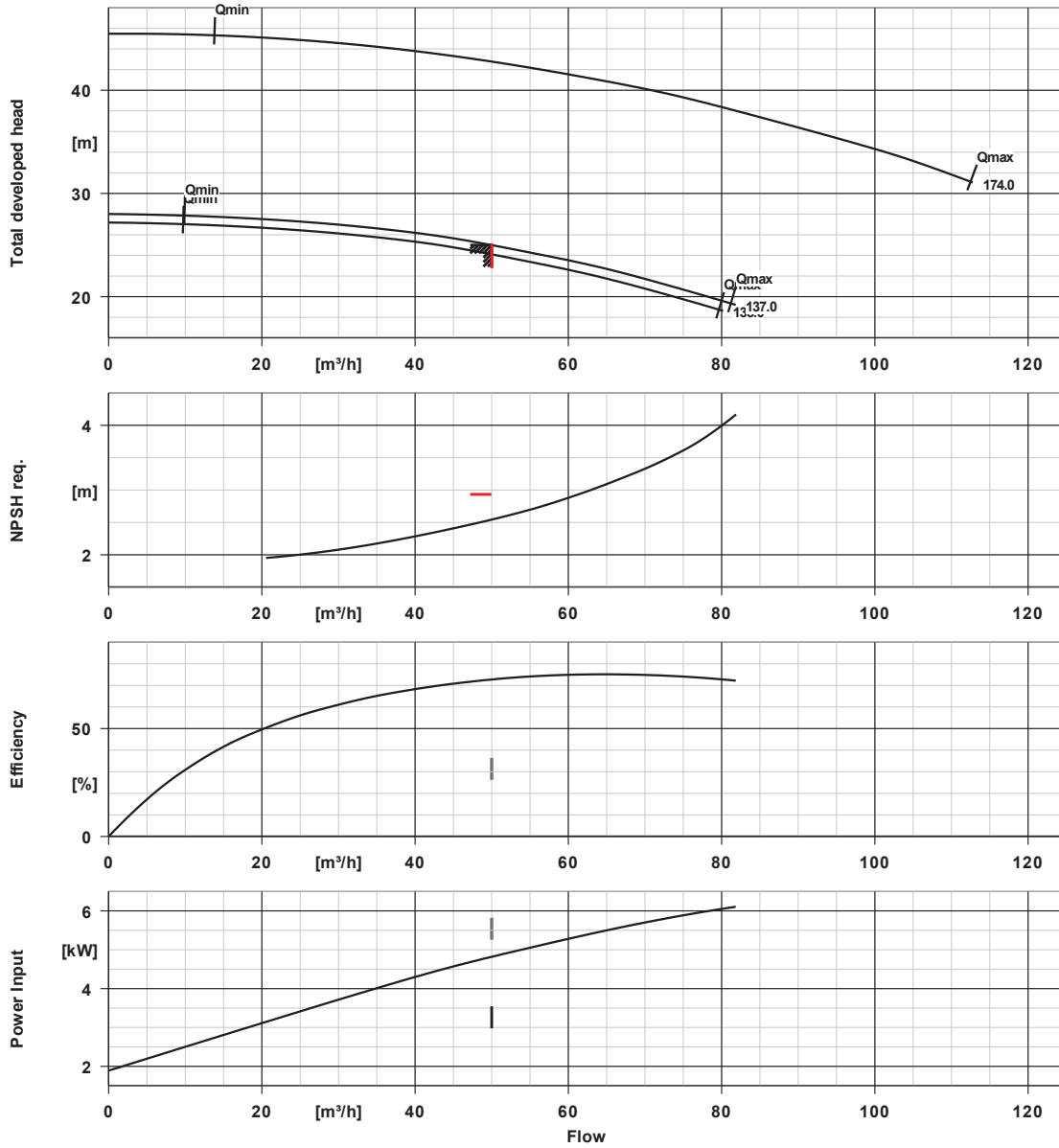


Customer item no.: 50 m³/h@25m
 Order dated:
 Order no.:
 Quantity: 1

Number: ES 2837045
 Item no.: 100
 Date: 12/03/2014
 Page: 3 / 6

MCPK080-050-160 CC NA 00752A
 Chemical pump to EN 22858/ISO 2858/ISO 5199

Version no.: 1



Curve data

Speed of rotation	2968 rpm	Requested developed head	25.00 m
Fluid density	1030 kg/m ³	Efficiency	72.8 %
Viscosity	1.37 mm ² /s	Power absorbed	4.82 kW
Flow rate	50.00 m ³ /h	NPSH required	2.54 m
Requested flow rate	50.00 m ³ /h	Curve number	KGP.452/31
Total developed head	25.00 m	Effective impeller diameter	137.0 mm



NIKKISO NON-SEAL PUMP DATA SHEET



(CENTRIFUGAL CANNED MOTOR PUMP) HQ21A-A1FGT-01D1XX-AZCHF4G1

PURCHASER _____
 OWNER _____
 SITE _____
 UNIT _____
 SERVICE **REFIGERATION PUMP**
 ITEM NO. **ITEM 3**
 NO. OF PUMP REQ **1** DRIVER **CANNED MOTOR**
 PUMP MFR. **NIKKISO CO., LTD.** MODEL NO. **HQ21A-A1**

DOC NO. **EKD73-8905 03REV.**
 PURCHASER JOB NO. _____
 ORDER NO. _____
 NIKKISO MASTER NO. _____
 MADE BY _____
 APPROVED BY _____
 SERIAL NO. _____

OPERATING CONDITION				PERFORMANCE	
LIQUID C02/R744	CAP. @PT (m ³ /h) NOR			SPEED (min ⁻¹)	2850
	RATED	3		NPSHR (WATER) (m)	0.91
PUMPING TEMP. (°C) -50	DISCH. PRESS (barG)	0.98		MIN. CONTINUOUS FLOW (m ³ /h)	0.6
SP. GR. @PT 1 #	SUCT. PRESS (barG) MAX			ROTATION (VIEWED FROM MOTOR)	CW
VAP. PRESS @PT (barA) #	NOR			PUMP EFF (%)	21.4
VISCOSITY @PT (mPa·s) 1 #	DIFF. PRESS (bar)	0.98		RATED BHP (KW)	0.38
SP. HEAT @PT (kJ/kg·°C) 2.09 #	DIFF. HEAD (m) #2	10		MAX. BHP (KW)	0.46
MELTING TEMP. (°C)	NPSHA (m)			HEAD (M)	11.1
CORR/EROS. CAUSED BY	HYD. hp (kW)	0.08		WITH RATED IMP.	

CONSTRUCTION				AUXILIARY PIPING	
CASING MOUNT FOOT	CASING SPLIT RADIAL			C. W. REQ (m ³ /h)	MAX 36 (CG)
TYPE SINGLE VOLUTE				REV. CIRCULATION (m ³ /h)	0.7
MAX. ALLOWABLE PRESS. (barG) 10	@ (°C) -50			LOSS IN REV. CIRC. LINE (m)	6
HYDROSTATIC TEST PRESS. (barG) 15				EXT. FLUSH FLUID	-
IMPELLER DIA. (mm) RATED 80	MAX 100	MIN 80		(m ³ /h)	-
MOUNT OVERHUNG	IMPELLER TYPE OPEN			(barG)	-
BEARING TYPE RADIAL SLEEVE	THRUST PLAIN				
LUBRICATION SELF (PUMPING LIQUID)					
NO. OF STAGES 1					
COUPLING NOT REQ'D	PACKING NOT REQ'D				
MECHANICAL SEAL NOT REQ'D	BASE COMMON				

MATERIALS					
CASING	SCS14A				
IMPELLER	SCS14				
SHAFT	SUS316				
STATOR LINER (CAN)	HC-N				
ROTOR SLEEVE (CAN)	HC-N				
BEARING	CG93				
SHAFT SLEEVE	SUS316/WC-NI				
THRUST WASHER	SUS316/WC-NI				
PUMP GASKET	PTFE-GL				
MOTOR GASKET	PTFE				
STATOR BANDS	SUS304				

BEARING MONITOR **E MONITOR FOR LOCAL INDICATION**

MOTOR DRIVER				INSPECTION & TESTS	
kW 0.8	SYNCHRONOUS SPEED (min ⁻¹) 3000			TEST	REQ WIT
VOLT / PHASE / HERTZ 400 / 3 / 50				PERFORMANCE	YES NO
FULL LOAD AMPS 2.1	LOCKED ROTOR AMPS 8			HYDROSTATIC	YES NO
MANUFACTURER NIKKISO					
TYPE SQUIRREL CAGE INDUCTION MOTOR					
INS. CLASS 155	ENCL/EX-PROOF IP55/TE				
CONDUIT TAP FOR MOTOR LEAD 28					
FOR THERMOSTAT 22					

INSPECTION & TESTS	
TEST	REQ WIT
PERFORMANCE	YES NO
HYDROSTATIC	YES NO
MASS (kg) (PUMP & MOTOR) 50	

REMARKS

PLEASE CONFIRM THE ABOVE SPECIFIC DATA MARKED AS # WHEN YOU SHOULD PLACE AN ORDER ON US.
#2 : WITH DISCHARGE ORIFICE
THERMOSTATS ARE NORMALLY CLOSE

PAINTING RAL 6011 (GREEN)

MATERIAL CODE (ASTM EQUIVALENT)

FC0450	DUCTILE IRON (A536 65-45-12)
SCW480	CAST STBBL (A216 WCB)
S25C	STBBL (A108 1025)
SCS13A	304 SS CASTING (A351 CF8)
SCS14A	316 SS CASTING (A351 CF8M)
SUS304	304 SS (A276 304)
SUS316	316 SS (A276 316)
HC	HASTELLOY C-276 (B675) EQUIV.
CG X	CARBON GRAPHITE NO. X (-)
V6501	NON-ASBESTOS SHEET (-)
PTFE	POLYTETRAFLUORO ETHYLENE (-)
HCR	HARD CHROMIUM PLATING (-)
GRA	GRAPHITE SHEET (-)



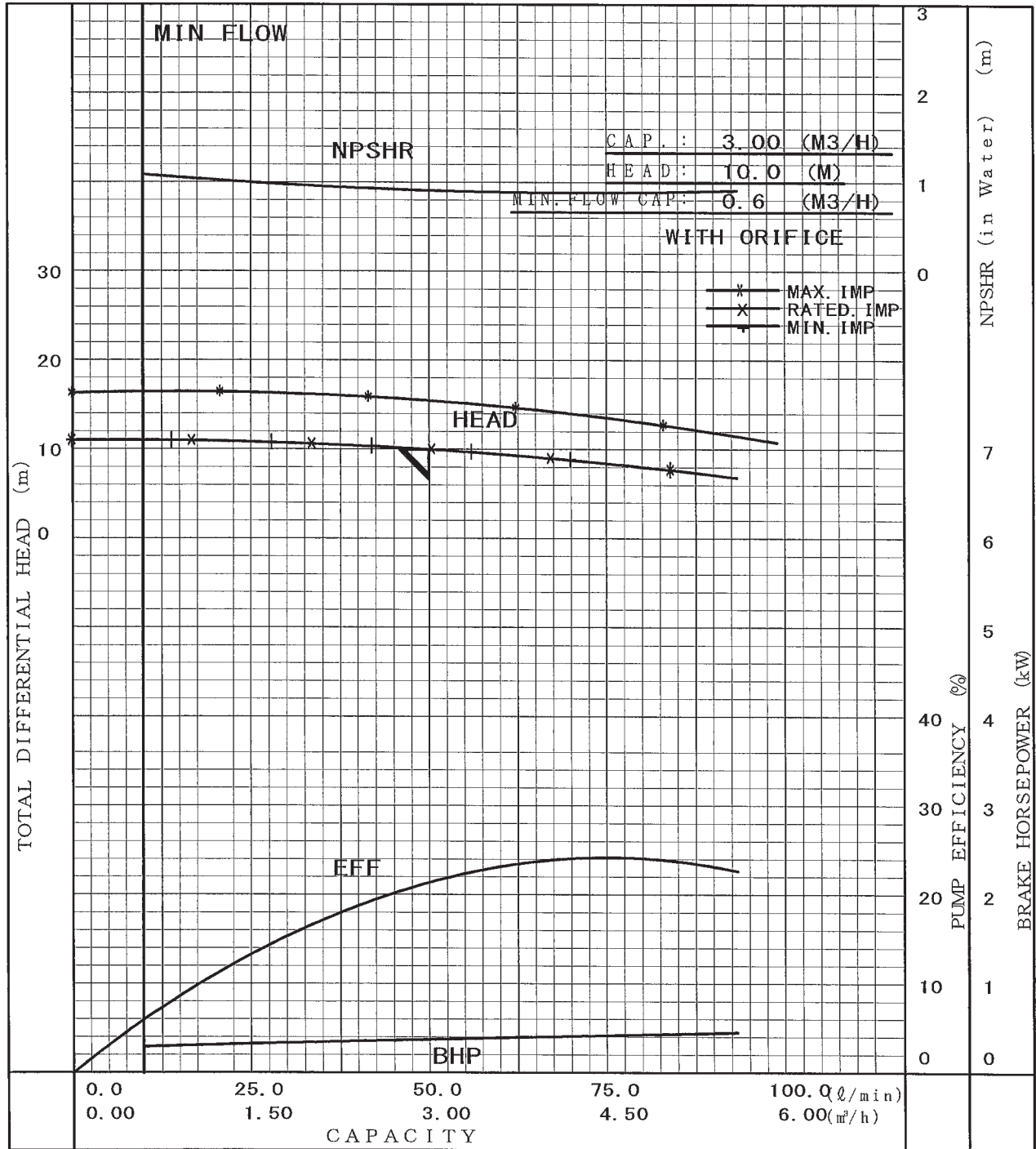
NON-SEAL PUMP EXPECTED PERFORMANCE CURVE

SHEET NO. 1 OF 1

ITEM NO. ITEM 3
 NO. REQ'D 1

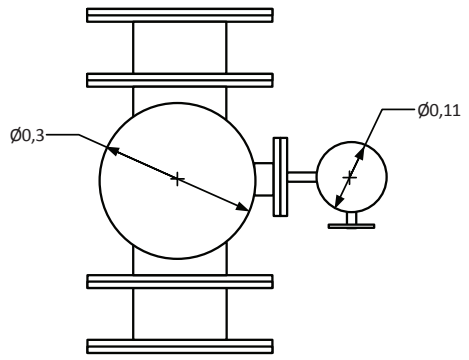
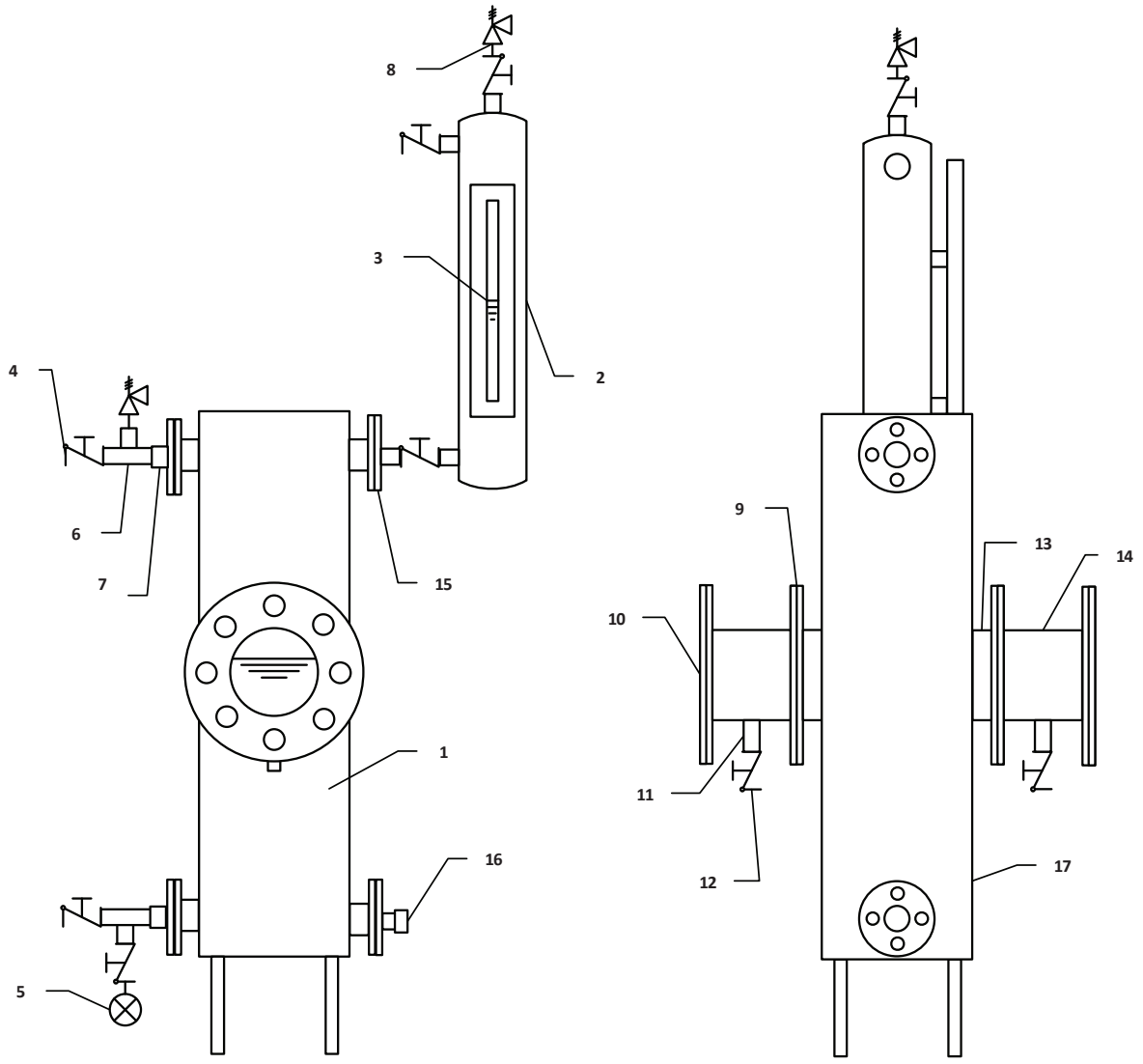
DOCUMENT NO. KD73-8905 -P21A 03
 MODEL HQ21A-A1
 SERIAL NO. _____

SPBC. LIQUID CO2/R744 TEMP. -50.0°C SP. MASS 1.000 kg/l VISC. 1.00 mPa·s SPECIFIED PT.



◇ ×					APPROVED BY	CHECKD BY	MADE BY
◇ ×							
◇ ×							
◇ ×							
REV.	DATE	DESCRIPTION	MADE BY	APPROVED BY			

Latent heat CO₂ storage system



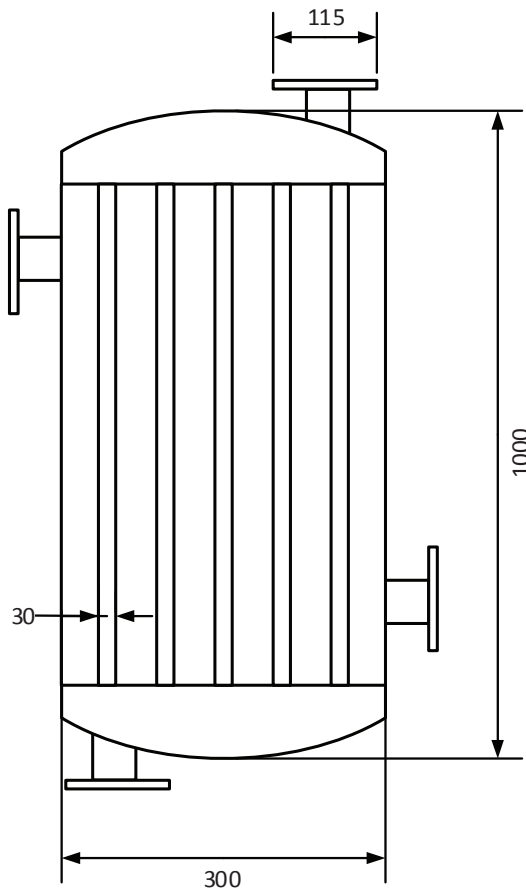
Facility requirements					SUM [NOK]	101128.95		
Nr.	Part	Quantity	Manufacturer	Specification	Type reference	Price per piece [NOK]	Total [NOK]	Contact
1	Shell & tube heat exchanger	1	Skala fabrikk	Tilbud nr 14009		54000.00	54000	Kjell.Walseth@skala.no Phone: +47 73 87 60 76
2	Liquid collector	1	KLIMAL/ Skala fabrikk			1271.41	1271.41	www.klimal.de Phone: +49/89-800624-0
3	Gauge glass	1	Klinger	1/2"; 400 mm	R25-DG	3583.40	3583.40	verena.enold@klinger-schoeneberg.de Phone: +49 6126 950 253
4	Ball valve	6	Swagelok/Svafas	1/2"	SS-AFSS8	2099.00	12594.00	ole.richard.bodtker@svafas.no Mobile: +47 90 24 79 02
5	Analog manometer	1	Empeo		SN120	492.00	492.00	http://www.empeo.de Phone: +49/2241-845230-0
6	Tee fitting, union	2	Swagelok/Svafas	1/2"	-810-3	318.00	636.00	ole.richard.bodtker@svafas.no Mobile: +47 90 24 79 02
7	Hex Reducing Nipples (Male NPT)	3	Swagelok/Svafas	1" to 1/2"	-16-HRN-8	246.00	738.00	ole.richard.bodtker@svafas.no Mobile: +47 90 24 79 02
8	Safety valve	2	HEROSE	1/2"	6801	2829.82	5659.64	Soeren.Thele@herose.com Phone: +49 4531 509-147
9	Gauge glass	2	ACI Industriarmaturen		N_230 (PN 25)	3118.50	6237.00	Gerd.Falck@aci-industriarmaturen.de Phone: +49/2403- 74885-12
10	Gauge glass	2	ACI Industriarmaturen		N_120 (PN 16)	1886.00	3772.00	
11	Tube Butt Weld, Bodies	2	Swagelok/Svafas	3/8"	6LV-4-HVCR-1-6TB7	124.00	248.00	ole.richard.bodtker@svafas.no Mobile: +47 90 24 79 02
12	Ball valve	2	Swagelok/Svafas	3/8"	SS-AFSS6	1950.00	3900.00	ole.richard.bodtker@svafas.no Mobile: +47 90 24 79 02
13	Pipe, stainless steel	2		DN 150, l = 75				
14	Pipe, stainless steel	2		DN 160, l = 125				
15	Flansh (diameter reducer)	4	Swagelok/Svafas	DN40, screw connection	SS-25M0-F25M-40-C	825.00	3300.00	ole.richard.bodtker@svafas.no Mobile: +47 90 24 79 02
16	Metal cap	1	Swagelok/Svafas	1"	SS-16-VCR-CP	629.00	629.00	ole.richard.bodtker@svafas.no Mobile: +47 90 24 79 02
17	Insulation	5	Armacell [m ²]	s = 32 mm	AF/Armaflex	813.70	4068.50	http://www.armacell.de Phone: +49/251-76 03-0

- Maximum pressure operation = 25 bar
- Minimum Temperature = -60°C
- CO₂ as process and cooling media

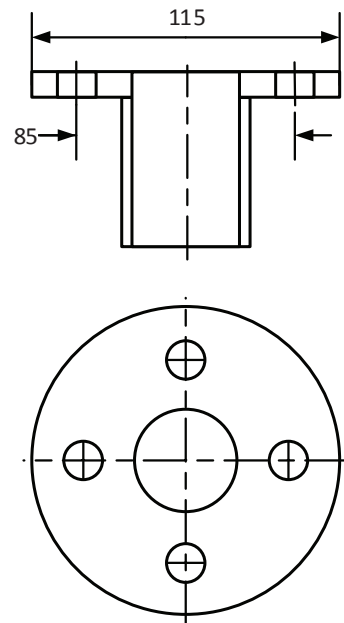
to verify!!!

Shell and heat tube exchanger

- DIN Flanges, Pressure class PN40, Flange DIN size DN25
- 10 tubes with a diameter of 30 mm



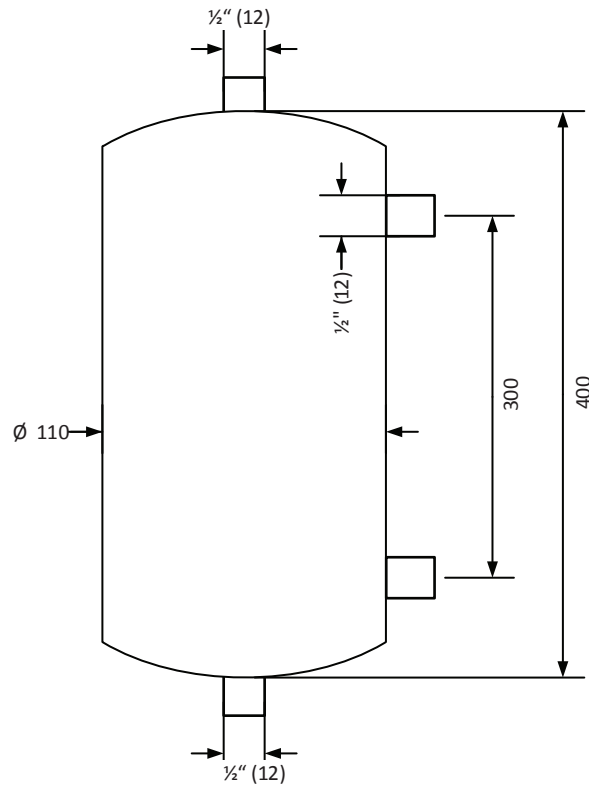
Heat exchanger



Flange connection (4x)

Liquid receiver

- All connections $\frac{1}{2}$ " (12 mm) with outer thread for further connection purposes



Ephraim Gukelberger
SINTEF Energy Research
Dept: Energy efficiency
Kolbjørn Hejes vei 1 A
Trondheim, Norway
E-mail: E.Gukelberger@gmail.com
Phone: +47 - 483 301 27

SINTEF Energi AS
Att: Ephrahim Gukelberger

Vår ref. Kjell Walseth

Trondheim, 05.02.2014

Tilbud nr 14009

Tube heat exchanger

Vi viser til tidligere kontakt, og Skala Fabrikk har med dette gleden av å gi tilbud på:

Pos. Ant. Beskrivelse:

1. 1 Varmeveksler

Pris

NOK 54.000,-

Prisforbehold Prisen er eksk. mva. og basert på dagens nivå for materialpriser og lønninger, samt på det statlige avgiftssystem. Det tas forbehold om prisendring, som er tillatt iht. den til enhver tid gjeldende prislovgivning.

Leveringsbet. EXW (Incoterms 2010)

Alm. bet. I følge NL-01

Leveringstid 14 dager etter bestilling.

Betalingsbet. Ved levering

Tilbudets gyldighet 30 dager fra tilbudsdato

Vi håper tilbudet er etter Deres ønske, og ser fram til å høre fra Dem igjen.

Vennlig hilsen
Skala Fabrikk AS



KLIMAL

Komponenten für Kälte- und Klimaanlage Vertriebs GmbH

D-82178 Puchheim · Grillenweg 21

Telefon: 089/80 06 24-0

Telefax: 089/80 06 24-25

e-Mail: info@klimal.de

Internet: www.klimal.de

Seite 1 / 1

SINTEF Energy Research
Herr Ephraim Gukelberger
Kolbjorn Hejes vei 1 A
TRONDHEIM
NORWEGEN

Angebot

Nr. **149640**

Datum: 18.02.2014

Unsere Ust-Id-Nr.: DE 128233379

Ihre Fax-Nr.:

Kunden-Nr.: 10528

Email: **e.gukelberger@gmail.com**

Ihre Anfrage E-Mail vom 12.02.2014

Vielen Dank für Ihre Anfrage. Gerne unterbreiten wir Ihnen ein Angebot auf der Grundlage von unseren Allgemeinen Geschäftsbedingungen:

Pos.	Bezeichnung Art.Nr.	Menge	Einzelpreis EUR	Pos.Wert EUR
1	Flüssigkeitssammler F 4.15 (M16/M16)28b(-60°C) Sintef FO70004150001616H028C -Konformitätserklärung und Betriebsanleitung liegen der Lieferung bei	1,00 STK	155,05	155,05

- **Lieferzeit 3-4 Wochen**
ab Bestellung
- **ab Lager Klimal, verpackt**

Anlage: Zeichnung/en
Codice 130.1505.A

Warenwert NETTO		ACHTUNG:	MwSt %
EUR 155,05		5 € Transportkostenpauschale bei NETTO-Bestellwert < 250 €	19,0%

Zahlungsbedingungen: 8 Tage 2,00% Skonto, 30 Tage netto

Lieferkondition: unfrei

Auf Ihren Auftrag würden wir uns freuen.

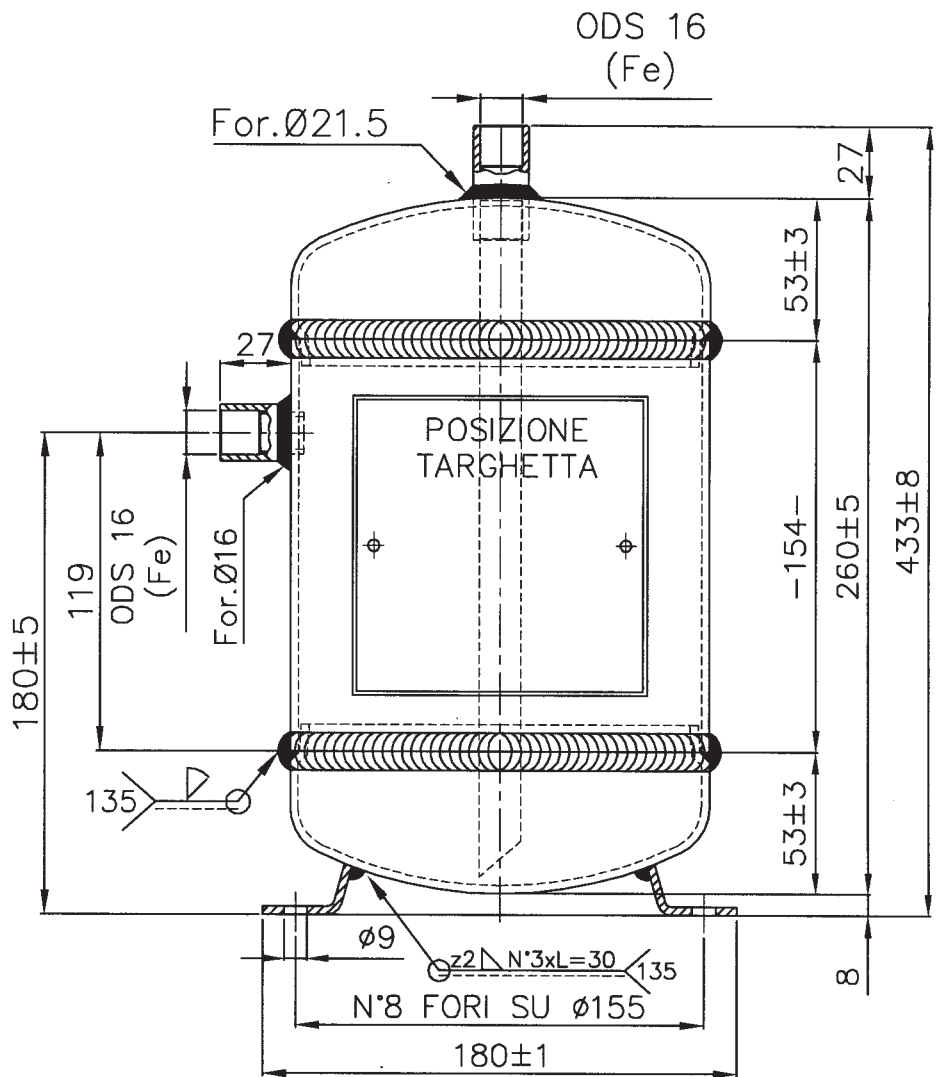
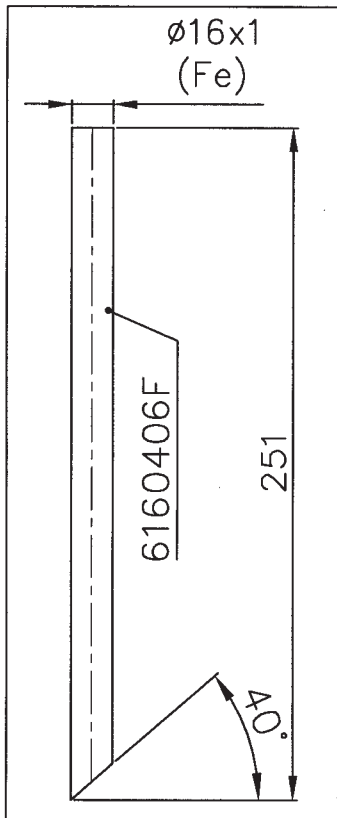
Mit freundlichen Grüßen

KLIMAL / Zikeli

Hypo Vereinsbank München
Konto: 2390333334
BLZ: 70020270
SWIFT: HYVEDEMMXXX
IBAN: DE58 7002 0270 2390 3333 34

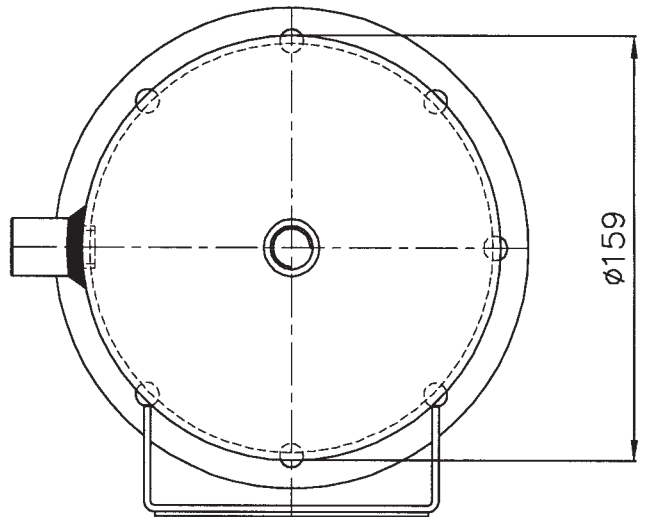
Sparkasse Fürstenfeldbruck
Konto: 1646066
BLZ: 70053070
SWIFT: BYLADEM1FFB
IBAN: DE95 7005 3070 0001 646066

KLIMAL GmbH
HRB München 75343
Geschäftsführer: Michael Zikeli, Hildegard Zikeli
St.Nr. 117/130/50565



ESEGUIRE SECONDO PROGETTO 3300/D PER TEMPERATURA MINIMA -60°C

KLIMAL D-82178 Puchheim bel München LEGNAGO VERONA-Italy I-37048		CE 0036
Type: Typ:	F4.15(M16/M16)	
Fabrikation- Manufacture- Fabbricazione- Nr.		
Herstellungsjahr Manufacture year Anno di fabbricazione		
Volumen Volume Volume	V: L	4
Temperatur Temperature Temperatura	TS- $^{\circ}\text{C}$	min: -60 -10 max: 120 120
Max.zulässiger Druck Max. Permissible pressure Pressione massima consentita	PS-bar:	21 28
Prüfdruck Test pressure Pressione di collaudo	PT-bar:	40.04
Fluid Gruppe/Fluids Group/Gruppo Fluidi Kategorie/Category/Categoria	2 / / 1 / /	Ausgenommen Excluded Escluso /



ATTACCHI SALDATI MAG 135

MARCHIO **CE** CAT. I

RESISTENZA ALLA CORROSIONE IN NEBBIA SALINA 504 ORE / SALT SPRAY TEST CORROSION RESISTANCE 504 HOURS

A TERMINI DELLE VIGENTI LEGGI SUI DIRITTI D'AUTORE, IL PRESENTE DISEGNO NON POTRA', ESSERE COPIATO, RIPRODOTTO O CONSEGNATO A TERZI ED A DITTE CONCORRENTI.

TOLLERANZE PER FORATURE ATTACCHI ± 0.2	VERNICIATURA	colore <u>NERO</u>	DICHIARAZIONE DI CONFORMITA': DA DEFINIRE			
	RAL <u>9005</u>	POLV. <input checked="" type="checkbox"/> LIQ. <input type="checkbox"/>	2	1	IM	
			SOSTITUISCE			
			SOSTITUITO			
		MATERIALE		PESO		
		PED-97/23/CE				
		Data	Disegnato	Controllato	Approvato	QUOTE SENZA INDICAZIONE DI TOLLERANZA
		15/02/2013	Venturini	Cattivelli	Vignoli	SECONDO PROCEDURA INTERNA PROS
		Firme	VENTURINI	CATTIVELLI	VIGNOLI	SCALA 1:1
		TIPO RICEVITORE DI REFRIGERANTE A NORME PED - (CE)				PROIEZIONE
		MODELLO F4.15(M16/M16)				
		CODICE 130.1505.A				FOLGIO 1/1
		 FRIGOMECC S.p.A. COSTRUZIONE COMPONENTI REFRIGERAZIONE CONDIZIONAMENTO S.PIETRO DI LEGNAGO (VR) TEL. ++39 0442 629006 FAX. ++39 0442 629091 www.frigomecc.com/Email: frigomecc@tin.it				



Reflex level gauges

Process application

[back to overview](#)

R 25*
PN 25
ANSI 150

*) former type designation LDR

Nom. pressure: PN 25, ANSI 150 with gauge cock DG with gauge valve RAV 946, 956, 947, 957

Construction to KLINGER material code FS/H, M/H
Gauge glass:
Klinger Reflex glass A
Material Borosilicate

Connection gauge body – gauge valve

Not rotatable: 1/2"-NPT double nipple gauge cock DG, gauge valve RAV 946, 956

Rotatable: Union nut and nipple 1/2"-NPT, gauge valve RAV 947, 957
Seal between nipple and gauge valve: joint ring.

Connection construction

End connection with gauge cock DG or gauge valve RAV 946 (see illustration) and RAV 947 with handwheel or weighted lever (page 40). Safety ball in the upper and lower shut-off fitting.

Gauges without gauge valves:

End, side or back connections with flanges or female thread.

Vessel connection with flanges or male thread to all recognized standards.

Weight: Gauges cock set with DN 25 flanges approx. 7,3 kg. Gauge valve set with DN 20 flanges approx. 8 kg.

Torque for body bolts 25 – 30 Nm, cold.

For gauge body, gauge cock and gauge valve part lists, dimensions of glasses and material specifications see pages 18, 37 and 40.

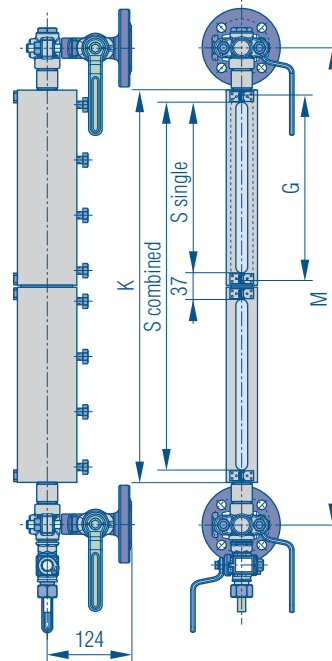
Suggested order specification
Reflex level gauge PN 25

KLINGER material code FS/H, M/H
Gauge glass Borosilicate, thermally prestressed
Connection gauge body – shut-off rotatable / not rotatable

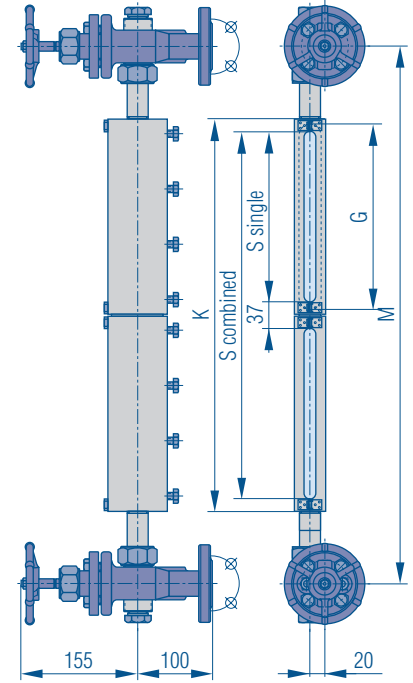
Shut-off fittings gauge cocks and gauge valves with safety balls

Ordering example:
R 25-DG, IX, FS/H
DN 25 / PN 16
M= 450 mm

R 25-DG



R 25-RAV 947



Overall and connection dimensions (mm)

Gauge size	Centre-to-centre distance M min			Body length K	Sight length S	Glass length G	Approx. weight of gauge (kg)
	R 25 DG	R 25 RAV 946/956	R 25 RAV 947/957				
II	215	250	290	153	118	140	3,40
III	240	275	315	178	143	165	3,70
IV	265	300	340	203	168	190	4,10
V	295	330	370	233	198	220	4,80
VI	325	360	400	263	228	250	5,40
VII	355	390	430	293	258	280	5,90
VIII	395	430	470	333	298	320	6,80
IX	415	450	490	353	318	340	7,10
2 x IV	470	505	545	408	373	190	8,40
2 x V	530	565	605	468	433	220	9,90
2 x VI	590	625	665	528	493	250	11,00
2 x VII	650	685	725	588	553	280	12,10
2 x VIII	730	765	805	668	633	320	13,80
2 x IX	770	805	845	708	673	340	14,50
3 x VI	855	890	930	793	758	250	16,50
3 x VII	945	980	1020	883	848	280	18,10
3 x VIII	1065	1100	1140	1003	968	320	20,70
3 x IX	1125	1160	1200	1063	1028	340	21,80
4 x VII	1240	1275	1315	1178	1143	280	24,20
4 x VIII	1400	1435	1475	1338	1303	320	27,70
4 x IX	1480	1515	1555	1418	1383	340	29,10
5 x VII	1535	1570	1610	1473	1438	280	30,20
5 x VIII	1735	1770	1810	1673	1638	320	34,60
5 x IX	1835	1870	1910	1773	1738	340	36,30
6 x VIII	2070	2105	2145	2008	1973	320	41,50
6 x IX	2190	2225	2265	2128	2093	340	43,60
7 x VIII	2405	2440	2480	2343	2308	320	48,40
7 x IX	2545	2580	2620	2483	2448	340	50,90

Shorter distance on request.

KLINGER SCHÖNEBERG GmbH · Cunoweg 7 · D-65510 Idstein

 Sintef Energy Research
 Hr. Gukelberger
 Trondheim
 NORWEGEN

A N G E B O T

Belegnr.:	1295950		Anfr.-Nr.:	e-mail		Bearb.:	Frau Enold
Datum :	23.01.2014		Anfr. vom:	21.01.2014		TelDW :	06126/950-253
Kd-Nr.	100000/100000		Zeichen :	Hr. Gukelberger		FaxDW :	06126/950-341
			Ihre U.ID:			U.ID :	DE 814 269 666
Steuernr:	30063/14265						verena.enold@klinger-schoeneberg.de

Sehr geehrter Herr Gukelberger,

wir danken für Ihre Anfrage und bieten Ihnen gerne wie folgt an:

Geltende Bedingungen: AGB-Verkauf vom 01.01.2012.

Pos.	Bezeichnung	Menge	Einh	Preis	Gesamt	EUR
	KLINGER-Reflexions-Flüssigkeitsanzeiger mit Hahnkopfgarnitur DG Geeignet für den Dampf- und Prozess- einsatzbereich Typ R25-DG Behälteranschluß : 1/2" Außengewinde NPT oder BSP Schaukörpergröße : 333 mm Mittentfernung : 400 mm Schaulänge : 298 mm Werkstoffausführung : FS/H Hahnkopfgarnitur DG bestehend aus: - oberer Hahnkopf mit Kugelsicherung - unterer Hahnkopf mit Kugelsicherung und Ablaßhahn ABL12					
1.00	699999999 REFLEX-A R25-DG 1/2" PN25 ME=400mm FS/H Größe VIII ABL12	1		437,00	437,00	

Fortsetzung nächste Seite

Seite 1 von 2

KLINGER SCHÖNEBERG GmbH · Cunoweg 7 · D-65510 Idstein

Fortsetzung Beleg-Nr.: 1295950

Kunden-Nr.: 100000

Datum: 23.01.2014

Pos.	Bezeichnung	Menge	Einh	Preis	Gesamt	EUR
------	-------------	-------	------	-------	--------	-----

Lieferzeit: ca. 6-8 Wochen ab Auftragseingang

netto	437,00
MwSt	0,00
=====	
Summe EUR	437,00

 Zahlungsbedingungen: Vorauskasse bei Erstbestellung
 Lieferbedingungen : ab Werk, zzgl. Verpackung
 Gültig bis : 28.02.2014

Mit freundlichen Grüßen

KLINGER SCHÖNEBERG GmbH


 i.V.
 J. Wössner


 i.A.
 V. Enold

Kundeninformation bezügl. Einlagerung und Kundenabnahmen:

Zum Versand fertiggestellte Warenlieferungen können bei bauseitigen Verzögerungen für einen Zeitraum von max. 6 Wochen nach Meldung der Versandbereitschaft kostenfrei bei uns eingelagert werden.

Danach werden wir Lagerkosten in Höhe von 1 % des Netto-Warenwertes pro Monat in Anrechnung bringen.

Kundenabnahmen werden pauschal mit 600,00 EURO pro Arbeitstag in Rechnung gestellt.

Seite 2 von 2

 Geschäftsführer:
 Manfred Goßmann

 Registergericht:
 Amtsgericht Mannheim HRB 71 28 36
 USt-Id.Nr.: DE 814 269 666

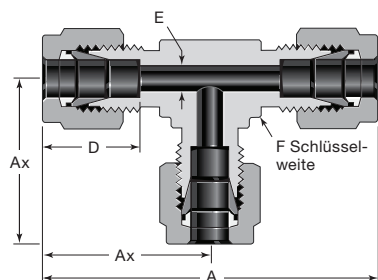
 Steuer-Nr.: 30063/14265
 IBAN: DE64 5105 0015 0107 0607 33
 SWIFT/BIC: NASS DE 55 XXX

 Bankverbindung:
 Nassauische Sparkasse Wiesbaden
 BLZ 510 500 15 Kto. 107 060 733

T-Verschraubungen

ROHR-
VERSCHRAUBUNGEN

T-Verschraubungen

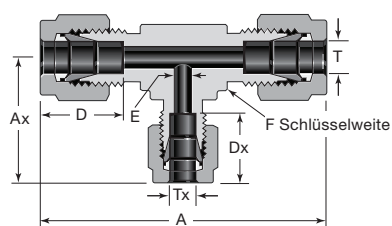


T-Verschraubung

Rohr-AD	Grund-Bestellnummer	Abmessungen				
		A	Ax	D	E	F
Abmessungen, Zoll						
1/16	-100-3	1,40	0,70	0,34	0,05	3/8
1/8	-200-3	1,76	0,88	0,50	0,09	3/8
3/16	-300-3	1,92	0,96	0,54	0,12	7/16
1/4	-400-3	2,12	1,06	0,60	0,19	1/2
5/16	-500-3	2,34	1,17	0,64	0,25	5/8
3/8	-600-3	2,40	1,20	0,66	0,28	5/8
1/2	-810-3	2,84	1,42	0,90	0,41	13/16
5/8	-1010-3	3,06	1,53	0,96	0,50	1
3/4	-1210-3	3,14	1,57	0,96	0,62	1 1/16
7/8	-1410-3	3,52	1,76	1,02	0,72	1 3/8
1	-1610-3	3,86	1,93	1,23	0,88	1 3/8
1 1/8	-1810-3	4,34	2,17	1,23	0,97	1 11/16
1 1/4	-2000-3	5,34	2,67	1,62	1,09	1 11/16
1 1/2	-2400-3	6,20	3,10	1,97	1,34	2
2	-3200-3	8,44	4,22	2,66	1,81	2 3/4

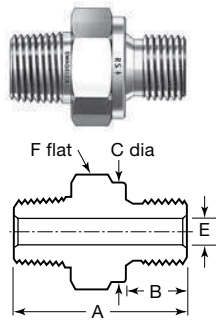
Rohr-AD	Grund-Bestellnummer	Abmessungen				
		A	Ax	D	E	F, Zoll
Abmessungen, mm						
2	-2M0-3	44,7	22,3	12,9	1,7	3/8
3	-3M0-3	44,7	22,3	12,9	2,4	3/8
4	-4M0-3	50,8	25,4	13,7	2,4	1/2
6	-6M0-3	53,9	27,0	15,3	4,8	1/2
8	-8M0-3	59,7	29,9	16,2	6,4	5/8
10	-10M0-3	63,0	31,5	17,2	7,9	11/16
12	-12M0-3	72,0	36,0	22,8	9,5	13/16
14	-14M0-3	77,6	38,8	24,4	11,1	1
15	-15M0-3	77,6	38,8	24,4	11,9	1
16	-16M0-3	77,6	38,8	24,4	12,7	1
18	-18M0-3	79,6	39,8	24,4	15,1	1 1/16
20	-20M0-3	89,3	44,6	26,0	15,9	1 3/8
22	-22M0-3	89,3	44,6	26,0	18,3	1 3/8
25	-25M0-3	98,3	49,1	31,3	21,8	1 3/8
28	-28M0-3	128	64,0	36,6	21,8	41 mm
30	-30M0-3	140	69,9	39,6	26,2	46 mm
32	-32M0-3	145	72,3	42,0	28,6	46 mm
38	-38M0-3	168	84,0	49,4	33,7	55 mm
50	-50M0-3	211	106	65,0	45,2	2 3/4

T-Reduzierschraubung (zöllig)



Rohr-AD		Grund-Bestellnummer	Abmessungen					
T	Tx		A	Ax	D	Dx	E	F
Abmessungen, Zoll								
3/8	1/4	-600-3-6-4	2,40	1,14	0,66	0,60	0,19	5/8
1/2	1/4	-810-3-8-4	2,84	1,25	0,90	0,60	0,19	13/16
	3/8	-810-3-8-6		0,66				
5/8	3/8	-1010-3-10-6	3,06	1,42	0,96	0,66	0,28	1
3/4	3/8	-1210-3-12-6	3,14	1,46	0,96	0,66	0,28	1 1/16
	1/2	-1210-3-12-8		1,57		0,90		
1	3/8	-1610-3-16-6	3,86	1,65	1,23	0,66	0,28	1 3/8
	1/2	-1610-3-16-8		1,76		0,90		
	3/4	-1610-3-16-12		1,76		0,96		
1 1/4	1	-2000-3-20-16	5,34	2,17	1,62	1,23	0,88	1 11/16
1 1/2	1	-2400-3-24-16	6,20	2,36	1,97	1,23	0,88	2
2	1	-3200-3-32-16	8,44	2,79	2,66	1,23	0,88	2 3/4

Hex Nipples



Male NPT to Male ISO Parallel Thread (RS)

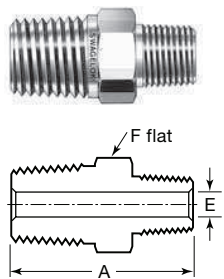
NPT Size in.	ISO Thread Size in.	Basic Ordering Number	Dimensions in. (mm)					Pressure Ratings ^② psig (bar)	
			A	B	C	E ^①	F	316 SS, Steel	Brass
1/8	1/8	-2-HN-2RS	1.09 (27.7)	0.32 (8.1)	0.54 (13.7)	0.16 (4.1)	9/16	11 400 (785)	5700 (392)
1/4	1/4	-4-HN-4RS	1.45 (36.8)	0.47 (11.9)	0.70 (17.8)	0.23 (5.8)	3/4	10 300 (709)	5100 (351)
3/8	3/8	-6-HN-6RS	1.48 (37.6)	0.47 (11.9)	0.86 (21.8)	0.31 (7.9)	7/8	10 300 (709)	5100 (351)
1/2	1/2	-8-HN-8RS	1.75 (44.4)	0.55 (14.0)	1.02 (25.9)	0.47 (11.9)	1 1/16	7 600 (523)	3800 (261)
3/4	3/4	-12-HN-12RS	1.93 (49.0)	0.63 (16.0)	1.25 (31.8)	0.62 (15.7)	1 5/16	7 300 (502)	3600 (248)
1	1	-16-HN-16RS	2.23 (56.6)	0.71 (18.0)	1.53 (38.9)	0.78 (19.8)	1 5/8	7 400 (509)	3700 (254)

For gasket information, see page 8.

① The E dimension is the minimum nominal opening. These fittings may have a larger opening at one end.

② Pressure ratings are for the NPT end connections. Pressure ratings for the male ISO end connections are dependent on the selected gasket. Contact your authorized Swagelok representative for more pressure-temperature ratings.

Hex Reducing Nipples



Male NPT

NPT Size in.	Basic Ordering Number	Dimensions, in. (mm)			Pressure Ratings, psig (bar)	
		A	E ^①	F	316 SS, Steel	Brass
1/8 to 1/16	-2-HRN-1	1.01 (25.6)	0.12 (3.0)	7/16	11 000 (757)	5500 (378)
1/4 to 1/8	-4-HRN-2	1.22 (31.0)	0.19 (4.8)	9/16	10 000 (689)	5000 (344)
3/8 to 1/8	-6-HRN-2	1.25 (31.8)	0.19 (4.8)	11/16	10 000 (689)	5000 (344)
3/8 to 1/4	-6-HRN-4	1.43 (36.3)	0.28 (7.1)	11/16	8 000 (551)	4000 (275)
1/2 to 1/8	-8-HRN-2	1.47 (37.3)	0.19 (4.8)	7/8	7 700 (530)	3800 (261)
1/2 to 1/4	-8-HRN-4	1.65 (41.9)	0.28 (7.1)	7/8	8 000 (551)	4000 (275)
1/2 to 3/8	-8-HRN-6	1.65 (41.9)	0.38 (9.6)	7/8	7 800 (537)	3900 (268)
3/4 to 1/4	-12-HRN-4	1.65 (41.9)	0.28 (7.1)	1 1/16	8 000 (551)	4000 (275)
3/4 to 1/2	-12-HRN-8	1.84 (46.7)	0.47 (11.9)	1 1/16	7 700 (530)	3800 (261)
1 to 1/4	-16-HRN-4	1.94 (49.3)	0.28 (7.1)	1 3/8	5 300 (365)	2600 (179)
1 to 1/2	-16-HRN-8	2.13 (54.1)	0.47 (11.9)	1 3/8	7 700 (530)	3800 (261)
1 to 3/4	-16-HRN-12	2.13 (54.1)	0.62 (15.7)	1 3/8	7 300 (502)	3600 (248)
Heavy-Wall Male NPT						
1/2 to 1/4	SS-8-HRN-4-10K	1.65 (41.9)	0.23 (5.8)	7/8	10 000 (689)	—

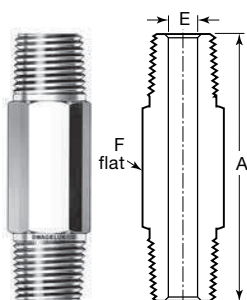
① The E dimension is the minimum nominal opening. These fittings may have a larger opening at the larger end.

Male ISO Tapered Thread (RT)

ISO Thread Size in.	Basic Ordering Number	Dimensions in. (mm)			Pressure Ratings psig (bar)	
		A	E ^①	F	316 SS, Steel	Brass
3/8 to 1/4	-6-HRNT-4RT	1.43 (36.3)	0.28 (7.1)	11/16	7800 (537)	3900 (268)
1/2 to 1/8	-8-HRNT-2RT	1.47 (37.3)	0.19 (4.8)	7/8	7700 (530)	3800 (261)
1/2 to 3/8	-8-HRNT-6RT	1.65 (41.9)	0.38 (9.6)	7/8	7800 (537)	3900 (268)

① The E dimension is the minimum nominal opening. These fittings may have a larger opening at the larger end.

Hex Long Nipples



Male NPT

NPT Size in.	A (Available Lengths) in.						Basic Ordering Number	Dimensions in. (mm)		Pressure Ratings psig (bar)	
	1.50	2.00	2.50	3.00	4.00	6.00		E	F	316 SS, Steel	Brass
1/8	✓	✓	✓	✓	—	—	-2-HLN-	0.19 (4.8)	7/16	10 000 (689)	5000 (344)
1/4	✓	✓	✓	✓	✓	—	-4-HLN-	0.28 (7.1)	9/16	8 000 (551)	4000 (275)
3/8	✓	✓	✓	✓	✓	—	-6-HLN-	0.38 (9.6)	11/16	7 800 (537)	3900 (268)
1/2	—	✓	—	✓	✓	✓	-8-HLN-	0.47 (11.9)	7/8	7 700 (530)	3800 (261)
3/4	—	✓	—	✓	✓	—	-12-HLN-	0.62 (15.7)	1 1/16	7 300 (502)	3600 (248)
1	—	—	—	✓	✓	—	-16-HLN-	0.88 (22.4)	1 3/8	5 300 (365)	2600 (179)

To order, insert the material designator as a prefix and the available length as a suffix to the basic ordering number.

Example: **SS-2-HLN-1.50**

Safety Valves

Type 06801 with bellow seal



Stainless steel bellow sealed Safety Valves, angle type, PN40, type tested TÜV-SV.1105. S/G/L orifice $d_0 = 12.5$ mm TÜV-SV.1105. S/G

Standard safety valve,
metal to metal seated, closed bonnet
"cleaned and degreased for oxygen service"

Part No. 06801.X.0000

Inlet: male thread type G (BSPP) acc. to ISO 228/1, Outlet: female thread type G (BSPP) acc. to ISO 228/1

Part No. 06801.X.2000

Inlet: male thread type R (BSPT) acc. to ISO 7/1, Outlet: female thread type G (BSPP) acc. to ISO 228/1

Part No. 06801.X.5000

Inlet: male thread NPT acc. to ANSI B 1.20.1, Outlet: female thread type G (BSPP) acc. to ISO 228/1

Part No. 06801.X.6000

Inlet: male thread NPT acc. to ANSI B 1.20.1, Outlet: female thread NPT acc. to ANSI B 1.20.1



Applications:

Provided as safety device for protection against excessive pressure in stationary and moveable gas cylinders. Approved for non-inflammable and inflammable vapours, gases and fluids.

Working temperature: $-270^{\circ}\text{C} / -454^{\circ}\text{F}$ (3K) up to $+225^{\circ}\text{C} / +437^{\circ}\text{F}$ (498K)

Maximum allowed back pressure: 15% of set pressure

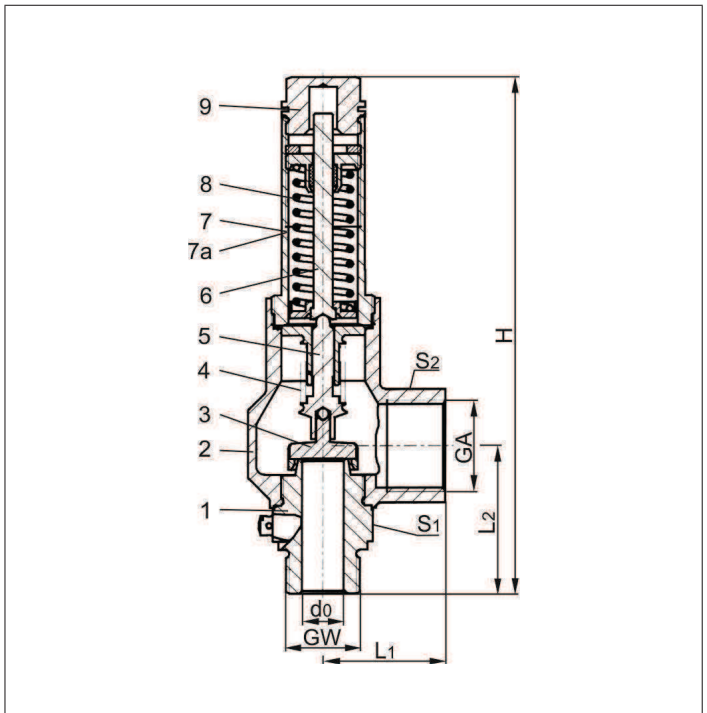
Materials	DIN EN	ASTM
1 Inlet body	1.4571	A 276 Grade 316Ti
2 Outlet body	1.4308	A 351 CF8
3 Disc	1.4541	A 276 Grade 321
4 Bellow	1.4571	A 276 Grade 316Ti
5 Bellow stem	1.4571	A 276 Grade 316Ti
6 Stem	CW453K	B 103 UNS C52100
7 Bonnet	1.4308	A 351 CF 8
7a Bonnet from GW 1	1.4305	A 276 Grade 303
8 Spring	1.4571	A 276 Grade 316Ti
9 Cap	1.4301	A 276 Grade 304

Important:

For nominal size GW 3/4 the back pressure reduces the blow off performance of the safety valve (see diagram 06801-3/4).

Essential: Valves are delivered at a set pressure, therefore when ordering please confirm set pressure, medium and temperature.

Standard marking acc. to Pressure Equipment Directive 97/23/EG (PED).



Type 06801	Technical data				
Nominal size	GW	1/2	3/4	1	1
Orifice	d_0	12.5	15	20	23
Dimension code	.X.	1204	1506	2010	2310
Set pressure range	bar	3.0-25.0	3.0-25.0	3.0-25.0	3.0-25.0
Outlet	GA	G 1	G 1	G 1-1/4	G 1-1/2
Height	H	186	190	205	255
Length	L_1	44	44	51	56
Length	L_2	52	54	63	65
Wrench size across flats	S_1	36	36	41	50
Wrench size across flats	S_2	41	41	50	55
Weight	ca. kg	1.03	1.05	1.70	2.45
Coeff. of discharge vapours, gases	α_w	0.60	0.50	0.60	0.66
Coeff. of discharge fluids	α_w	-	0.39	0.45	0.48

Dimensions in mm.

Safety Valves

Type 06801 with bellow seal



Discharge capacities

Calculation of mass flow acc. to AD2000-Merkblatt A2 / DIN EN ISO 4126-1

Medium:

Air in m³/h at 0°C and 1013.25 mbar

Water in kg/h

Saturated steam in kg/h

The capacity indicated below is for a fully opened valve.

Maximum allowed back pressure: 15% of set pressure.

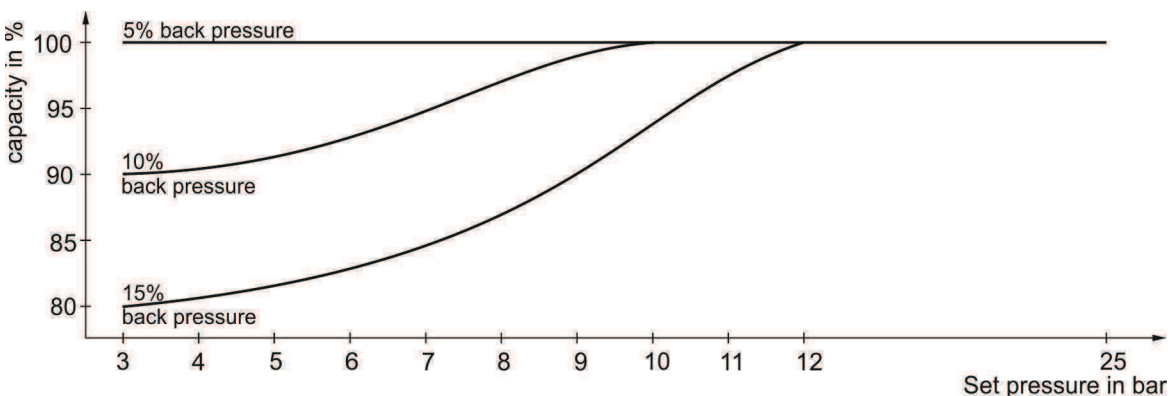
For nominal size GW 3/4 the back pressure reduces the blow off performance of the safety valve (see diagram 06801-3/4).

d_0 - orifice

A_0 - flow area

Set pressure in bar (\bar{u})	GW	1/2	1/2	3/4	1	1/2	1/2	3/4	1	1/2	3/4	1	
	d_0 (mm)	12.5	15.0	20.0	23.0	12.5	15.0	20.0	23.0	15.0	20.0	23.0	
	A_0 (mm ²)	122.7	176.7	314.2	415.5	122.7	176.7	314.2	415.5	176.7	314.2	415.5	
	Medium	Air				Saturated steam				Water			
3.0		216	260	555	807	169	203	433	630	6369	13065	18431	
4.0		272	326	696	1013	211	253	540	786	7355	15087	21283	
5.0		328	393	839	1221	252	303	647	942	8223	16868	23796	
6.0		383	460	981	1428	294	353	753	1096	9008	18479	26067	
7.0		438	526	1123	1634	335	402	859	1249	9730	19960	28157	
8.0		495	594	1269	1846	376	452	964	1403	10402	21338	30101	
9.0		551	661	1411	2053	417	501	1069	1555	11033	22633	31928	
10.0		608	729	1556	2265	458	550	1174	1708	11631	23858	33656	
12.0		719	863	1842	2679	540	648	1384	2013	12741	26135	36868	
14.0		830	997	2127	3094	622	746	1592	2317	13761	28229	39822	
16.0		942	1130	2412	3509	703	844	1802	2621	14712	30178	42572	
18.0		1053	1264	2697	3924	785	942	2010	2924	15604	32009	45154	
20.0		1176	1411	3011	4380	866	1040	2219	3228	16452	33748	47607	
22.0		1288	1546	3298	4799	948	1137	2427	3531	17255	35395	49931	
25.0		1457	1748	3730	5427	1070	1284	2739	3985	18394	37731	53226	

Diagram 06801-3/4



HEROSE



HEROSE GMBH - Postfach 1561 - D-23835 Bad Oldesloe

SINTEF Energi AS
Sem Saelands vei 11
SE-7034 TRONDHEIM

Delivery address

SINTEF Energi AS
Sem Saelands vei 11
SE-7034 TRONDHEIM

Invoice address

SINTEF Energi AS
Sem Saelands vei 11
SE-7034 TRONDHEIM

Quotation

Seite 1/ 3

Number/Date
20033685 /17.01.2014
Reference no./Date of receipt
e-mail /16.01.2014
Delivery upon receipt PO, ex factory
4 weeks
Cust. no. / Orderer
2500001 / Ephraim Gukelberger
Vendor no. / Fax
UNKNOWN / +49 4531 509 120
Validity period
17.01.2014 bis30.04.2014
Contact
Sören Thele
Tel./ Fax. / Email
+49(0)4531-509-147 /- 120
soeren.thele@herose.com

We deliver according to the following conditions:

Currency EUR

Terms of payment Payment in advance

Terms of delivery EXW Bad Oldesloe

Our sales conditions 04/2009 available at <http://www.herose.com> are valid.

Any damage of lead seals or sealing labels on HEROSE Valves results in exclusion of guarantee.

Item	Material	Qty	Description	Price	Price unit	Value
000010	06801.1204.0000		FABA-Sicherheitsventil Za G1/2 do=12,5			
	Customs tariff no. 84814010					
		2 PC		345,10	EUR	1 PC
	Material : 1.4308					690,20
	Bellow sealed safety valve angle type, type tested					

HEROSE GMBH
ARMATUREN UND METALLE
Elly-Heus-Knapp-Straße 12
D-23843 Bad Oldesloe

TEL. +49 4531-509-0
FAX +49 4531-509-120
info@herose.com
www.herose.com
UST.-IdNR. DE 118564125
St-Nr.: 30 292 11842
HRB 1517 Bad Oldesloe

Bankverbindungen:
HSH Nordbank
HypoVereinsbank Hamburg
Hamburger Sparkasse
Commerzbank Hamburg
Sparkasse Holstein
Postbank Hamburg

Bankleitzahl:
210 500 00
200 300 00
200 505 50
200 400 00
213 522 40
200 100 20

Konto-Nr.
530 520 10
4 008 888
1354 122754
49 1444600
20 024
030 355 204

IBAN
DE84 2105 0000 0053 0520 10
DE89 2003 0000 0004 0088 88
DE32 2005 0550 1354 1227 54
DE46 2004 0000 0491 4446 00
DE17 2135 2240 0000 0200 24
DE97 2001 0020 0030 3552 04

SWIFT (BIC)
HSHNDEHH
HYVEDEMM300
HASPDEHHXXX
COBADEFFXXX
NOLADE21HOL
PBNKDEFF



HEROSE GMBH - Postfach 1561 - D-23835 Bad Oldesloe

SINTEF Energi AS
Sem Saelands vei 11
SE-7034 TRONDHEIM

Quotation

Seite 2/ 3

Number/Date
20033685 /17.01.2014
Reference no.
e-mail

Item	Material	Qty	Description	Price	Price unit	Value
000020	06801.1506.0000	2 PC	<p>for vapours and gases cleaned and degreased for oxygen services working temperature -270°C up to +225°C bonnet 1.4308/CF8 st.st. closed without lifting device inlet 1.4571 st.st. 1/2"BSPP male thread outlet 1.4308 st.st. 1"BSPP female thread disc 1.4541 st.st. metal to metal seated orifice 12.5mm With the following configuration: 16,00 bar</p> <p>FABA-Sicherheitsventil Za G3/4 do=15 Customs tariff no. 84814010</p>	345,10	EUR	1 PC 690,20
000030	06801.2010.0000	2 PC	<p>Material : 1.4308 Bellow sealed safety valve angle type, type tested for vapours, gases and fluids cleaned and degreased for oxygen services working temperature -270°C up to +225°C bonnet 1.4308/CF8 st.st. closed without lifting device inlet 1.4571 st.st. 3/4"BSPP male thread outlet 1.4308 st.st. 1"BSPP female thread disc 1.4541 st.st. metal to metal seated orifice 15mm With the following configuration: 16,00 bar</p> <p>FABA-Sicherheitsventil Za G1 do=20 Customs tariff no. 84814010</p>	590,60	EUR	1 PC 1.181,20
			<p>Material : 1.4308 Bellow sealed safety valve angle type, type tested for vapours and gases cleaned and degreased for oxygen services working temperature -270°C up to +225°C bonnet 1.4308/CF8 st.st. closed without lifting device inlet 1.4571 st.st. 1"BSPP male thread outlet 1.4308 st.st. 11/4"BSPP female thread</p>			

HEROSE GMBH
ARMATUREN UND METALLE
Elly-Heus-Knapp-Straße 12
D-23843 Bad Oldesloe

TEL. +49 4531-509-0
FAX +49 4531-509-120
info@herose.com
www.herose.com
UST.-IdNR. DE 118564125
St-Nr.: 30 292 11842
HRB 1517 Bad Oldesloe

Bankverbindungen:
HSH Nordbank
HypoVereinsbank Hamburg
Hamburger Sparkasse
Commerzbank Hamburg
Sparkasse Holstein
Postbank Hamburg

Bankleitzahl:
210 500 00
200 300 00
200 505 50
200 400 00
213 522 40
200 100 20

Konto-Nr.
530 520 10
4 008 888
1354 122754
49 1444600
20 024
030 355 204

IBAN
DE84 2105 0000 0053 0520 10
DE89 2003 0000 0004 0088 88
DE32 2005 0550 1354 1227 54
DE46 2004 0000 0491 4446 00
DE17 2135 2240 0000 0200 24
DE97 2001 0020 0030 3552 04

SWIFT (BIC)
HSHNDEHH
HYVEDEMM300
HASPDEHHXXX
COBADEFFXXX
NOLADE21HOL
PBNKDEFF

Geschäftsführer:
Dipl.-Jur. Dirk M. Zschalich, MBE



HEROSE GMBH - Postfach 1561 - D-23835 Bad Oldesloe

SINTEF Energi AS
Sem Saelands vei 11
SE-7034 TRONDHEIM

Quotation

Seite 3/ 3

Number/Date
20033685 /17.01.2014
Reference no.
e-mail

Item	Material	Qty	Description	Price	Price unit	Value
	disc	1.4541	st.st. metal to metal seated orifice 20.0mm With the following configuration: 16,00 bar			
Items total						2.561,60
Output Tax			0,000		2.561,60	0,00
Final amount						2.561,60

Additionally we offer following certificates which need to be mentioned in the purchase order.

TÜV, pressure test certificate for safety valve EN10204-3.2:

1-5 pc / 6-10 pc / >10 pc
34,- Euro / 22,- Euro / 17,- Euro each per safety valve

pressure test certificate EN10204-3.1:

37,- Euro per order line item

material certificate EN10204-3.1:

37,- Euro per line item

combined test and material certificate EN10204-3.1:

52,- Euro per order line item

Thank you for your enquiry and we hope our quotation meets your expectations.

We hope this allows you to release your order but should you require any additional information please contact us.
Please include our quotation number in any future correspondence.

HEROSE GMBH

HEROSE GMBH
ARMATUREN UND METALLE
Elly-Heus-Knapp-Straße 12
D-23843 Bad Oldesloe

TEL. +49 4531-509-0
FAX +49 4531-509-120
info@herose.com
www.herose.com
UST.-IdNR. DE 118564125
St-Nr.: 30 292 11842
HRB 1517 Bad Oldesloe

Bankverbindungen:
HSH Nordbank
HypoVereinsbank Hamburg
Hamburger Sparkasse
Commerzbank Hamburg
Sparkasse Holstein
Postbank Hamburg

Bankleitzahl:
210 500 00
200 300 00
200 505 50
200 400 00
213 522 40
200 100 20

Konto-Nr.
530 520 10
4 008 888
1354 122754
49 1444600
20 024
030 355 204

IBAN
DE84 2105 0000 0053 0520 10
DE89 2003 0000 0004 0088 88
DE32 2005 0550 1354 1227 54
DE46 2004 0000 0491 4446 00
DE17 2135 2240 0000 0200 24
DE97 2001 0020 0030 3552 04

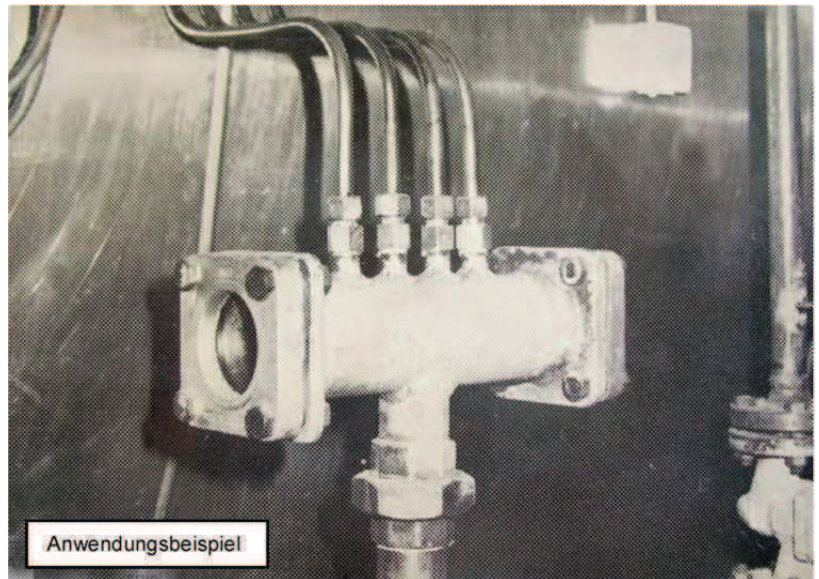
SWIFT (BIC)
HSHNDEHH
HYVEDEMM300
HASPDEHHXXX
COBADEFFXXX
NOLADE21HOL
PBNKDEFF

Verwendung:

Schauglasflanschen mit Anschweißstutzen eignen sich zum Einschweißen in Rohrleitungen, Kesseln, Tanks und Apparaturen aller Art. Einsatzmöglichkeiten sind überall dort gegeben, wo Sichtkontrollen von Füllung oder Strömung gefordert wird. Für Flüssigkeiten und Gase gleichermaßen geeignet, empfehlen sie sich insbesondere auch für Sonderkonstruktionen auf den verschiedensten Einsatzgebieten.

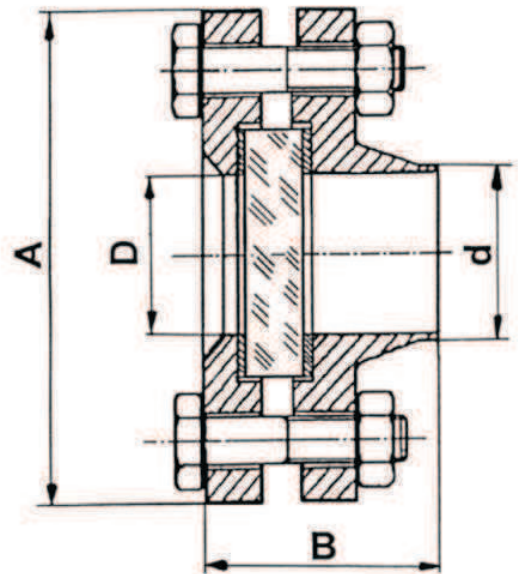
Sonderausführung:

andere Nennweiten
für höhere Drücke
verschiedene Werkstoffe



Werkstoffe:

Anschweiß-Stutzen	WN 1.4571/1.4541 oder C-Stahl
Deckel	WN 1.4571/1.4541 oder C Stahl
Glasplatten	Borosilikatglas (280°C max.) Natron-Kalk-Glas (150°C max.)
Dichtungen	Aramidfaser (oder nach Wunsch)



Durchblick Ø = Größe D	A	B	d
40	150	63	48,3
50	165	70	60,3
65	185	70	76,1
80	200	74	88,9
100	220	83	114,3
125	250	88	139,7
150	285	94	168,3
200	340	107	219,1

Verwendung:

Schraub-Schauglas-Armaturen werden zur Beobachtung von Vorgängen im Innern von Kesseln, Behältern und Rohrleitungen eingesetzt. Sie finden Anwendung im Lebensmittelbereich, Molkereien, Brauereien, Getränkeindustrie und in der Pharma- und Medizintechnik. Auf Grund der hohen zulässigen Temperaturen ist eine Sterilisierung möglich.

Betriebsbedingungen:

Betriebsdruck: max. 6 bar

Vakuum: max. 1 Torr

Temperatur: max. 220°C

Werkstoffe:

Anschweiß-Stutzen: WN 1.4404 oder 1.4301

Nutmutter: WN 1.4301

Glasplatte: Borosilikatglas
Natron-Kalk-Glas

Zwischenlage: Aramidfaser/PTFE

Dichtung: Silikon/Viton/EPDM/PTFE-Umhüllt

Sonderausführungen:

Höhere Betriebsdrücke

Scheibenwischer Bauform N-190

Schauglasleuchten

Bestellbeispiel:

Schraub-Schauglas Bauform N-127

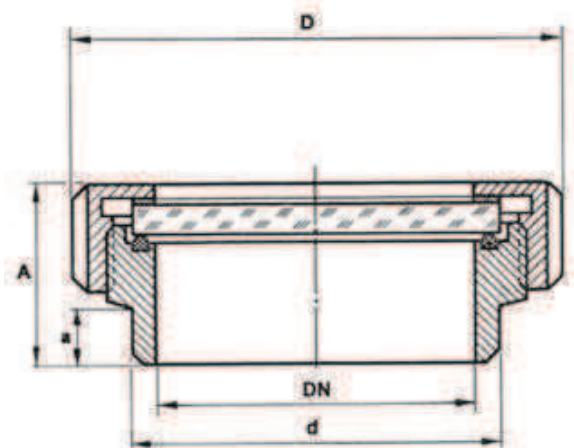
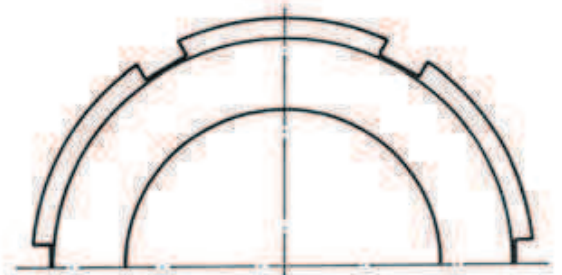
Stutzen WN 1.4571

Nutmutter: WN 1.4301

Borosilikatglas

Dichtung Silikon

DN 80



Abmessungen

DN	a	A	d	D
50	18	46	55	92
65	22	49	72	112
80	23	54	87	127
100	32	65	106	148
125	20	60	132	178

Verwendung:

Beobachtung und Beleuchtung des Inneren von geschlossenen Behältern (Kesseln, Tanks, Silos usw.)

Lieferumfang:

Komplett, bestehend aus Grund- und Deckflansch, Glasplatte, Dichtungen und Stiftschrauben mit Muttern

Betriebsbedingungen:

Betriebsdruck: 10 und 16 bar
(6 und 25 bar auf Anfrage)

Werkstoffe:

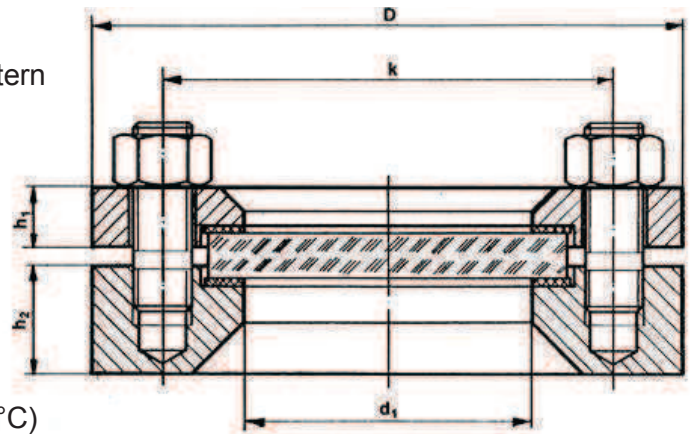
Blockflansch: RSt. 37-2, H II, C 22.8
WN 1.4541, WN 1.4571
oder nach Wunsch

Schauglas: Borosilikatglas DIN 7080 (280°C)
Preßhartglas DIN 8902 (150°C)

Dichtungen: Asbestfrei oder nach Wunsch

Schrauben und

Muttern: 5.6 verzinkt, A4-70



Sonderausführungen:

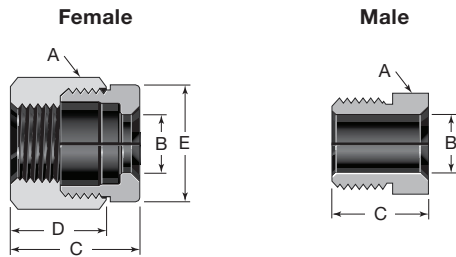
- mit Scheibenwischer Bauform N-190 + N-195
- mit Sprühvorrichtung Bauform N-198
- mit Doppelverglasung Bauform N-126 und 120-D
- mit Befestigungsbohrungen für Leuchten
- mit Schutzüberzug, Ausführung B nach DIN 28120
- mit O-Ring-Dichtung (Vakuumausführung)
- Sonderausführung nach Kundenwunsch



DN	PN	d ₁	d ₃	s	D	k	h ₁	h ₂	Gewinde
25	10/16	48	63	10	115	85	16	25	4 x M 12
40	10/16	65	80	12	150	110	16	30	4 x M 16
50	10/16	80	100	15	165	125	16	30	4 x M 16
80	10/16	100	125	15/20	200	160	20	30	8 x M 16
100	10/16	125	150	20/25	220	180	22	30	8 x M 16
125	10/16	150	175	20/25	250	210	25	30	8 x M 16
150	10/16	175	200	25/30	285	240	30	36	8 x M 20
200	10	225	250	30	340	295	35	36	8 x M 20

Nuts, Caps, and Plugs

Split-Nut Assemblies

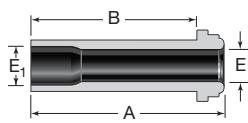


VCR Size	Split Nut Type	Ordering Number	Dimensions				
			A	B	C	D	E
Dimensions, in. (mm)							
1/4	Female	SS-4-VCR-1-SN	3/4	0.36 (9.1)	0.81 (20.6)	0.63 (16.0)	0.68 (17.4)
1/4	Male	SS-4-VCR-4-SN	5/8	0.36 (9.1)	0.60 (15.2)	—	—

High-Flow Connections—“H” Type VCR

“H” Type VCR connections are compatible with 1/4 in. VCR connections and are designed for use with Swagelok high-flow diaphragm valves and gas regulators. For uniform flow, use 1/4 in. side-load retainer style gasket. See page 17.

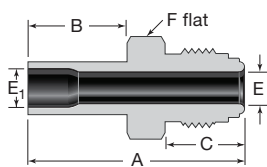
Glands



Tube Butt Weld

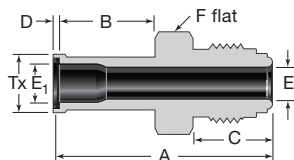
Tube Size	Nominal Wall Thickness	VCR Size	Ordering Number	Dimensions				Working Pressure		
				A	B	E	E ₁	Ni	SS	Cu
Dimensions, in. (mm)								psig (bar)		
3/8	0.035	1/4	6LV-4-HVCR-3-.60SR	0.60 (15.2)	0.41 (10.4)	0.25 (6.4)	0.31 (7.9)	3300 (227)	3300 (227)	3300 (227)
			6LV-4-HVCR-3-1.19SR	1.19 (30.2)	1.00 (25.4)					
			6LV-4-HVCR-3-1.31SR	1.31 (33.3)	1.12 (28.4)					

Bodies



Tube Butt Weld

Tube Size	VCR Size	Ordering Number	Dimensions						Working Pressure		
			A	B	C	E	E ₁	F	Ni	SS	Cu
Dimensions, in. (mm)									psig (bar)		
3/8	1/4	6LV-4-HVCR-1-6TB7	1.68 (42.7)	0.75 (19.1)	0.62 (15.7)	0.25 (6.4)	0.31 (7.9)	5/8	3300 (227)	3300 (227)	3300 (227)



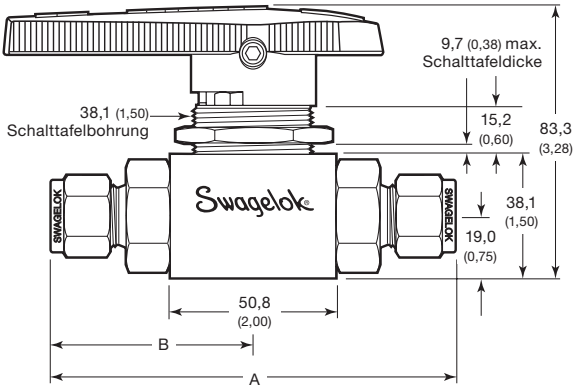
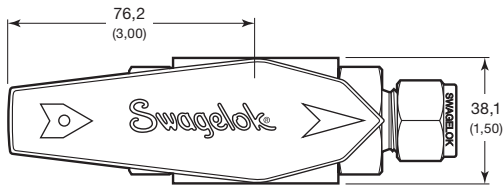
Automatic Tube Weld

Tube Size	VCR Size	Ordering Number	Dimensions							Working Pressure			
			A	B	C	D	E	E ₁	F	Tx	Ni	SS	Cu
Dimensions, in. (mm)										psig (bar)			
3/8	1/4	316L-4-HVCR-1A6	1.71 (43.4)	0.75 (19.1)	0.62 (15.7)	0.03 (0.8)	0.25 (6.4)	0.31 (7.9)	5/8	0.41 (10.4)	3300 (227)	3300 (227)	3300 (227)

Bestellinformationen und Abmessungen

Eine Bestellnummer auswählen.

Die Abmessungen in Millimeter (Zoll) dienen nur als Referenz und können sich ändern.



Endanschlüsse ^①		Bestellnummer	C _v	Bohrung mm (Zoll)	Abmessungen mm (Zoll)	
Typ	Größe				A	B
Zöllige Swagelok Rohrverschraubung	3/8 Zoll	SS-AFSS6	4,0	7,1 (0,281)	116 (4,57)	58,2 (2,29)
	1/2 Zoll	SS-AFSS8	7,2	10,3 (0,406)	122 (4,80)	61,0 (2,40)
	3/4 Zoll	SS-AFSS12	7,1	12,0 (0,472)	122 (4,80)	61,0 (2,40)
	1 Zoll	SS-AFSS16 ^②	6,5	12,0 (0,472)	130 (5,10)	64,8 (2,55)
Metrische Swagelok Rohrverschraubung	12 mm	SS-AFSS12MM	5,2	10,3 (0,406)	112 (4,40)	55,9 (2,20)
	16 mm	SS-AFSS16MM	12,4	12,0 (0,472)	122 (4,80)	61,0 (2,40)
NPT- Innengewinde	3/8 Zoll	SS-AFSF6	11,0	12,0 (0,472)	102 (4,00)	50,8 (2,00)
	1/2 Zoll	SS-AFSF8	13,8		102 (4,00)	50,8 (2,00)
	3/4 Zoll	SS-AFSF12 ^②	7,8		105 (4,12)	52,3 (2,06)
Kegeliges ISO- Innengewinde ^③	1/2 Zoll	SS-AFSF8RT	13,8	12,0 (0,472)	102 (4,00)	50,8 (2,00)

Die Abmessungen gelten bei fingerfest angezogenen Überwurfmuttern der Swagelok Rohrverschraubungen.

- ① Die Hähne können mit zwei unterschiedlichen Endanschlüssen bestellt werden. Wenden Sie sich bitte an Ihren autorisierten Swagelok Vertriebs- und Servicevertreter.
- ② Nicht erhältlich mit AGA, IAS und ECE R110 Zertifizierungen; nicht für Schalttafelmontage empfohlen; nicht erhältlich mit pneumatischem Antrieb.
- ③ ISO/BSP Gewinde (kegelig), nach DIN 3852, Swagelok RT Fittings. Siehe Spezifikationen ISO 7/1, BS EN ISO 10226-1 und JIS B0203.

KUGELHÄHNE
KÜHENHÄHNE

Optionen und Zubehör

Griffoptionen

Griffe aus schwarzem Nylon sind Standard.

- Wenn Sie einen Griff in einer anderen Farbe wünschen, fügen Sie zur Hahnbestellnummer eine Farbkennung hinzu.

Grifffarbe	Kennung
Blau	-BL
Grün	-GR
Orange	-OG
Rot	-RD
Gelb	-YW

Beispiel: SS-AFSS6-**RD**

- Zum Bestellen eines Ovalgriffs aus Nylon, der Hahnbestellnummer **-K** hinzufügen.



Beispiel: SS-AFSS6-**K**

- Zum Bestellen eines schwarzen Aluminiumgriffs mit Richtungsanzeige, der Hahnbestellnummer **-AHD** hinzufügen.

Beispiel: SS-AFSS6-**AHD**

Griffsätze

Der Ersatzgriffsatz enthält einen Griff, eine Befestigungsschraube und Montageanleitung.

- Bestellnummer für Griffsatz mit schwarzem Nylongriff: **NY-5K-AFS-BK**
Wenn Sie einen Griffsatz in einer anderen Farbe als schwarz bestellen möchten, ersetzen Sie das **-BK** in der Griffsatz-Bestellnummer durch eine andere Farbkennung.

Beispiel: NY-5K-AFS-**RD**

- Bestellnummer für Griffsatz mit ovalem Nylongriff: **NY-5K-AFSK-BK**
- Bestellnummer für Griffsatz mit schwarzem Aluminiumgriff mit Richtungsanzeige: **A-5K-AFS-BK**

Werkstoffoption für Spindeldichtung

Tieftemperatur-Fluorkautschuk FPM ist Standard. Tieftemperatur-Nitril (Buna C) als Option zur Verlängerung der Zykluslebensdauer des Hahns erhältlich. Hähne mit Tieftemperatur-Nitril haben einen Temperatureinsatzbereich von -40 bis 93°C (-40 bis 200°F) **und haben keine AGA, IAS oder ECE R110 Zertifizierung.**

Zum Bestellen, der Hahnbestellnummer **-BCS** hinzufügen.

Beispiel: SS-AFSS6-**BCS**

Griffverriegelungen



- Zum Abschließen in offener oder geschlossener Stellung
- Für Schlossbügel bis zu einem Durchmesser von 8,7 mm (0,344 Zoll)
- Wenn Sie die Griffverriegelung werkseitig montiert bestellen möchten, fügen Sie an die Bestellnummer des Hahns **-LH** an.

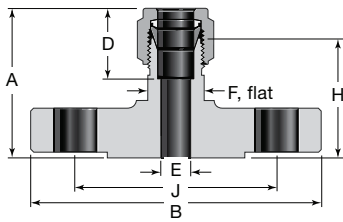
Beispiel: SS-AFSS6-**LH**

Wenn sie die Griffverriegelung zum Nachrüsten bestellen möchten, verwenden Sie die Bestellnummer für den Griffverriegelungssatz: **SS-51K-AFS-LH**

Ordering Information and Dimensions

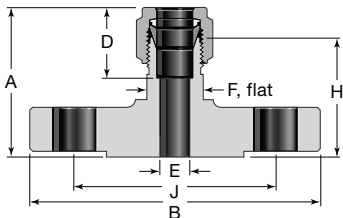
Dimensions are for reference only and are subject to change.

DIN Flanges, Pressure Class PN 40



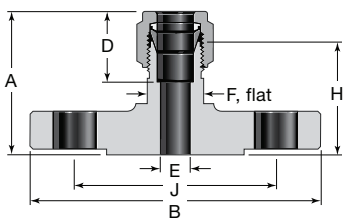
Tube OD mm	DIN Flange Size DN	Ordering Number Raised Face Flange	Dimensions mm						
			A	B	D	E	F	H	J
6	25	SS-6M0-F25M-40-C	47.5	115	15.3	4.8	20	40.1	85.0
12	15	SS-12M0-F15M-40-C	48.5	95.0	22.8	9.5	20	38.4	65.0
	25	SS-12M0-F25M-40-C	50.5	115				40.4	85.0
	50	SS-12M0-F50M-40-C	55.3	165				45.2	125
18	15	SS-18M0-F15M-40-C	51.8	95.0	24.4	15.1	32	41.7	65.0
	25	SS-18M0-F25M-40-C	53.8	115				43.7	85.0
25	25	SS-25M0-F25M-40-C	64.0	115	31.3	21.8	35	51.8	85.0
38	50	SS-38M0-F50M-40-C	90.4	165	49.4	33.7	55	62.7	125
50	50	SS-50M0-F50M-40-C	103	165	65.0	45.2	70	66.3	125

EN Flanges, Pressure Class PN 40



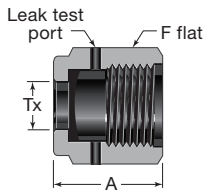
Tube OD mm	EN Flange Size DN	Ordering Number Raised Face Flange	Dimensions mm						
			A	B	D	E	F	H	J
6	25	SS-6M0-F25E-40-B1	47.5	115	15.3	4.8	20	40.1	85.0
12	15	SS-12M0-F15E-40-B1	48.5	95.0	22.8	9.5	20	38.4	65.0
	25	SS-12M0-F25E-40-B1	50.5	115				40.4	85.0
	50	SS-12M0-F50E-40-B1	55.3	165				45.2	125
18	15	SS-18M0-F15E-40-B1	51.8	95.0	24.4	15.1	32	41.7	65.0
	25	SS-18M0-F25E-40-B1	53.8	115				43.7	85.0
25	25	SS-25M0-F25E-40-B1	64.0	115	31.3	21.8	35	51.8	85.0
38	50	SS-38M0-F50E-40-B1	90.4	165	49.4	33.7	55	62.7	125
50	50	SS-50M0-F50E-40-B1	103	165	65.0	45.2	70	66.3	125

JIS Flanges, Pressure Class 10K



Tube OD	JIS Flange Size DN	Ordering Number Raised Face Flange	Dimensions						
			A	B	D	E	F	H	J
Dimensions, in.									
1/4	15	SS-400-F15A-10K-RF	1.66	3.74	0.60	0.19	13/16	1.37	2.76
3/8		SS-600-F15A-10K-RF	1.72		0.66	0.28			
1/2		SS-810-F15A-10K-RF	1.83		0.90	0.41			
3/4		SS-1210-F15A-10K-RF	1.91		0.96	0.62		1 1/4	
1	25	SS-1610-F25A-10K-RF	2.40	4.92	1.23	0.88	1 3/8	1.92	3.54
2	50	SS-3200-F50A-10K-RF	4.01	6.10	2.66	1.81	2 3/4	2.54	4.72
Dimensions, mm									
12	15	SS-12M0-F15A-10K-RF	46.5	95.0	22.8	9.5	20	36.3	70.0
18	15	SS-18M0-F15A-10K-RF	48.5	95.0	24.4	15.1	32	38.4	70.0
25	25	SS-25M0-F25A-10K-RF	61.0	125	31.3	21.8	35	48.8	90.0

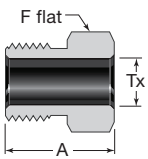
Nuts, Caps, and Plugs



Female Nut

VCR Size	Ordering Number	Dimensions		
		A	F	Tx
Dimensions, in. (mm)				
1/8	SS-2-VCR-1	0.53 (13.5)	7/16	0.21 (5.3)
1/4	SS-4-VCR-1	0.81 (20.6)	3/4	0.36 (9.1)
1/2	SS-8-VCR-1	0.88 (22.4)	1 1/16	0.61 (15.5)
5/8	SS-10-VCR-1	0.88 (22.4)	1 3/16	0.74 (18.8)
3/4	SS-12-VCR-1	1.12 (28.4)	1 1/2	0.89 (22.6)
1	SS-16-VCR-1	1.34 (34.0)	1 3/4	1.20 (30.5)

Male Nut

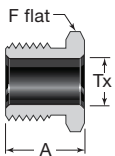


VCR Size	Ordering Number	Dimensions		
		A	F	Tx
Dimensions, in. (mm)				
1/8	SS-2-VCR-4	0.50 (12.7)	3/8	0.21 (5.3)
1/4	SS-4-VCR-4 ^①	0.71 (18.0)	5/8	0.36 (9.1)
1/2	SS-8-VCR-4	0.81 (20.6)	15/16	0.61 (15.5)
5/8	SS-10-VCR-4	0.81 (20.6)	1 1/16	0.74 (18.8)
3/4	SS-12-VCR-4	1.00 (25.4)	1 5/16	0.89 (22.6)
1	SS-16-VCR-4	1.19 (30.2)	1 5/8	1.20 (30.5)

① A taper at the hex end allows the nut to move around 90° tube bends.

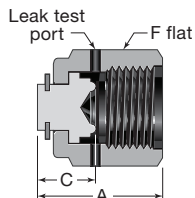
Short Male Nut

For use with short gland.



VCR Size	Ordering Number	Dimensions		
		A	F	Tx
Dimensions, in. (mm)				
1/4	SS-4-VCR-4-.54NC	0.54 (13.7)	5/8	0.36 (9.1)
	SS-4-VCR-4-.65NC	0.65 (16.5)		

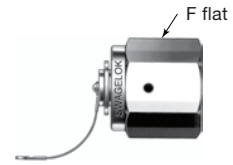
Cap



VCR Size	Ordering Number	Dimensions		
		A	C	F
Dimensions, in. (mm)				
1/8	SS-2-VCR-CP	0.63 (16.0)	0.30 (7.6)	7/16
1/4	SS-4-VCR-CP	0.94 (23.9)	0.44 (11.2)	3/4
1/2	SS-8-VCR-CP	1.01 (25.6)	0.45 (11.4)	1 1/16
3/4	SS-12-VCR-CP	1.29 (32.8)	0.54 (13.7)	1 1/2
1	SS-16-VCR-CP	1.54 (39.1)	0.63 (16.0)	1 3/4

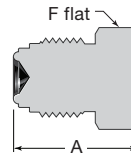
Cap with Lanyard

Lanyard material is 302 SS.
Lanyard length is 6 in. (15.2 cm).



VCR Size	Ordering Number	Dimensions		
		A	C	F
Dimensions, in. (mm)				
1/4	SS-4-VCR-CP-BP	0.94 (23.9)	0.44 (11.2)	3/4
1/2	SS-8-VCR-CP-BP	1.01 (25.6)	0.45 (11.4)	1 1/16

Plug



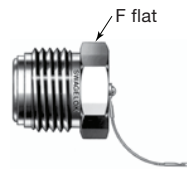
VCR Size	Ordering Number	Dimensions	
		A	F
Dimensions, in. (mm)			
1/8	SS-2-VCR-P ^①	0.68 (17.3)	3/8
1/4	SS-4-VCR-P ^②	0.92 (23.4)	5/8
1/2	SS-8-VCR-P	1.08 (27.4)	15/16
3/4	SS-12-VCR-P	1.43 (36.3)	1 5/16
1	SS-16-VCR-P	1.52 (38.6)	1 5/8

① Not designed for gasket retainer assembly.

② Also available as a rotatable plug.
Ordering number: **SS-4-VCR-RP**

Plug with Lanyard

Lanyard material is 302 SS.
Lanyard length is 6 in. (15.2 cm).



VCR Size	Ordering Number	Dimensions	
		A	F
Dimensions, in. (mm)			
1/4	SS-4-VCR-BP	0.92 (23.4)	5/8
1/2	SS-8-VCR-BP	1.08 (27.4)	15/16

Technische Daten - AF/Armaflex

Kurzbeschreibung	Hochflexibles, geschlossenzelliges Dämmmaterial mit hohem Wasserdampf-Diffusionswiderstand, niedriger Wärmeleitfähigkeit und integriertem antimikrobiellem Schutz durch Microban.				
Materialtyp	Elastomerschaum auf Basis synthetischen Kautschuks. Werkmässig hergestellte Produkte aus flexiblem Elastomerschaum (FEF) gemäss EN 14304.				
Farbe	schwarz				
Spezielle Materialhinweise	Selbstklebebeschichtung: Haftkleber-Beschichtung auf modifizierter Acrylat-Basis mit Gitternetzstruktur und einer Abdeckung aus Polyethylen-Folie. Die Schutzfolie der Klebeschicht von selbstklebenden Produkten kann Spuren von Silikon enthalten.				
Anwendungen	Dämmung und Schutz von Rohren, Luftkanälen und Behältern (inkl. Rohrbogen, Armaturen, Flanschen) in Kälte- und Klimaanlage sowie verfahrenstechnischen Anlagen, zur Tauwasserverhinderung und Energieeinsparung. Reduzierung der Körperschallübertragung bei Wasser und Abwasser-Installationen.				
Besonderheiten	Zunehmende Dämmschichtdicken der Schläuche stellen gleichbleibende Oberflächentemperaturen bei steigendem Rohrdurchmesser sicher.				
Hinweise	EG-Konformitätszertifikat Nr. 0543 und 0551 der Güteschutzgemeinschaft Hartschaum e.V., Celle				
Eigenschaft	Wert/Beurteilung		Prüfzeugnis^{*1}	Überwachung^{*2}	Besondere Hinweise
Temperaturbereich					
Anwendungsbereich	Obere Anwendungsgrenztemperatur	+ 110 °C	(+ 85 °C bei vollflächiger Verklebung von Platte oder Band auf dem Objekt.)	D 4869 EU 5315 EU 4955	● Prüfung nach DIN EN 14706, DIN EN 14707 und DIN EN 14304
	Untere Anwendungsgrenztemperatur ¹	-50 °C			
Wärmeleitfähigkeit					
Wärmeleitfähigkeit	ϑ_m	+/-0	°C	$\lambda =$	
	Schläuche λ	$\leq 0,033$	W/(m · K)	$[33 + 0,1 \cdot \vartheta_m + 0,0008 \cdot \vartheta_m^2]/1000$	D 4892 EU 5315 EU 5493
	Schläuche λ	$\leq 0,036$	W/(m · K)	$[36 + 0,1 \cdot \vartheta_m + 0,0008 \cdot \vartheta_m^2]/1000$	○/● Deklariert nach EN ISO 13787 Prüfung nach EN 12667 und EN ISO 8497
	Platten, Streifen, Band λ	$\leq 0,033$	W/(m · K)	$[33 + 0,1 \cdot \vartheta_m + 0,0008 \cdot \vartheta_m^2]/1000$	
	Platten λ	$\leq 0,036$	W/(m · K)	$[36 + 0,1 \cdot \vartheta_m + 0,0008 \cdot \vartheta_m^2]/1000$	
Wasserdampfdiffusionswiderstand					
Wasserdampfdiffusionswiderstand	Platten (AF-10MM bis AF-32MM) und Schläuche (AF-1 bis AF-4)	μ	\geq	10.000	D 4532 D 4981 EU 5315 EU 4955
	Platten (AF-50MM) und Schläuche (AF-5 bis AF-6)	μ	\geq	7.000	○/● Prüfung nach EN 12086 und EN 13469
Brandverhalten					
Baustoffklasse ²	Euroklasse				EU 5315 EU 5493 CH 3497
	Schläuche		B _L -s3,d0 (Z-56.269-3530)		○/● Deklariert nach EN 13501-1 Prüfung nach EN 13823 und EN ISO 11925-2 Prüfung nach VKF
	Platten		B / B _L -s3-d0 (Z-56.269-768)		
	selbstklebendes Band		B-s3-d0 (Z-56.269-768)		
	Brandkennziffer 5 (200 °C).2 schwerbrennbar bis		200 °C		
Sonstige Brandklasse	UL-zugelassen			UL: D 4613 D 3763 FM: D 4592	○/● UL: Prüfung nach UL94, IEC 60695 und Can/CSA-C.22.2 No0.17., UL 746C FM: Prüfung nach UBC26-3, Klasse No.4924
	FM-zugelassen				
Praktisches Brandverhalten	Selbstverlöschend, nicht tropfend, leitet kein Feuer				
Akustische Eigenschaften					
Reduzierung der Körperschallübertragung	Dämmwirkung		$\leq 28,00$ dB(A)	D 3660	Prüfung nach DIN 52219 und EN ISO 3822-1
Bewerteter Schallabsorptionsgrad α_w			$\leq 0,45$	D 4763	Prüfung nach EN ISO 354
Sonstige technische Eigenschaften					
Abmessungen und Toleranzen	Gemäss EN 14304, Tabelle 1			EU 5315 EU 5493	○ Prüfung nach EN 822, EN 823, EN 13467

Technische Daten - AF/Armaflex

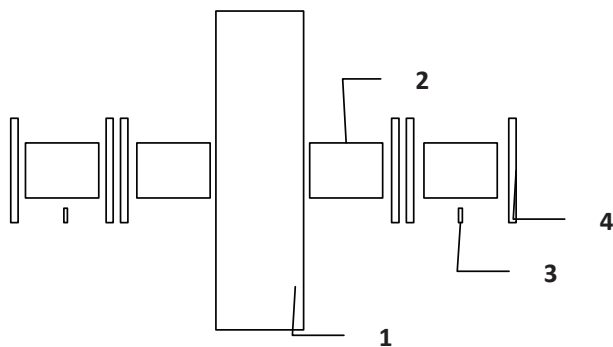
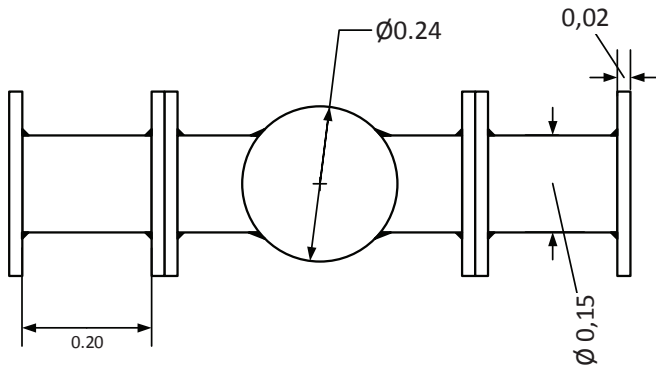
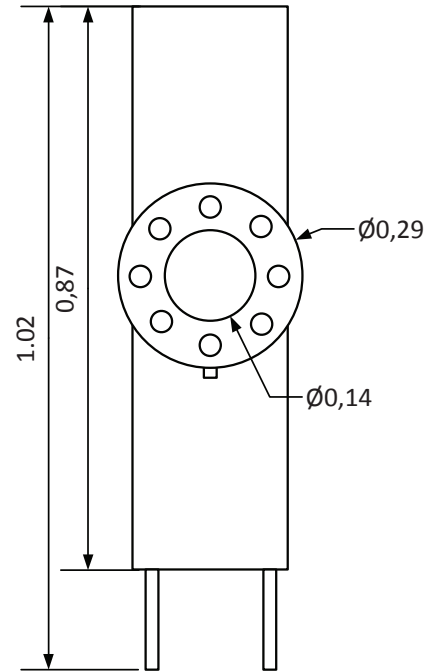
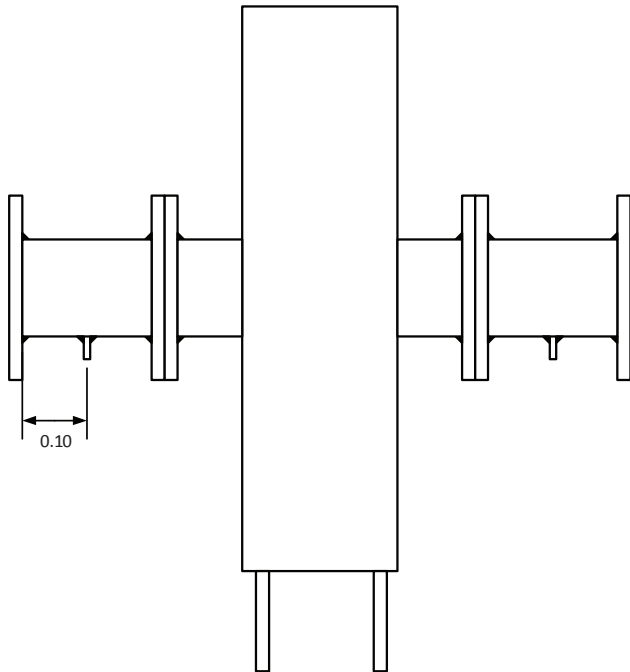
Lagerung und Haltbarkeit	Selbstklebende Bänder, selbstklebende Platten, selbstklebende Schläuche, Streifen: 1 Jahr		Lagerung in trockenen, sauberen Räumen bei normaler Luftfeuchte (50-70%) und Raumtemperatur (0-35 °C).
Antimikrobielles Verhalten	Mit aktivem antimikrobiellem Microban Produktschutz für zusätzliche Sicherheit gegen Bakterien und Schimmelpilzbefall	D 5524 D 4640 D 4641	Prüfung nach ASTM G21 und ASTM C 1338

1. Bei Temperaturen unter -50 °C fragen Sie bitte unseren Kundenservice nach den entsprechenden technischen Informationen.
 2. Die Baustoffklasse gilt für metallische oder feste mineralische Untergründe.
- *1 Weitere Dokumente wie Prüfzeugnisse, Genehmigungen und ähnliches können unter Nennung der angegebenen Registriernummer angefordert werden.
- *2 ●: Offizielle Überwachung durch unabhängige Institute und/oder Prüfbehörden
○: Werkseigene Produktionskontrolle

Alle Daten und technischen Informationen basieren auf Ergebnissen, die unter typischen Anwendungsbedingungen erzielt wurden. Empfänger dieser Informationen sollten in ihrem eigenen Interesse und auf eigene Verantwortung rechtzeitig mit uns klären, ob die Daten und Informationen für den beabsichtigten Anwendungsbereich anwendbar sind. Installationsanweisungen finden Sie in unserem Armaflex Montagehandbuch. Bitte wenden Sie sich an unseren Kundenservice, bevor Sie Edelstahl dämmen. Einige Kühlmittel können Austrittstemperaturen über +110 °C erreichen; fragen Sie bitte unseren Kundenservice nach weiteren Informationen. Bei Anwendung im Freien sollte Armaflex innerhalb von 3 Tagen mit einer Ummantelung geschützt werden.

SINTEF Energi AS (Armin Hafner) – Inquiry for a welding assignment

09.01.14



- $p_N = 16$ bar
- $T_{min} = -55^\circ\text{C} \dots -60^\circ\text{C}$
- CO_2 as storage media
- stainless steel 1.4541
- parts simplified

Nr.	Part	Quantity
1	Shell & tube heat exchanger	1x
2	Pipe piece $d_v = 140$ mm	4x
3	Pipe piece $d_v = 20$ mm	1x
4	Flansh $d_h = 140$ mm	6x